DEPARTMENT OF SCIENCE AND TECHNOLOGY
GRADUATE SCHOOL OF ENGINEERING
NAGASAKI UNIVERSITY

Design and Evaluation of Dual Band MIMO Antennas

ERFAN ROHADI

DOCTORAL
DISSERTATION

Preface

First and foremost, I would like to raise my infinite thanks to God, the Most Gracious and the Most Merciful. Alhamdulillah.

The research work presented in this thesis was performed between the years of October 2011 – September 2014 at Nagasaki University. The research works were carried out at the Graduate School of Engineering, Department of Science and Technology, under Electrical and Electronics group. The research and financial supports from Ministry of Education and Culture of Republic Indonesia, General Higher Education and The State Polytechnic of Malang is gratefully acknowledged.

I would like to express my most sincere gratitude and appreciation to my supervisor, Professor Mitsuo Taguchi for accepting me as one of his doctoral students. His trust, supports, encouragement and faithful guidance were the main reason for the emergence of this thesis.

I would like to thank the pre-examiners of my thesis, Professor Takashi Takenaka and Associate Professor Takafumi Fujimoto for their reviews and comments in order to improve the quality of the thesis.

For my colleagues and laboratory mates, administrative staffs and everybody in the department; thank you very much. I am glad to know all of you. My Indonesian friends in Nagasaki especially, also my foreign student friend from many countries, thank you for all the enjoyable moments that we shared together throughout the years.

Finally, I would like to express my warmest gratitude to lovely people; for my daughter Gabie and my son Michel, thank you for the love, patience, understanding and nicely behaved during papa's busy days. I love you both a lot. Special thank deliver to Aida, thank you for your love, prayers, patience, and support.

Nagasaki, July 30, 2014,
Erfan Rohadi

Contents

List of Publication

1. M. Taguchi and E. Rohadi, ”Unbalanced Fed Ultra Low Profile Inverted L Antenna on a Rectangular Conducting Plane; Equivalent Circuit Expression”, *Proc. Int. Conf. APCAP,* pp. 533-536, July 2014.
2. E. Rohadi and M. Taguchi, ”Dual Band MIMO Antenna Composed of Two Profile Unbalanced Fed Inverted L Antennas for Wireless Communications”, *Journal of Wireless Engineering and Technology*. Vol.5, No.3, pp. 54-61, July 2014.
3. E. Rohadi and M. Taguchi, ”Two Low Profile Unbalanced Fed Inverted L Elements on Square Conducting Plane for MIMO Application”, *Journal of Wireless Engineering and Technology*, Vol.5, No.2, pp .34-43, April 2014.
4. E. Rohadi and M. Taguchi, ”Two element ultra low profile inverted L antennas on finite conducting plate for MIMO applications”, *Proc. International Conference on Advanced Tech. for Communications.* (ATC), pp. 74-77, October 2013.
5. E. Rohadi and M. Taguchi, ”Ultra low profile, unbalanced fed inverted F antenna for 2.45 GHz wireless communication system”, *Proc. International conference of EMTS-URSI*, pp. 585-588, may 2013.
6. E. Rohadi and M. Taguchi, ”Ultra Low Profile Antenna for 2.45 GHz Wireless Communications”, *Proc. Int. Conference on Communication and Satellite (Comnetsat)*, pp. 103-107, July 2012.
7. E. Rohadi and M. Taguchi, ”Ultra Low profile, Unbalanced Fed Inverted F Antenna on Finite Conducting Plane”, *Proc. International Conference ACES*,

pp. 969-971, April 2012.

I. Introduction

1.1 Background

The evolution of cellular systems began in 1970s, starting with the first generation (1G) comprising of analog systems supporting basic voice transmission [1]. The second generation (2G) of cellular systems, global system for mobile communications (GSM) was developed in early 90's. The 2G systems provided digital encryption of the signal and improved the transmission quality and coverage. As the need for packet data arose, general packet radio service (GPRS) and enhanced data rates for GSM evolution (EDGE) technologies were introduced as an extension to the 2G systems.

The advent of the 20th century brought the third generation (3G) systems, which improved the data rates from several hundreds of kilobits per second (EDGE) to several megabits per second. This increased the inter-net usage from mobile devices, thereby fuelling the growth of the mobile broadband industry. Recently introduced fourth generation (4G) systems provide even higher data rates enabling a wide range of telecommunication services, including mobile broadband internet access, internet protocol (IP) telephony, high-definition mobile TV, etc. The 4G system is aimed at providing peak data rates of up to 1 gigabit per second [2]. Two candidates of the 4G systems are commercially deployed around the world, namely long-term evolution (LTE) systems and worldwide interoperability for microwave access (WiMAX) technology [1, 3]. Both systems are based on packet-oriented communication. Meanwhile, new radio spectrum to accommodate new wireless systems is scarce and expensive. Therefore, available radio spectrum must be used efficiently without any increase on bandwidth or transmit power.

In a conventional communication link between the base station and a mobile terminal, a single antenna is used at both ends and thus is referred to as a single-input single-output (SISO) system. Capacity of a SISO system depends on the bandwidth, transmit power, and signal to noise ratio. The bandwidth and transmit

power are limited by frequency regulations. In addition to noise, impairment due to the unavoidable phenomenon such as fading and shadowing exists in wireless communication systems. This limits the channel capacity of a SISO system.

In the late 1990s, multiple-input multiple-output (MIMO) systems that utilize multiple antennas at both ends of the link were introduced. This enables the use of multiple spatial channels at the same frequency. Hence, channel capacity of a MIMO system increases with the number of channels as compared to a SISO link. The number of spatial channels is limited to the number of antenna elements at an end of the link [4–7].

Implementation of MIMO in mobile communication system necessitates at least two antennas in one terminal. MIMO specific antenna design challenges are related to mutual coupling among antenna elements and degradation of antenna performance due to a user holding the mobile terminal [8–17]. The number of antennas to be incorporated in today's mobile terminal is restricted by the size of the terminal [18, 19]. This is contrary to a less severe space limitation at the base station. More-over, the performance of a MIMO system depends not only on the antenna performance, but also on the propagation environment. The design of MIMO antennas for mobile terminals should also incorporate selection of optimal placement locations, topology, type and number of antenna elements. Therefore, a definitive and general conclusion on this subject has became major interest in antenna design community over the past few years [11, 12, 20–22].

1.2 Objective of the thesis

The main objective of this thesis is to provide the dual band MIMO antenna and valuable insights for the small size and simple design of multi element antennas for wireless communication systems. The low profile unbalance fed inverted L antenna on finite conducting plane is investigated as antenna element of the dual band MIMO antenna. Particularly, Equivalent circuit expression and the performance of inverted L antenna have been studied in the presence of the impedance matching. A comparison with the base fed inverted F antenna have been investigated. The performance of unbalanced fed inverted L antenna such as the gain and

return loss bandwidth are examined. Then, the comparison of the performance between the unbalanced fed inverted L antenna and unbalanced inverted F antenna has been examined to ensure which one is better to design the MIMO antenna. The MIMO antenna composed two low profile inverted L antenna for 2.45 GHz on finite conducting plane have been investigated. The develop knowledge is used to reduce the mutual coupling between antenna elements and also the diversity performance is examined with investigating the correlation coefficient.

Finally, the dual band MIMO antenna composed of two low profile inverted L antennas for 2.45 GHz and 5 GHz has been studied based on calculation and measurement data.

1.3 Contents and organization of the thesis

The main scientific results of this thesis are presented in articles (II) – (VI). The thesis is divided into two parts. In the first part of the thesis, the expression of equivalent circuit of ultra low profile inverted L antenna in (II) and the characterization methods of ultra low profile unbalanced fed inverted L, base fed inverted F and unbalanced inverted F antennas performances are studied in (III), and (IV). The performances of the antennas with different type of inverted element are analyzed extensively. The investigations are focused on impedance matching, antenna gain and the return loss bandwidth at the design frequency of 2.45 GHz. The second part of the thesis is dedicated to the design of MIMO antenna structures operating at the 2.45 GHz (V) and dual band MIMO antenna structures operating at 2.45 GHz and 5 GHz (VI). The design and performance of the proposed MIMO antenna is investigated and compared. A summary of the publications describing the contributions of this thesis is presented in Chapter VII. Finally, Chapter VIII presents general conclusions and possible ideas for future research.

1.4 Scientific contributions

The scientific merit of the thesis is in the design, analysis, performance evaluation and design rules for MIMO antennas for wireless communication application. The highlights are:

1. The study of equivalent circuit of the ultra low profile unbalanced fed inverted L antenna is performed. The investigation on inverted L elements has been examined to obtain the impedance matching.
2. An empirical investigation on the impact of the height of inverted L and inverted F antenna, the conducting plane size and impedance matching. The evaluation is performed using calculation and measurement based on scattering parameters data.
3. Systematic analysis and evaluation on the performance of MIMO antenna composed of inverted L antennas are performed.
4. A simple design and good performance of dual band MIMO antenna has been realized. The proposed structure is operating at 2.45 GHz and 5 GHz bands.

1.5 The MoM of electromagnetic simulator WIPL-D

In the calculation the WIPL-D electromagnetic simulator based on Method of Moment is used.

References Chapter-I

[1] E. Dahlman, S. Parkvall, J. Skold, and P. Beming, *3G Evolution: HSPA and LTE for Mobile Broadband*. Academic Press, Elsevier, 2008.

[2] E. Dahlman, S. Parkvall, and J. Skold, *4G LTE/LTE- advanced for mobile broadband*. Academic Press, Elsevier, 2011.

[3] Q. Li, X. Lin, J. Zhang, and W. Roh, "Advancement of MIMO technology in WiMAX: from IEEE 802.16d/e/j to 802.16m," *IEEE Commun. Mag.*, vol. 47, no. 6, pp. 100–107, June 2009.

[4] R. Vaughan and J. Andersen, "Antenna diversity in mobile communications," *IEEE Trans. Veh. Technol.*, vol. 36, no. 4, pp. 149–172, Nov. 1987.

[5] G. J. Foschini and M. J. Gans, "On limits of wireless communications in a fading environment when using multiple antennas," *Wireless Pers. Commun.*, vol. 6, no. 3, pp. 311–335, Mar. 1998.

[6] S. Anderson, B. Hagerman, H. Dam, U. Forssen, J. Karlsson, F. Kronestedt, S. Mazur, and K. Molnar, "Adaptive antennas for GSM and TDMA systems," *IEEE Pers. Commun.*, vol. 6, no. 3, pp. 74–86, June 1999.

[7] M. Jensen and J. Wallace, "A review of antennas and propagation for MIMO wireless communications," *IEEE Trans. Antennas Propag.*, vol. 52, no. 11, pp. 2810–2824, Nov. 2004.

[8] B. Green and M. Jensen, "Diversity performance of dual-antenna handsets near operator tissue," *IEEE Trans. Antennas Propag.*, vol. 48, no. 7, pp. 1017–1024, July 2000.

[9] K. Ogawa and T. Matsuyoshi, "An analysis of the performance of a handset diversity antenna influenced by head, hand, and shoulder effects at 900 MHz .I. effective gain characteristics," *IEEE Trans. Veh. Technol.*, vol. 50, no. 3, pp. 830–844, May 2001.

[10] K. Ogawa, T. Matsuyoshi, and K. Monma, "An analysis of the performance of a handset diversity antenna influenced by head, hand, and shoulder effects at 900 MHz .II. correlation characteristics," *IEEE Trans. Veh. Technol.*, vol. 50, no. 3, pp. 845–853, May 2001.

[11] M. Karaboikis, V. Papamichael, G. Tsachtsiris, C. Soras, and V. Makios,

"Integrating compact printed antennas onto small diversity/MIMO terminals," *IEEE Trans. Antennas Propag.*, vol. 56, no. 7, pp. 2067–2078, July 2008

[12] B. K. Lau and J. Andersen, "Unleashing multiple antenna systems in com-pact terminal devices," in *IEEE Int. Workshop Antenna Technol.*, Mar. 2009, pp. 1–4.

[13] V. Plicanic, B. K. Lau, A. Derneryd, and Z. Ying, "Actual diversity performance of a multiband diversity antenna with hand and head effects," *IEEE Trans. Antennas Propag.*, vol. 57, no. 5, pp. 1547–1556, May 2009.

[14] C. Luxey and D. Manteuffel, "Highly-efficient multiple antenna-systems for small MIMO devices," in *IEEE Int. Workshop Antenna Technol.*, Mar. 2010, pp. 1–6.

[15] F. Harrysson, J. Medbo, A. Molisch, A. Johansson, and F. Tufvesson, "Efficient experimental evaluation of a MIMO handset with user influence," *IEEE Trans. Wireless Commun.*, vol. 9, no. 2, pp. 853–863, Feb. 2010.

[16] F. Harrysson, A. Derneryd, and F. Tufvesson, "Evaluation of user hand and body impact on multiple antenna handset performance," in *Proc. IEEE Int. Symp. Antennas Propag.*, July 2010, pp. 1–4.

[17] J. Nielsen, B. Yanakiev, I. Bonev, M. Christensen, and G. Pedersen, "User influence on MIMO channel capacity for handsets in data mode operation," *IEEE Trans. Antennas Propag.*, vol. 60, no. 2, pp. 633–643, Feb. 2012.

[18] R. Vaughan and J. B. Andersen, *Channels, Propagation and Antennas for Mobile Communications*. The IEE, 2003.

[19] Z. N. Chen, *Antennas for Portable Devices*. John Wiley & Sons, Ltd, 2007.

[20] T. Brown, "Antenna diversity for mobile terminals," 2002, PhD thesis, University of Surrey, 2002. [Online]. Available: http://personal.ee.surrey.ac.uk/Personal/T.Brown/thesis.html

[21] C. Waldschmidt, C. Kuhnert, M. Pauli, and W. Wiesbeck, "Integration of MIMO antenna arrays into handhelds," in *5th IEE Int. Conf. 3G Mobile Commun. Technol.*, 2004, pp. 16–23.

[22] P. Vainikainen, J. Holopainen, C. Icheln, O. Kivekäs, M. Kyrö, M. Mustonen, S. Ranvier, R. Valkonen, and J. Villanen, "More than 20 antenna elements in future mobile phones, threat or opportunity?" in *Proc. 3rd Euro-*

pean Conf. Antennas Propag., Mar. 2009, pp. 2940–2943.

II. Unbalanced Fed Ultra Low Profile Inverted L Antenna on a Rectangular Conducting Plane; Equivalent Circuit Expression

2.1 Introduction

The input impedance of horizontal dipole located very close to a perfect conducting plane becomes low due to the existence of a metallic structure, and it approaches zero as the distance decreases toward zero [1 - 3]. An "ultra low profile dipole (ULPD) antenna", which is a horizontal dipole very closely located to an infinite conducting plane was proposed to solve the impedance matching issue [4]. A half wavelength dipole is excited at the offset points from its center, so that reasonable impedance can be obtained even with a conducting plane in proximity to the dipole. The maximum gain of 8.4 dBi, which is higher than that of a half-wave dipole with a quarter wavelength distance between the dipole and the reflector, is obtained. In order to realize ULPD, however, a 3 dB coupler and a $90°$ phase shifter are needed. In [5], the unbalanced feed to the ultra low profile inverted L antenna located very close on a rectangular conducting plane and analyzed numerically and experimentally. This antenna may call this antenna as "ULPIL antenna" for convenience.

As a low profile antenna, the base fed inverted F (BFIF) antenna is well known [6-12]. This antenna is composed of the base fed inverted L antenna and the short-circuited stub for impedance matching. In this chapter, the characteristics of ULPIL antenna are compared with those of the BFIF antenna. The mechanisms of impedance matching of two antennas are compared. In the numerical analysis, the electromagnetic simulator WIPL-D based on the Method of Moments is used [13].

2.2 Structure of proposed antenna

Fig. 2.1(a) shows the structure of the ULPIL antenna located on a rectangular conducting plane. The size of conducting plane is *pxp*+*pxm* by *pyp*+*pym*. The

semi-rigid coaxial cable with the characteristic impedance of 50 Ω is mounted on the conducting plane. The radius of the outer conductor is 1.095 mm and that of the inner conductor is 0.255 mm, and the polytetrafluoroethylene is filled within a coaxial cable [14]. This antenna consists of a horizontal arm in the y-direction and a small leg in the z-direction. The coaxial cable is extended behind ground plane. The generator is connected to the bottom end of coaxial cable. The inner conductor of the coaxial cable is extended from the end of outer conductor, that is, this antenna is excited at the end of outer conductor in the numerical analysis. The height of horizontal element is *h*. Fig. 2.1(b) shows the conventional, base fed inverted F antenna. The design frequency is 2.45 GHz.

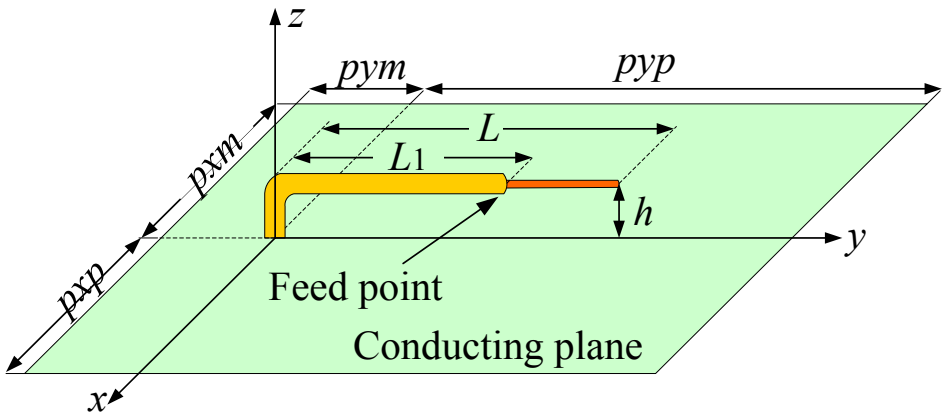

(a) ULPIL antenna

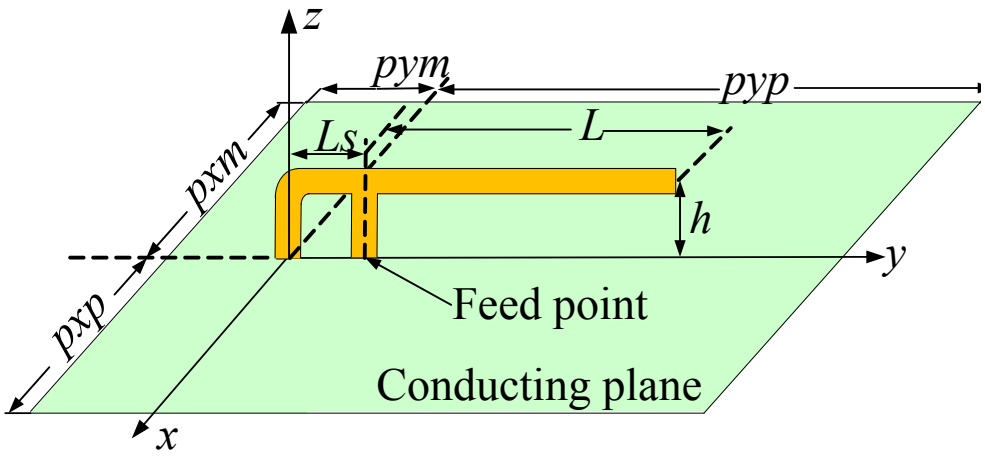

(b) BFIF antenna

Figure 2.1. ULPIL antenna and BFIF antenna on a rectangular conducting plane.

2.3 Result and discussion

2.3.1 *ULPIL antenna*

The fixed antenna parameters are as follows; *pxp* = *pxm* = 15 mm, *pym* = 10 mm, *pyp* = 44 mm. Table 2.1 shows the return loss bandwidth and the directivity of ULPIL antenna for different antenna height *h*. The length of horizontal element *L* and the feed point position L_1 are optimized so that the resonant frequency becomes to be 2.45 GHz.

Table 2.1 Return Loss and directivity of ULPIL antenna for different antenna height.

h	***L***	L_1	**Return Loss Bandwidth**			**Directivity at 2.45GHz**
(mm)	**(mm)**	**(mm)**	f_{low} **(GHz)**	f_{high} **(GHz)**	**(%)**	**(dBi)**
2	31.8	26.9	2.439	2.459	0.82	4.79
4	31.0	22.6	2.417	2.480	2.57	4.34
6	29.8	18.2	2.392	2.509	4.78	4.18
8	28.3	14.2	2.386	2.545	6.49	4.01
10	26.8	9.9	2.334	2.581	10.08	3.81

pxm = *pxp* = 15 mm, *pym* = 10 mm, *pyp* = 44 mm

Fig. 2.2 shows the input impedance characteristics of ULPIL for different *L*. L_1 = 22.6 mm, *h* = 4mm are fixed. In the case of *L* = 31 mm, the resonant frequency becomes to be 2.45 GHz. In the figure, the input impedances at the design frequency of 2.45 GHz are indicated by "x". When *L* is 30 mm, the input reactance becomes capacitive. On the other hand, when *L* is 32 mm, the input reactance becomes inductive. This is easily explained by the transmission line theory [15]. The input reactance of the open-circuited parallel line becomes capacitive if its length becomes shorter than a quarter wavelength. Fig. 2.3 shows the reflection coefficient for different *L*. L_1 is optimized so that the S11 becomes smallest at the resonant frequency in each case. The resonant frequencies in the case of *L* = 30 mm, 31 mm, and 32 mm are 2.535 GHz, 2.45 GHz, and 2.375 GHz, respectively. The length of *L* becomes almost a quarter wavelength at each resonant frequency. This means that the resonant frequency can be adjusted by *L*.

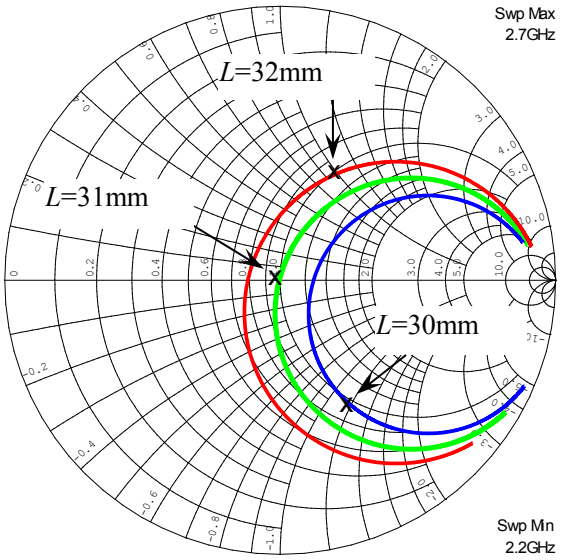

Figure 2.2. Input impedance characteristics of ULPIL antenna for different L. h = 4 mm, L_1 = 22.6 mm, pxm = pxp = 15 mm, pym = 10 mm, pyp = 44 mm.

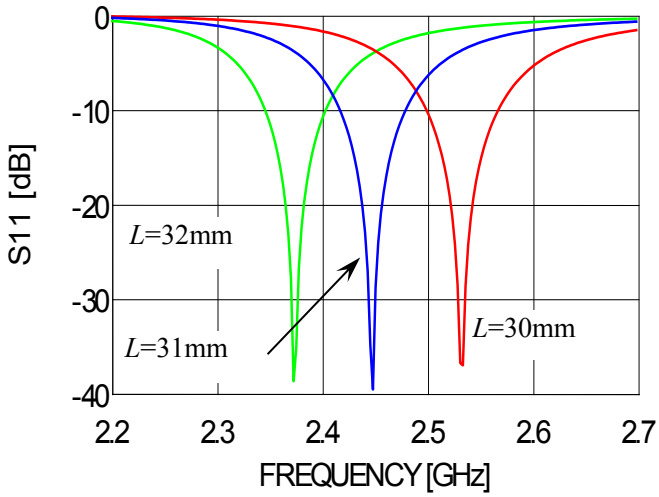

Figure 2. 3. S11 characteristics of ULPIL antenna for different L. L_1 is optimized. h = 4 mm, pxm = pxp = 15 mm, pym = 10 mm, pyp = 44 mm.

Fig. 2.4 shows the calculated current distributions of ULPIL with L_1 = 22.6 mm and that of the base fed inverted L antenna. The input impedance is defined by the ratio of the impressed voltage and the feed point current. Therefore the input resistance becomes smaller, as L_1 becomes smaller. The input impedance

is 50 Ω in the case of L_1 is 22.6 mm. That of base fed inverted L antenna is 4.06+j26.85 Ω. The directivity of ULPIL with L_1 = 22.6 mm and the base fed inverted L antenna are 4.34 dBi and 4.86 dBi, respectively. Since the input impedance of the base fed inverted L antenna is mismatched to 50 Ω, its actual gain becomes small.

2.3.2. *BFIF antenna*

The parameters of conducting plane are fixed as *pxp* = *pxm* = 15 mm, *pym* = 10 mm, and *pyp* = 44 mm. Table 2.2 shows the return loss bandwidth and the directivity of the BFIF antenna for different antenna height *h* in the case of the length of short stub L_s =3.3 mm. Fig. 2.5 shows the input impedance characteristics of the BFIF antenna for different *h*. In the BFIF antenna, the input impedance is adjusted by changing the element length *L* and short-circuited stub length L_s.

Table 2.2 Return Loss and directivity of BFIF antenna for differenet antenna height.

Ls	***h***	***L***	**Return Loss Bandwidth**			**Directivity at 2.45GHz**
(mm)	**(mm)**	**(mm)**	f_{low} **(GHz)**	f_{high} **(GHz)**	**(%)**	**(dBi)**
3.3	7	26.2	2.388	2.520	5.39	4.02
3.3	8	25.6	2.353	2.556	8.29	3.92
3.3	9	24.9	2.334	2.587	10.33	3.80
3.3	10	24.3	2.312	2.610	12.16	3.69

pxm = *pxp* = 15 mm, *pym* = 10 mm, *pyp* = 44 mm

Fig. 2.6 shows the comparison of the return loss bandwidth between ULPIL antenna and BFIF antenna. When the height *h* of the BFIF antenna is less than 7 mm (about 0.05 λ) the return loss bandwidth larger than 10 dB is not satisfied even though the short stub is added. Therefore, in Fig. 2.6, data are not shown in the case of *h* is less than 7 mm.

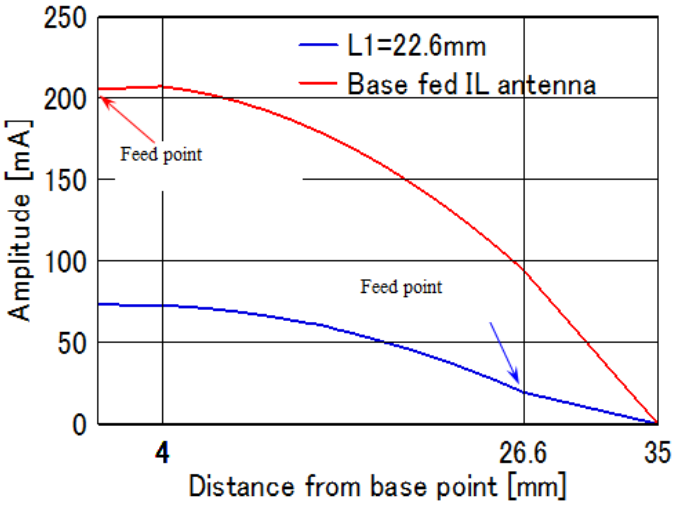

Figure 2.4. Calculated current distribution at 2.45 GHz for different L_1. h = 4 mm, L =31 mm, *pxm* = *pxp* = 15 mm, *pym* = 10 mm, *pyp* = 44 mm.

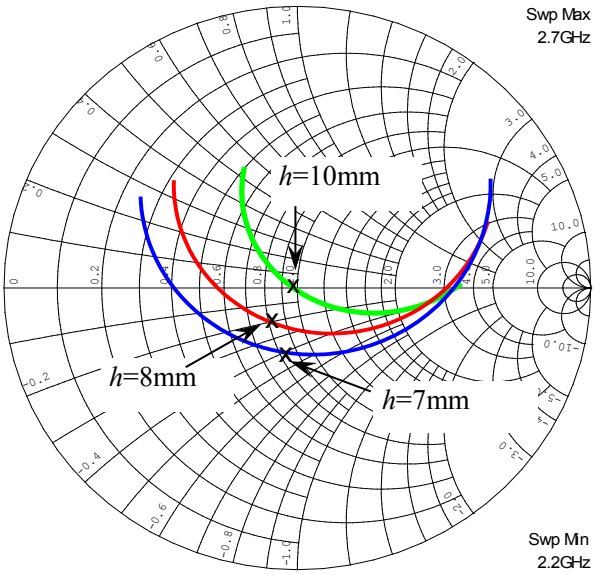

Figure 2.5. Input impedance characteristics of base fed inverted F antenna for different h. *pxm* = *pxp* = 15 mm, *pym* = 10 mm, *pyp* = 44 mm, *Ls* = 3.3 mm.

2.3.3 *Equivalent circuits*

The BFIF antenna is composed of the base fed inverted L antenna and the short-circuited stub. Fig. 2.7 shows the base fed inverted L antenna and the

short-circuited stub. In order to evaluate the electrical length of vertical element of antenna, the monopole antenna with its height *h* shown in Fig. 2. 7(c) is calculated. Fig. 2. 8 shows the equivalent circuit of BFIF antenna. The input admittance of the base fed inverted L antenna is shown at A. The short-circuited stub is connected in parallel with the base fed inverted L antenna at the bend (B).

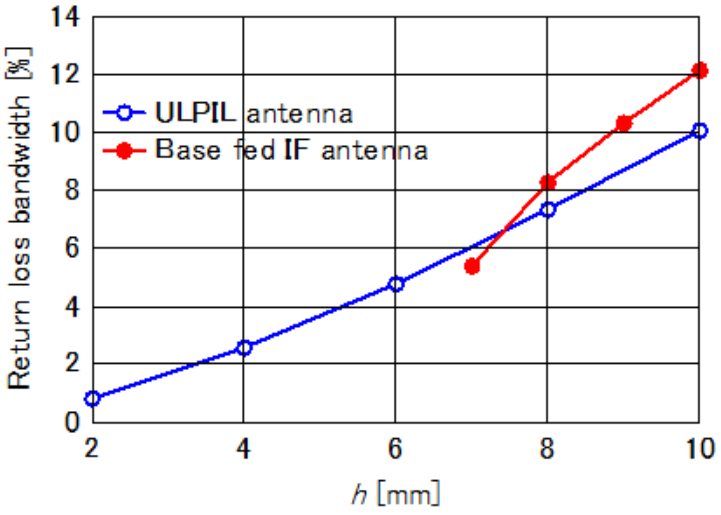

Figure 2.6. Comparison of return loss bandwidth between ULPIL antenna and base fed inverted F antenna. $pxm = pxp = 15$ mm, $pym = 10$ mm, $pyp = 44$ mm, $Ls = 3.3$ mm.

Fig. 2.9 shows the how the short-circuited stub works as the matching circuit. The antenna height *h* is 6 mm, the length of short-circuited stub *Ls* is 3.3 mm. In this case, the return loss larger than 10 dB is not satisfied. The input admittances of base fed inverted L antenna and BFIF antenna at the design frequency of 2.45 GHz are indicated as A (Y_{BFIL}) and D (Y_{BFIF}), respectively. In the figure, the input admittances of base fed inverted L antenna at the frequency of 2.4 GHz and 2.5 GHz are indicated as $A_{2.4}$ and $A_{2.5}$, respectively. The input admittances of BFIF antenna are shown as $D_{2.4}$ and $D_{2.5}$. The input admittances of the short-circuited stub and the monopole antenna are shown as F (Y_{SS}) and G (Y_{Mono}), respectively. The short-circuited stub is connected at the bend of inverted L antenna. Therefore the observation point is moved from the feed point to the bend. Therefore, the phase shift from A to B on the Smith chart is considered corre-

sponding to the length of antenna height. The normalized susceptance at B is *j*2.252. This susceptance is partially cancelled by the short-circuited stub. Consequently, the input admittance of BFIF antenna is shown at D. In order to match the input admittance, larger susceptance of short-circuited stub is needed as the antenna height becomes shorter. This is why the return loss larger than 10 dB is not satisfied in the case of h = 6 mm and Ls = 3.3 mm.

Next, the matching mechanism of the ULPIL antenna is discussed. Fig. 2.10 shows the base fed inverted L antenna. Fig. 2.11 shows the equivalent circuit of ULPIL antenna. The input impedance of base fed inverted L antenna (BFIL) is shown at A. The short-circuited stub seen to the base and the open-circuited stub seen to the antenna end are connected at the feed point B of ULPIL antenna. Therefore the observation point of the input impedance is moved from the base to the feed point.

(a) Base fed inverted L antenna (BFIL)

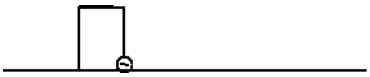

(b) Short-circuited stub (SS)

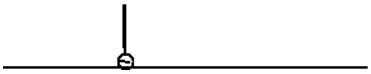

(c) Monopole antenna

Figure 2.7. Components of BFIF antenna.

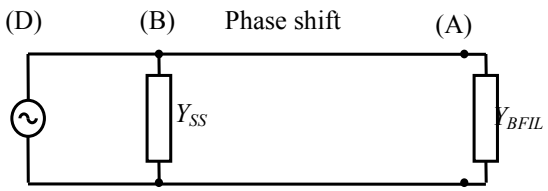

Figure 2.8. Equivalent circuit of BFIF antenna.

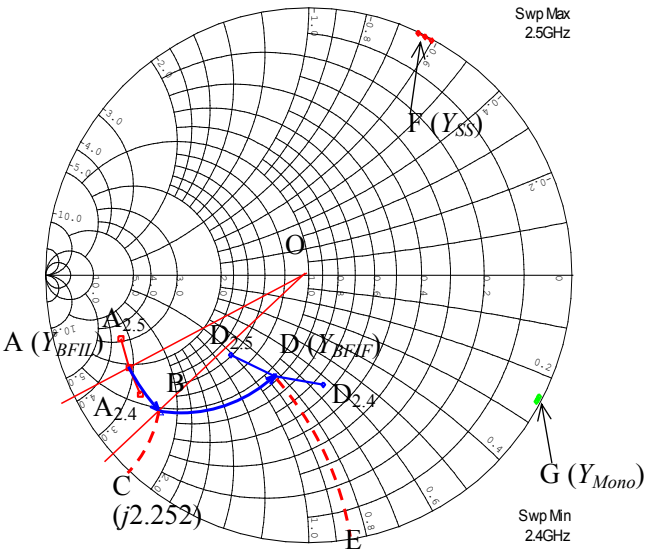

Figure 2.9. Impedance matching of BFIF antenna.

h=6mm, *L*=23.3mm, *Ls*=5mm, *pxp*=*pxm*=15mm, *pym*=10mm, *pyp*=44mm.

Figure 2.10. Base fed inverted L antenna (BFIL).

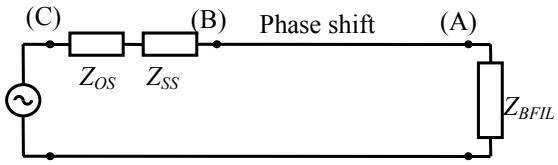

Figure 2.11. Equivalent circuit of ULPIL antenna.

Fig. 2.12 shows the how the input impedance is matched. The input impedance of base fed inverted L antenna and ULPIL antenna at the design frequency of 2.45 GHz are indicated as A and C, respectively. In the figure, the input impedances of base fed inverted L antenna at the frequency of 2.4 GHz and 2.5 GHz are indicated as $A_{2.4}$ and $A_{2.5}$, respectively. The input impedances of ULPIL antenna are also shown as $C_{2.4}$ and $C_{2.5}$. The phase shift from the base to the feed point of ULPIL antenna is shown as A to B in the Smith chart. At the feed point, the

short-circuited stub and the open-circuited stub are connected in series. The input impedance of two stubs is almost opposite phase to the input capacitance at B. Therefore, the input capacitance at B is cancelled by the two stubs connected in series. As a result, the input impedance of ULPIL antenna is matched to 50 Ω at C.

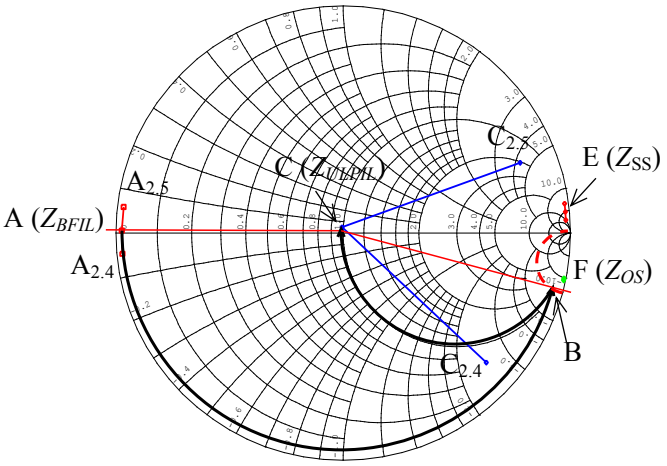

Figure 2.12. Impedance matching of ULPIL antenna. h=2mm, L=31.8mm, L_1=26.9mm, pxp=pxm=15mm, pym=10mm, pyp=44mm

2.4 Conclusion

The ULPIL antenna has been analyzed numerically and its characteristics have been compared with those of the BFIF antenna. The mechanism of impedance matching of these two antennas have been discussed. In the BFIF antenna, the short-circuited stub is connected in parallel with the base fed inverted L antenna. As the antenna height becomes shorter, the short-circuited stub with shorter length is needed. On the other hand, in the ULPIL antenna, the short-circuited stub seen to the base and the open-circuited stub seen to the antenna end are connected in series at the feed point. The input impedance of base fed inverted L antenna is compensated with two stubs. This means that the ULPIL antenna has a built-in automatic tuning circuit.

References Chapter-II

[1] J. D. Kraus: Antennas. New York: McGraw-Hill, pp. 425–427 and 461-467, 1988.

[2] C. A. Balanis: Antenna Theory Analysis and Design. New York: Wiley, pp. 175–180, 1997.

[3] S. A. Schelkunoff and H. T. Friis: Antennas Theory and Practice. New York: Wiley, 1952.

[4] A. Thumvicit, T. Takano and Y. Kamata: "Characteristics verification of a half-wave dipole very close to a conducting plane with excellent impedance matching", IEEE Trans. on Antennas and Propagat., vol.55, no.1, pp.53-58, Jan.2007.

[5] T. Yamashita and M. Taguchi: "Ultra Low Profile Inverted L Antenna on a Finite Conducting Plane", Proc. 2009 International Symp. on Antennas and Propagation, pp.361-364, Oct.2009.

[6] H. Attia, M. M. Bait-Suwalian and O. M. Ramahi, "Enhanced Gain Planar Inverted-F Antenna with Metamaterial Superstrate for UMTS Applications", *Proc. PIERS.,* Cambridge, USA, pp. 494-497, 2010.

[7] Z. N. Chen, K. Hirasawa, "A New Inverted F Antenna with a Ring Dielectric Resonator", IEEE Trans. On Vehicular Technology, Vol. 48, No. 4, pp. 1029-1032, 1999.

[8] D. Liu and B. P. Gaucher, "The inverted-F antenna height effects on bandwidth", Proc. IEEE Antenna Propag. Symp., Vol. 2A, pp. 367-370, 2005.

[9] D. Liu and B. P. Gaucher, "A branched inverted-F antenna for dual band WLAN applications", Proc. IEEE Int. Symp. Antenna Propagations, Vol.3, pp. 2263-2626, 2004.

[10] E. Rohadi and M. taguchi M. Taguchi, "Ultra Low Profile Antenna for 2.45 GHz Wireless Communications", Proc. 2012 IEEE Int. Conf. on Communication and Networks and Satellite, pp. 103-107, 2012.

[11] S. Schulteis, C. Waldschmidt, C. Kuhnert and W. Wiesbeck, “Design of a Capacitively Loaded Inverted F Antenna **for** Wireless-LAN Application**s**”, Proc. International ITG-Conference on Antennas, 178:187-190, 2003.

[12] K. Ito and T. Hose, “Study on the characteristics of planar inverted F antenna mounted in laptop computers for wireless LAN”, Proc. IEEE Int. Symp. Antennas Propag., Vol. 2, pp. 22-25, 2003.

[13] “WIPL-D Pro v11.0 3D Electromagnetic Solver Professional Edition User’s Manual”, WIPL-D, 2013.

[14] http://www.coax.co.jp/english/semi/219.html.

[15] D. M. Pozar, “Microwave Engineering”, Chapter 6, Addison-Wesley Publishing, Reading, MA, 1993.

III. Ultra Low Profile Antenna for 2.45 GHz Wireless Communications

3.1 Introduction

Recent technologies enable wireless communication devices to become physically smaller in size. Antenna size is obviously a major factor that limits miniaturization. In the few years, the designs of low-profile antennas for handheld wireless devices have been developed [1]. The low profile antennas do not extend very far from the surface they are mounted on.On the other hand, the height of previous antennas are $\lambda/10$ (λ: wavelength) or more. An example of low profile antennas is a base fed inverted L antenna. The input impedance of base fed inverted L antenna is close to that of the monopole antenna with reactance value due to additional horizontal section parallel to the antenna ground plane. It has a low resistance and high reactance characteristics. The degradation due to impedance mismatch can be recovered by feeding the antenna on the horizontal element.

Since the mismatch loss decreases radiation efficiency, it is desirable to modify the structure of the inverted L antenna to achieve a nearly resistive input impedance that is easily matched to a standard coaxial line. Reducing the antenna height has the disadvantage of reducing the bandwidth, but offers the advantages of smaller size and improved radiation characteristics.

The authors have proposed an ultra low profile, unbalanced fed inverted L antenna located very close on a rectangular conducting plane [2]. We may call this antenna as "ULPIL antenna" for convenience. This antenna consists of a coaxial cable. The inner conductor of the coaxial cable is extended from the end of outer conductor. Therefore, this antenna is excited at the end of outer conductor. The antenna height is around $\lambda/30$. This antenna is a horizontally polarized antenna. The length of horizontal element of this antenna is almost $\lambda/4$. The input impedance of this antenna is matched to 50 Ω by adjusting the position of feed point. When the size of conducting plane is 0.245 λ by 0.49λ, the return loss bandwidth less than -10 dB becomes 2.45 % and the directivity

is 4.24 dBi. In this antenna, the current flows on the conducting plane. Therefore the current on the horizontal element and on the conducting plane contribute to the radiation.

The inverted F antenna and planar inverted F antenna are well known as the other typical low-profile antennas. The inverted F antenna can be configured by bending a quarter wavelength monopole element mounted on a conducting plane into an L shape and by feeding at a point offset from the mounting point [3]. The inverted F antenna possesses good properties as required for wireless local area network application and mobile application at 2.45 GHz and it also provide a fairly return loss bandwidth [4, 5, 6, 7 and 8].

In this chapter, the ultra low profile, conventional base fed inverted F antenna (ULPIF antenna) on a rectangular conducting plane is numerically analyzed and its characteristics are compared with the previously proposed ULPIL antenna. The inverted F antenna in Figure 1(b) is identical to a transmission line antenna of length $h + L + Ls$ fed at the tap point (shorted element) Ls. Alternately, the configuration is treated as a small loop inductor, consisting of the feed probe and the inverted-L element behind the feed point, resonated with the capacitance of a horizontal wire above a ground plane. The addition of the element is done to simplify the input impedance settings. The elements may be extruded from the wire form to a planar form to realize an increase in impedance and gain bandwidth. However, a small degradation in gain may be seen [9].

In the numerical analysis, the electromagnetic simulator WIPL-D based on the method of moment is used. The method of moment is effective for analyzing the characteristics of antennas mounted on the portable radio equipment with the dimensions comparable to the wavelength. To improve the characteristics of the ULPIF antenna such as the impedance characteristics, the return loss bandwidth and the electric fields radiation pattern, the length of antenna element, the antenna height, the length of shorting element, and the size conducting plane are optimized [3, 10]. The advantages of the design of the antenna are the small size, the height less than $\lambda/10$ and the low cost material.

3.2 Analytical model

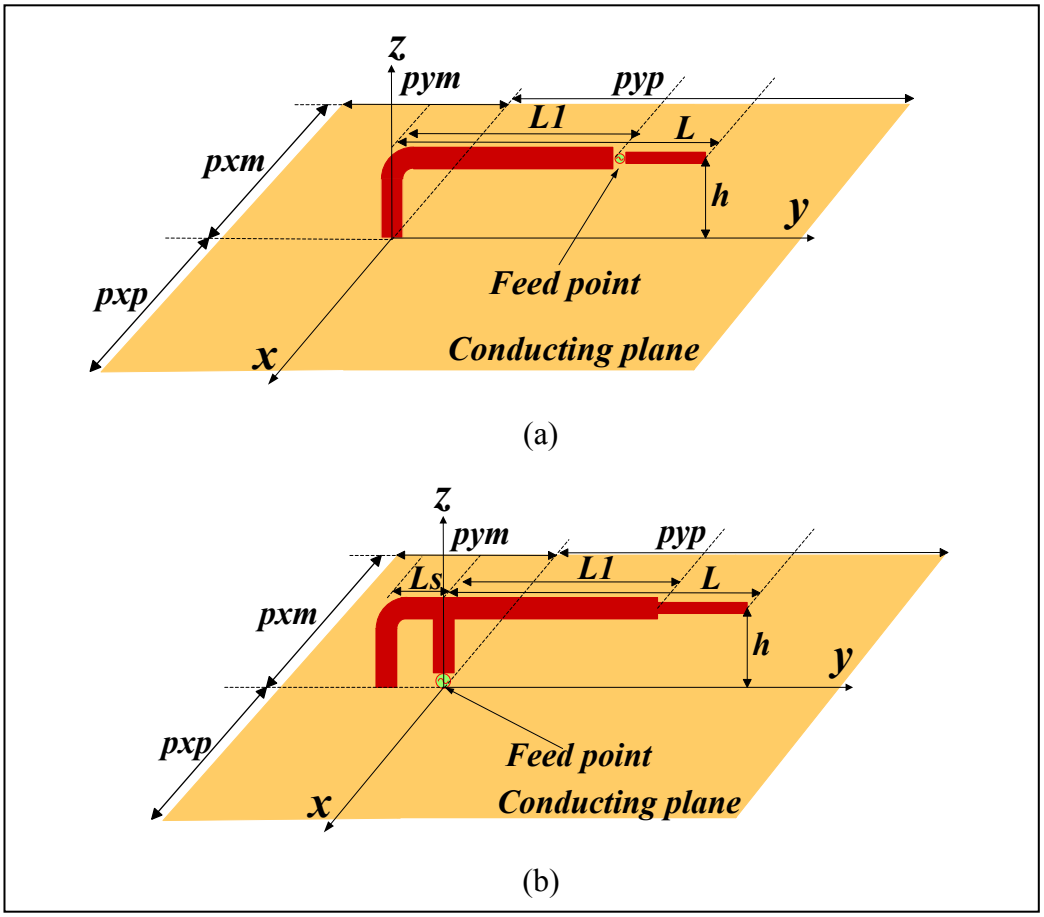

Figure 3. 1. The structure of Unbalanced fed Ultra Low Profile Inverted L Antenna (ULPIL Antenna) and Conventional base fed Ultra Low Profile Inverted F Antenna (ULPIF Antenna) on finite conducting plane.

Figure 3 . 1(a) shows the structure of the unbalanced fed ULPIL antenna located on a rectangular conducting plane, and Figure 3 . 1(b) shows the conventional base fed ULPIF antenna. The size of conducting plane is *pxp*+*pxm* by *pyp*+*pym*. The coaxial radiator is mounted on the conducting plane. The radius of the outer conductor is 1.095 mm and that of the inner conductor is 0.255 mm. The inner conductor of the coaxial cable is extended from the end of outer conductor, this antenna is excited at the end of outer conductor. The height *h* of antenna is from 5 mm to 12 mm, and the length *Ls* of shorted antenna element is from 3.3 mm to 10mm. The length of horizontal elements *L* and

L1 are optimized. The design frequency is 2.45 GHz. The wavelength λ at 2.45 GHz is 122.45 mm. The size of conducting plane is considered as 20.8 mm by 60 mm. At the design frequency of 2.45 GHz, the size of conducting plane becomes 0.17 λ by 0.49λ.

3.3 Results and discussion

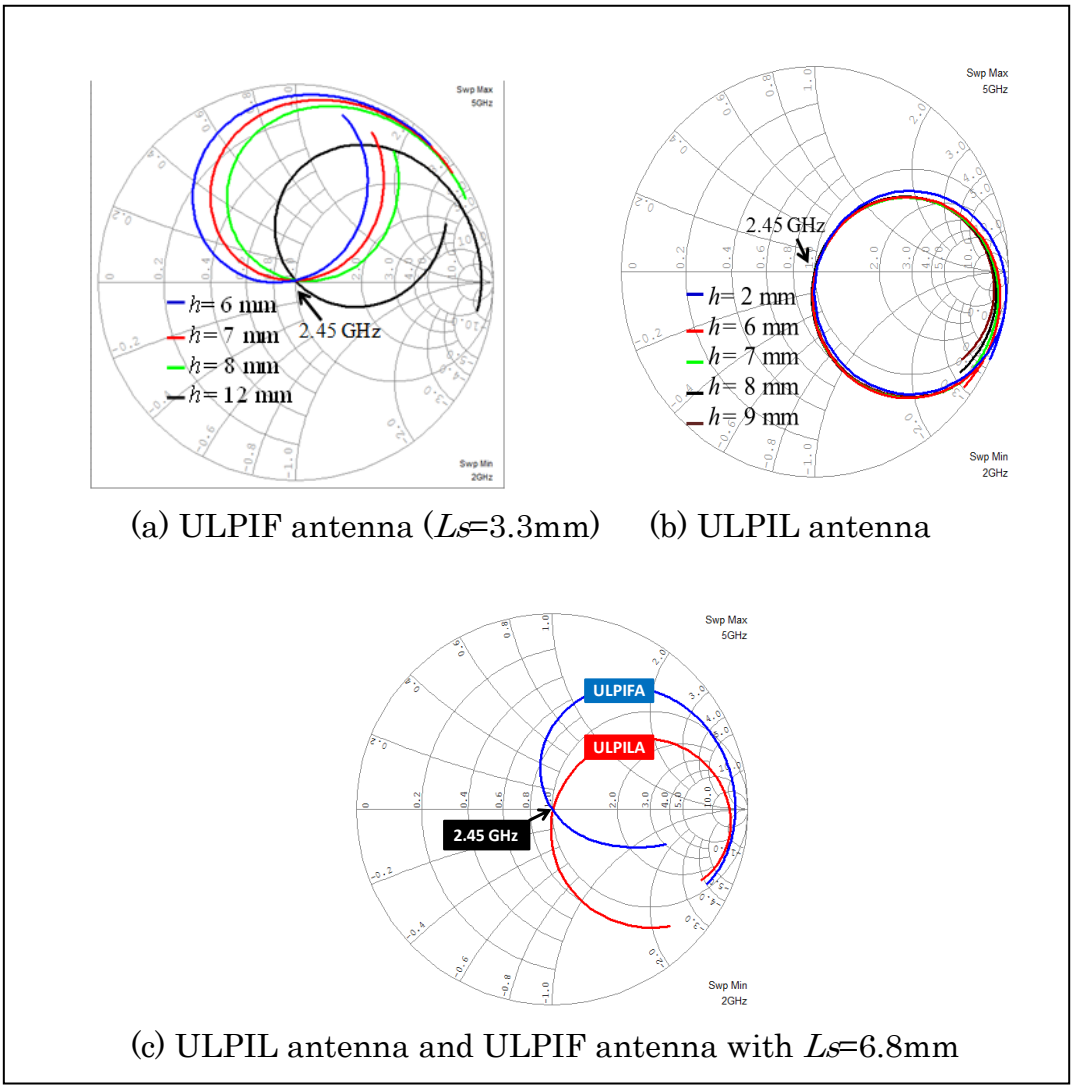

(a) ULPIF antenna (*Ls*=3.3mm) (b) ULPIL antenna

(c) ULPIL antenna and ULPIF antenna with *Ls*=6.8mm

Figure 3.2. Input impedance characteristics of Unbalanced fed ULPIL antenna and Conventional base fed ULPIF antenna (*Ls*=6.8 mm).

In the ULPIF antenna, the addition of the extra inverted *L* element behind the feed point tunes the input impedance of the antenna. To obtain the impedance of 50 Ω, the length of horizontal elements *L, L1,* and shorted element *Ls* must be adjusted, while considering the current distribution on the conducting plane by adjusting its size. For ULPIF antenna, the impedance is adjusted by also changing the antenna height *h*, otherwise the size of finite conducting plane may be not changed [3].

3.3.1 Impedance and Electric field radiation pattern characteristics

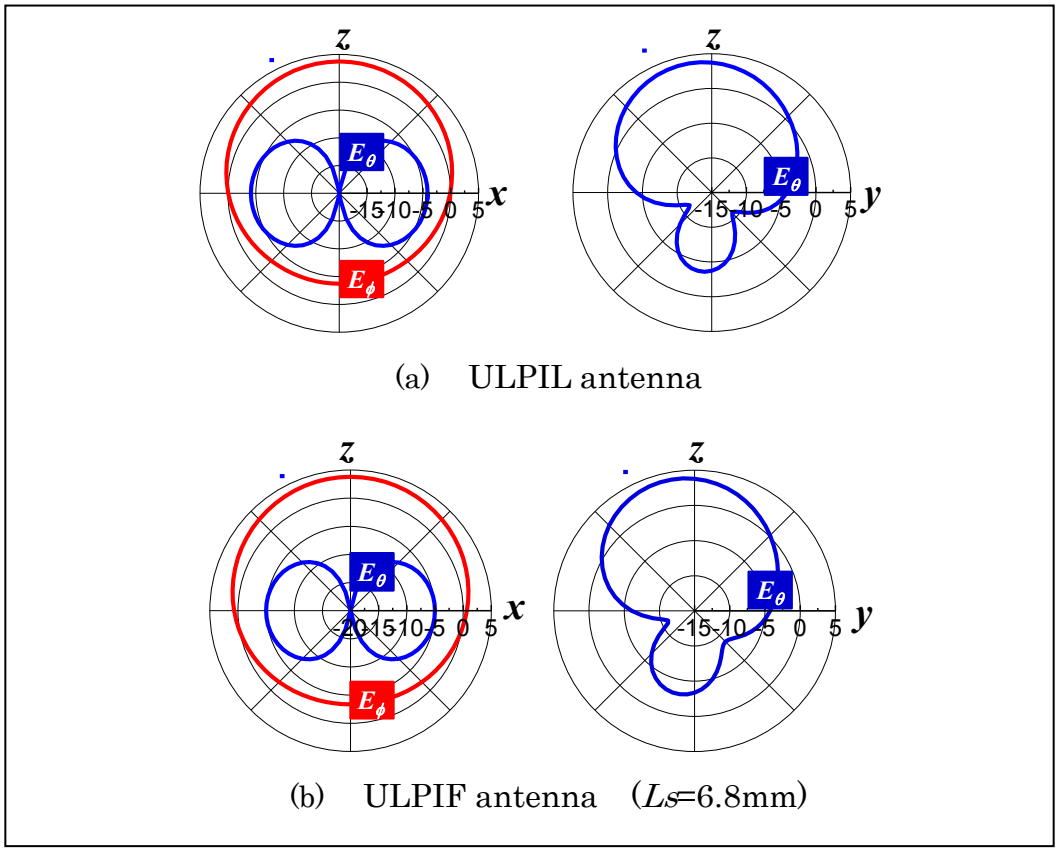

Figure 3.3. Electric field radiation patterns of Unbalanced fed ULPIL antenna and Conventional base fed ULPIF antenna (*Ls*=6.8 mm) at 2.45 GHz

Figure 3.3 (a) illustrates how the calculated input impedance of an ULPIF antenna changes when the antenna height *h* is altered while the length of shorted

antenna element is fixed as *Ls* = 3.3 mm. Figure 3 . 2 (b) shows the calculated input impedance of ULPIL antenna with different antenna height *h*.

Figure 3 . 2 (c) shows the calculated input impedance of ULPIF antenna with antenna height *h* = 10 mm, length of horizontal antenna elements *L* = 26.6 mm and *L1* = 14 mm, the shorted antenna element *Ls* = 6.8 mm, the size of conducting plane is 20.8 mm by 60 mm and ULPIL antenna with antenna height *h* = 10 mm, length of horizontal antenna elements *L* = 27 mm and *L1* = 10.2 mm, and the size of conducting plane is 30 mm by 60 mm.

In Figure 3.2(c), the length of shorted antenna element *Ls* is extended to 6.8 mm for the ease of fabrication.

The energy radiated by the antenna in a particular direction is m easured in terms of field strength at a point which is at a particular distance from antenna. The radiation pattern of the antenna is a graph which shows the variation of actual field strength of electromagnetic field at all points which are at equal distance from antenna [12].

Figure 3 . 3 (a) shows the computed electric field radiation patterns of ULPIL antenna and Figure 3 . 3 (b) shows the computed electric field radiation patterns of the base fed ULPIF antenna. The calculation condition are antenna height *h* = 10 mm, horizontal antenna elements *L* = 26.6 mm and *L1* = 14 mm, shorted element *Ls* = 6.8 mm, and the size of conducting plane is 20.8 mm by 60 mm and ULPIL antenna with antenna height *h* = 10 mm, horizontal elements *L* = 27 mm and *L1* = 10.2 mm, and the size of conducting plane 30 mm by 60 mm. From these figures it is clear that the antenna will give desired radiation characteristics.

The vertically polarized gain of the ULPIF antenna is maximum in the equatorial plane with a vertical null in the z direction. There is not a null in the y-z plane due to currents on the horizontal antenna elements. The maximum directivities in the z direction are 3.88 dBi for ULPIL antenna and 3.94 dBi for ULPIF antenna. The vertically directed currents on the ULPIF antenna cause a cross polarization component in the x-z plane.

3.3.2. Returns Loss Bandwidth Characteristics

Table 3.1 Return loss band width and directive gain of conventional base fed ULPIF antenna for different *h* and *Ls.*

h [mm]	Ls [mm]	L [mm]	L1 [mm]	Return Loss Bandwidth [%]	Directive gain at 2.45 GHz[dBi]
12	3.30	24.10	15.60	11.84	3.44
	6.00	24.40	16.10	14.29	3.53
	7.00	24.40	16.20	14.69	3.54
	10.00	24.40	16.20	13.88	3.47
11	3.30	24.70	16.00	12.24	3.58
	6.00	25.10	16.30	13.88	3.67
	10.00	25.30	16.40	11.02	3.62
10	3.30	25.10	17.00	11.43	3.69
	6.00	25.60	17.10	11.84	3.78
	10.00	25.90	17.30	5.71	3.74
9	3.30	26.50	13.10	9.80	3.88
	6.00	26.80	13.10	8.57	3.97
	8.00	27.00	13.20	4.49	3.99
	9.00	27.00	13.30	N/A	3.98
8	3.30	27.10	13.30	7.76	3.98
	6.00	27.40	13.40	2.04	4.08
	7.00	27.50	13.50	N/A	4.09
7	3.30	27.80	13.60	5.71	4.08
	4.00	27.80	13.70	4.08	4.12
	5.00	27.90	13.70	N/A	4.16
6	3.30	28.40	14.30	2.45	4.17
	4.00	28.40	14.30	N/A	4.20
5	3.30	29.10	14.80	N/A	4.25

Table 3.1 shows the calculated return loss bandwidth less than -10 dB and the directive gain of ULPIF antenna in the z direction by adjusting the antenna height *h* and length of shorted antenna element *Ls.* Since the height of ULPIF antenna is reduced, the shorted element becomes narrower.

Table 3.2 shows the calculated return loss bandwidth of ULPIL antenna and the directive gain in the z direction for different antenna height *h*. The

parameters of horizontal antenna element *L* and *L*1 are optimized to match the input impedance to 50 Ω at the frequency of 2.45 GHz.

Table 3.2 Return loss band width and directive gain of unbalanced fed ULPIL antenna for different *h*.

h [mm]	L [mm]	L1 [mm]	Return Loss Bandwidth			Directive gain at 2.45 GHz [dBi]
			f_low [GHz]	f_high [GHz]	%	
6	29.9	18.3	2.4	2.51	4.490	4.09
7	29.4	16.4	2.38	2.52	5.714	4.00
8	28.3	14.3	2.36	2.56	8.163	3.94
9	27.9	12.3	2.35	2.56	8.571	3.84
10	27.0	10.2	2.34	2.57	9.388	3.88

Table 3.3 Return loss band width and directive gain of conventional base fed ULPIF antenna for different *h* (*Ls=6.8mm*).

h [mm]	L [mm]	L1 [mm]	Return Loss Bandwidth			Directive gain at 2.45 GHz [dBi]
			f_low [GHz]	f_high [GHz]	%	
6	28.5	17.0	2.12	2.67	22.45	3.79
7	28.1	16.0	2.19	2.63	17.96	3.83
8	27.6	15.6	2.18	2.64	18.78	3.92
9	27.0	15.2	2.22	2.63	16.74	3.95
10	26.6	14.0	2.24	2.63	15.92	3.94

Table 3.3 shows the calculated return loss bandwidth and the directive gain in the z direction of the conventional base fed ULPIF antenna for different antenna height *h*. The shorted element *Ls* is fixed as 6.8 mm. When the antenna height *h* is 10 mm, the directive gain of ULPIF antenna becomes larger than that of ULPIL antenna. This may be due to that the total length of horizontal element of the ULPIF antenna *L+L1 + Ls* is a little bit longer than that of ULPIL antenna.

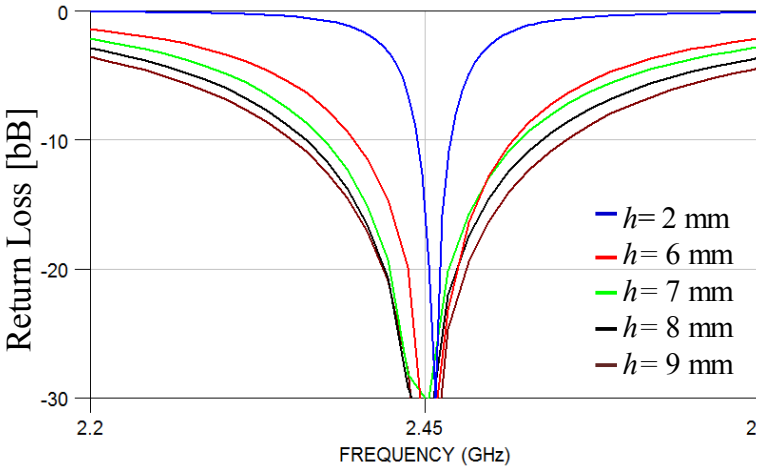

(a) ULPIL antenna

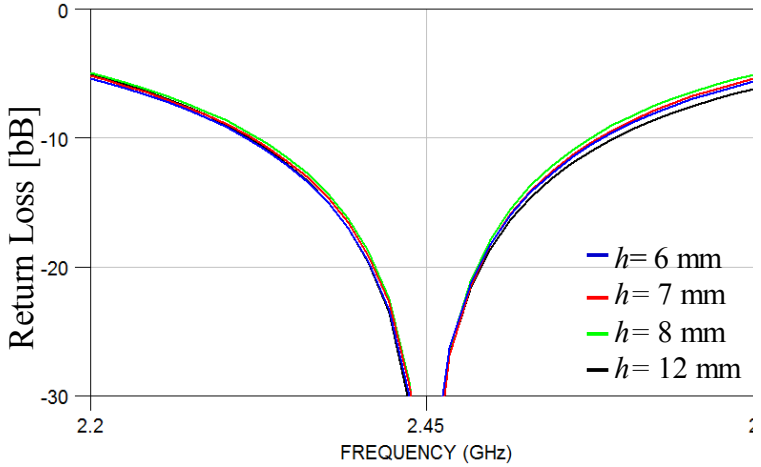

(b) ULPIF antenna (*Ls*=3.3mm)

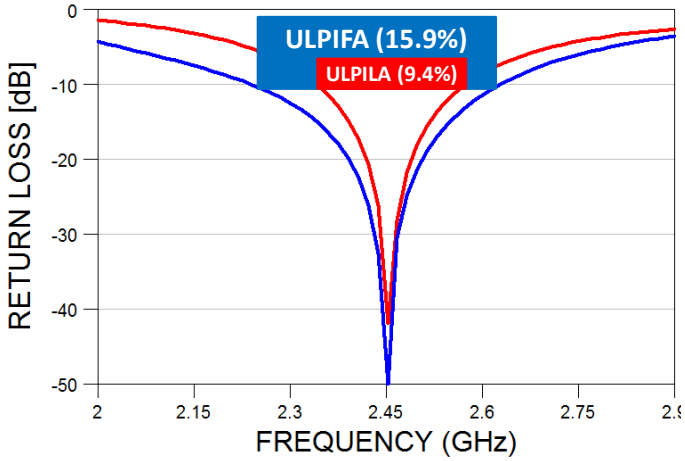

(c) ULPIL antenna and ULPIF antenna-*Ls*=6.8mm

Figure 3.4. Return Loss Characteristics of Unbalanced fed ULPIL antenna and Conventional base fed ULPIF antenna at 2.45 GHz.

Figure 3.4 (a) shows the calculated return loss characteristics of ULPIL antenna for different antenna height *h*. Figure 3.4 (b) shows the return loss characteristics of ULPIF antenna. The lengths of shorted element *Ls* and antenna height *h* are adjusted. Figure 3.4 (c) shows the calculated return loss characteristics of ULPIF antenna with antenna height h = 10 mm, horizontal antenna elements L = 26.6 mm and $L1$ = 14 mm, shorted element Ls = 6.8 mm, and the size of conducting plane is 20.8 mm by 60 mm and ULPIL antenna with antenna height h = 10 mm, horizontal elements L = 27 mm and $L1$ = 10.2 mm, and the size of conducting plane 30 mm by 60 mm.

As the antenna height of the ULPIL antenna becomes higher, the upper frequency of the return loss bandwidth less than -10 dB increases and the lower frequency decreases. On the other hand, the return loss characteristics of the ULPIF antenna is almost same for different antenna height for shorted element *Ls* of 3.3 mm.

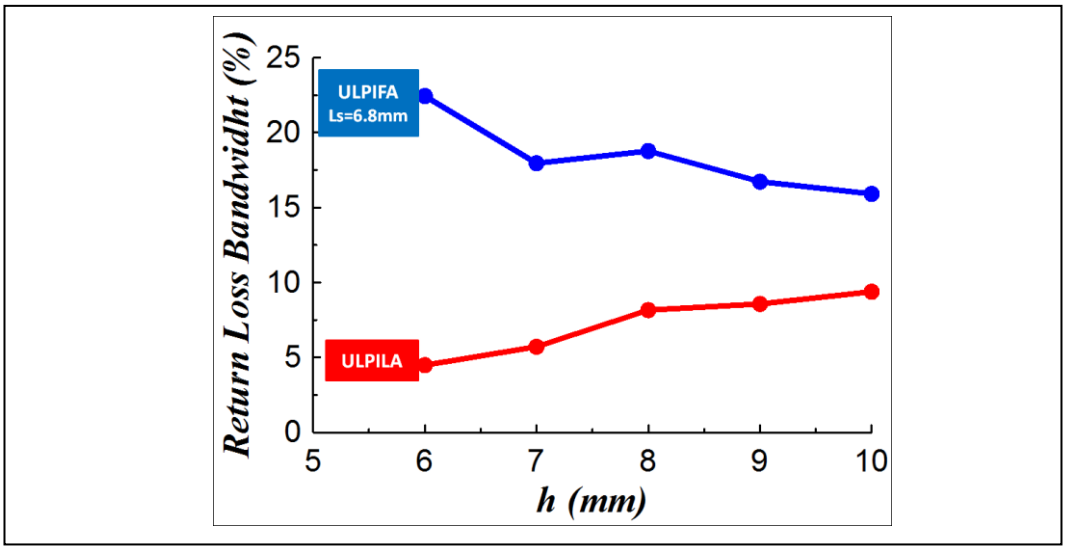

Figure 3.5. Return Loss Bandwidth of Unbalanced fed ULPIL antenna and Conventional base fed ULPIF antenna (*Ls*=6.8 mm) at 2.45 GHz.

The directive gain becomes larger as the antenna height *h* becomes lower when the minimum length of shorted element *Ls* is 3.3 mm while the minimum

height *h* of this antenna is 6 mm. On the other hand, its return loss bandwidth becomes narrow.

Figure 3.5 shows the calculated return loss bandwidth with different antenna height *h* of ULPIF antenna with shorted antenna element *Ls* = 6.8 mm and ULPIL antenna. The ULPIF antenna has smaller mutual coupling between currents on the antenna and on the conducting plane. On the ULPIL antenna, the stronger coupling occurs between the currents on the antenna element on the conducting plane and its bandwidth is narrower than ULPIF antenna.

3.4 Conclusion

The ultra low profile, base fed inverted F antenna (ULPIF antenna) on a rectangular conducting plane has been analyzed numerically. The calculated return loss and the directive gain of this antenna has been compared with those of the unbalanced fed ULPIL antenna. The directive gain of ULPIF antenna is higher than that of ULPIL antenna. When the size of conducting plane is 0.17 λ by 0.49λ and antenna height is 0.08 λ, the return loss bandwidth less than -10 dB becomes 15.92 % and the directivity is 3.94 dBi. The antenna height is less than 0.1 λ, this may be promising as the base station antenna or mobile terminal antenna of the wireless communication system. The proposed antenna will be validated through measurement.

References Chapter - III

[1] Douglas B. Miron, *"Small Antenna Design*", Communication Engineering Series, pp. 2-5, Elsevier Inc. Burlington, USA 2006.

[2] T. Yamashita and M. Taguchi, "*Ultra Low Profile Inverted L Antenna on a Finite Conducting Plane*", Proceedings of the 2009 International Symposium on Antennas and Propagation, pp.361-364, Oct. 2009.

[3] K. Fujimoto, A. Henderson, K. Hirasawa and J. R. James, *Small Antennas*, pp.116-151, 160-161, Research Studies Press, Letchworth, 1987.

[4] Y. Rahmat-Samii and Z. Li, Handset communication antenna, including human interactions, in *Wireless Network: From Physical Layer to Communication, Computing, Sensing and Control*, G. Franceschetti and S. Stonelli (Eds.), Academic Press, New York, 2006.

[5] Y. X. Guo, M. Y. W Chia, and Z. N. Chia, "Miniature built-in multiband antennas for mobile handset", *IEEE Trans. on Antennas Propagation,* vol. 52, pp 1936-1944. August 2004.

[6] G. Y. Lee and K. L. Wong, " Very low profile bent planar monopole antenna for GSM/ DCS dual-band mobile phone", *Microwave and Optical Technology Letters*, Vol. 34, No. 6 September, 2002.

[7] D. Liu and B. P. Gaucher, The inverted-F antenna height effects on bandwidth, *Proc. IEEE Antenna Propag. Symp.*, Vol. 2A, pp. 367-370, July 2005.

[8] C. Rowell, A brief survey of internal antennas in GSM phones: 1998 to 2004, Proc. *UNSC/URS/National Radio Science Meeting*, July 2005.

[9] T. Taga, Analysis of planar inverted-F antennas and antenna design for portable radio equipment, in *Analysis, Design, and Meauserement of Small and Low-Profile Antenna*, K. Hirasawa and M. Haneishi (Eds.), Arctech House, Norwood, MA, 1992.

[10] WIPL-D d.o.o.: http://www.wipl-d.com/, WIPL-D Pro v7.0, 2008.

[11] Kazuhiro Hirasawa, Misao Haneishi: *Analysis, Design, and Measurement of Small and Low-Profile Antennas,* pp. 165-169, Artech house, Inc. 1992.

[12] Constantine A Balanis., "*Antenna Theory Analysis and Design*." 3rd ed., pp. 873, 1021-1023, Hoboken, NJ, John Willey & Sons. Inc., 2005

IV. Ultra Low Profile, Unbalanced Fed Inverted F Antenna for 2.45 GHz Wireless Communication System

4. 1 Introduction

The small and low-profile antenna for the miniaturization of communication equipment is needed for mobile communication systems. The low profile antennas do not extend very far from the surface they are mounted on. The well known low profile antenna is inverted F antenna for its abilities to allow a simplify impedance matching and to controlling both the return loss bandwidth and directive gain [1]. The inverted F antenna possesses good properties as required for wireless local area network application and mobile applications and it also provide a fairly return loss bandwidth. For further information refer to [2], [3], [4], [5] and [6]. In this chapter, the ultra low profile, unbalanced fed inverted F antenna is proposed and its characteristics are compared with the previous proposed low profile unbalanced inverted L antenna which is located very close on rectangular conducting plane [7] and [8]. Measured trough the fabrication is needed to validate its calculation characteristics. The proposed ultra low profile, unbalanced inverted F antenna, and then we called ULPIF for the convenience. In the numerical analysis, the electromagnetic simulator "WIPL-D" is used [9].

4.2 Analytical Model

The unbalanced fed inverted F antenna is identical to a transmission line antenna of length $h + L + Ls \approx \lambda/4$. Alternately, the configuration is treated as a small loop inductor, consisting of the feed probe and the inverted L element behind the feed point, resonated with the capacitance of a horizontal wire above a ground plane, shown by Fig. 1. The sum of horizontal elements, *L, Ls* and the height antenna effects to the resonant frequency of the antenna. If the antenna height *h* is low, a capacitive coupling between conducting plane

and the upper part of antenna occurs; hence the total length of horizontal element can be reduced. The length of short stub *Ls* has no effect onto the resonant frequency but to the input Impedance [10].

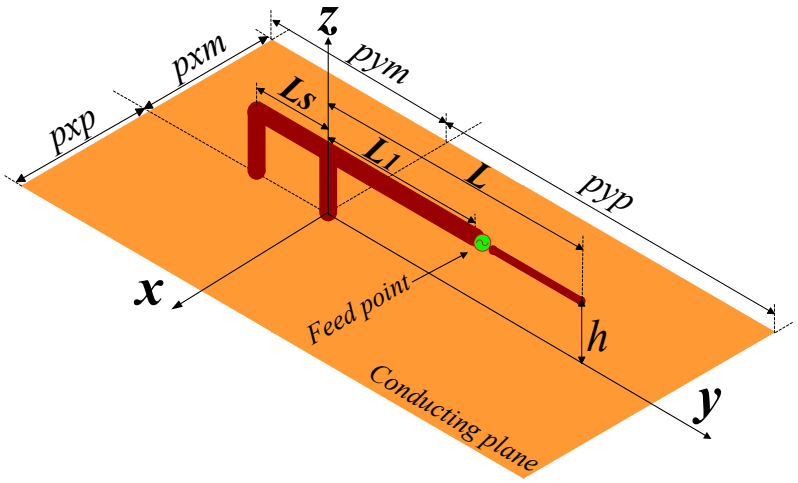

Fig. 4.1. Structure of the proposed ULPIF

Fig. 4.1 shows the structure of the proposed ULPIF antenna located on a rectangular conducting plane (*pxp*+*pxm* by *pyp*+*pym*) and its size is fixed as *pxp*=*pxm*=15mm, *pyp*=43.2mm and *pym*=16.8mm when the length of short stub *Ls* is 6.8mm. The coaxial radiator is mounted on the conducting plane. The radius of the outer conductor is 0.8 mm and that of the inner conductor is 0.16 mm. The inner conductor of the coaxial cable is extended from the end of outer conductor. Therefore, this antenna is excited at the end of outer conductor. The height of horizontal element is *h*. The design frequency is 2.45 GHz. The wavelength λ at 2.45 GHz is 122.45 mm.

4.3 Results and discussion

The ULPIF antenna is analyzed by adjusting the antenna height *h*. The limitation maximum *h* is 1/10 λ (wavelength). The heights *h* are 6mm, 8mm and 10 mm for the calculation analysis. The length of short stub *Ls* is adjusted in order to enhance the antenna gain even though it has limitation when the horizontal antenna very closed to the conducting plane. The length of horizontal

antenna *L1* is adjusted in order to tune at the frequency design, on the other hand other horizontal *L* is adjusted due to impedance matching 50 Ohm. The length of horizontal elements *L* and *L1* are increased by reducing the antenna height.

Table 4.1 shows the calculated return loss bandwidth and the directive gains in the z direction of ULPIL antenna, ULPIF antenna and low profile conventional base fed inverted F (Base Fed IF) antenna for different antenna height *h*. The directive gain of ULPIF antenna is larger than that of ULPIL antenna. This may be due to that the total length of horizontal element of the ULPIF antenna *L*+*L1* + *Ls* is a little bit longer than that of ULPIL antenna. When the height h is 0.08λ, the total length element of ULPIF and ULPIL are 0.34 λ and 0.3λ, respectively. The base fed IF antenna has wider the bandwidth antenna and smaller gain than the ULPIF. Increasing the antenna height decreases the total of horizontal element. The calculation results indicate the antenna return loss bandwidth increases nearly linearly with the antenna height; on the other hand the directivity reduces.

Table 4,1 Return loss bandwidth and directive gain of ULPIL and ULPIF antenna for different height of antenna at 2.45 GHz.

h	*L*	*L1*	Return Loss Bandwidth			Directive Gain at 2.45 GHz [dBi]
[mm]			f-low [GHz]	f-high [GHz]	%	
ULPIL			2.40	2.50	4.08	4.03
6	29.7	18.3				
8	28.4	14.2	2.38	2.53	6.12	3.88
10	26.8	10.0	2.35	2.55	8.16	3.68
ULPIF, *Ls*=6.8 mm			2.41	2.50	3.67	4.15
6	30.0	19.2				
8	29.1	15.2	2.38	2.52	5.71	4.03
10	27.8	11.1	2.46	2.55	7.76	3.85
Base Fed IF,			2.15	2.64	20.00	3.67
6	29.0	17.2				
8	28.1	15.8	2.22	2.61	15.92	3.76
10	27.0	14.6	2.27	2.61	13.88	3.76

Table 4 . 2 shows the calculated return loss bandwidth of ULPIF antenna and the directive gain in the z direction for different length of short stub *Ls* and antenna height *h* when the size conducting plane *pxp*=*pxp*=15mm by *pym*=16.8mm + *pyp*=42.2 mm at 2.45 GHz The length of short stub *Ls* can be reduced due to the antenna gain enhancement, on the other hand the bandwidth antenna little bit becomes narrower. The Ls adjustment almost doesn't affect on the length of horizontal elements *L* and *L1*.

Table 4,2 Return loss bandwidth and directive gain of ULPIL and ULPIF antenna for different height and length short stub of antenna at 2.45 GHz

Ls	*L*	*L1*	Return Loss Bandwidth			Directive Gain at 2.45 GHz [dBi]
[mm]			f-low [GHz]	f-high [GHz]	%	
h=6mm			2.40	2.50	4.08	4.18
4	30.4	18.8				
5.6	30.1	19.0	2.40	2.50	4.08	4.17
6.8	30.0	19.2	2.41	2.50	3.67	4.15
8	29.9	19.2	2.41	2.50	3.67	4.13
h=8mm			2.38	2.53	6.12	4.05
4	29.1	15.0				
5.6	29.1	15.0	2.38	2.53	6.12	4.04
6.8	29.1	15.2	2.38	2.52	5.71	4.03
8	29	15.5	2.38	2.52	5.71	4.00
h=10mm			2.35	2.56	8.57	3.88
4	27.8	10.9				
5.6	27.8	11.0	2.36	2.56	8.16	3.87
6.8	27.8	11.1	2.36	2.55	7.76	3.85
8	27.7	11.3	2.36	2.55	7.76	3.82

Figure 4.2a and Figure 4.2b show the calculated input impedance and return loss characteristics result between ULPIF (*h*=10mm, *Ls*=6.8mm, *pxp*=*pxm*=15mm, *pym*=16.8mm, *pyp*=43.2mm), ULPIL (*h*=10mm, *pxp*=*pxm*=15mm, *pym*=10mm, *pyp*=50mm) and Base Fed IF antenna (*h*=10mm, *Ls*=6.8mm, *L1*+*Ls*=21.4mm, *L*+*Ls*=33.8mm, *pxp*=*pxm*=10.4mm, *pym*=16.8mm, *pyp*=43.2mm).

Figure 4.2c and Figure 4.2d show comparison return loss bandwidth and the directive gain between ULPIL (*pxp*=*pxm*=15mm, *pym*=10mm, *pyp*=50mm),

ULPIF (*Ls*=6.8mm, *pxp*=*pxm*=15mm, *pym*=16.8mm, *pyp*=43.2mm) with different *h* at 2.45 GHz and Base Fed IF antenna (*h*=10mm, *Ls*=6.8mm, *L1*+*Ls*=21.4mm, *L*+*Ls*=33.8mm, *pxp*=*pxm*=10.4mm, *pym*=16.8mm, *pyp*=43.2mm). The antenna bandwidth increases linearly, by increase the antenna height. Figure 4.3 shows the directive gain of ULPIF antenna (*h*=10mm, *pxp*=*pxm*=15mm, *pym*=16.8mm, *pyp*=43.2mm) by investigate on length of short stub *Ls*.. Figure 4.4a shows the photograph of fabricated ULPIF antenna. Figure 4.4b and Figure 4.4c show the return loss and the input impedance characteristics of the ULPIF antenna, respectively. In the calculation the parameters are *h*=10mm, *Ls*=6.8mm, *L1*+*Ls*=17.9mm, *L*+*Ls*=34.6mm, *pxp*=*pxm*=15mm, *pym*=10mm, *pyp*=50mm and in the measurement are *h*=10mm, *Ls*=6.6mm, *L1*+*Ls*=17.1mm, *L*+*Ls*=34.1mm, *pxp*=*pxm*=15mm, *pym*=16.8mm, *pyp*=43.2mm. The measured results are agree well with the calculated results..

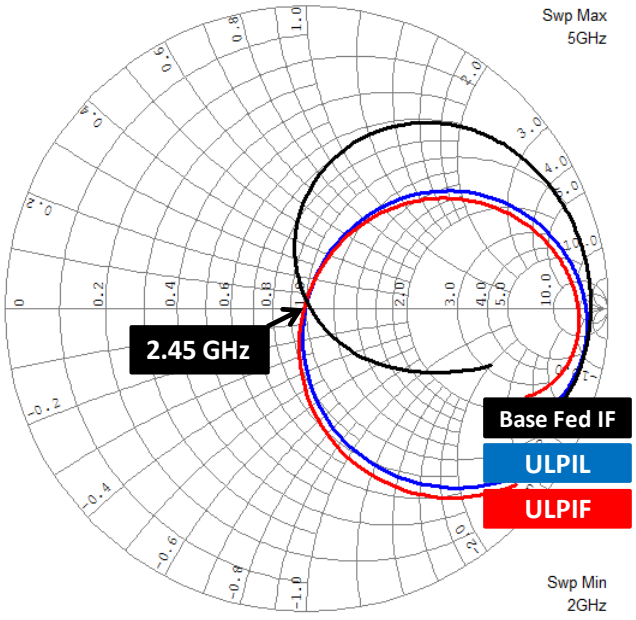

Fig. 4.2a. Input Impedance characteristic of ULPIL (*h*=10mm, *pxp*=*pxm*=15mm, *pym*=10mm, *pyp*=50mm), ULPIF (*h*=10mm, *Ls*=6.8mm, *pxp*=*pxm*=15mm, *pym*=16.8mm, *pyp*=43.2mm) and Base Fed IF antenna (*h*=10mm, *Ls*=6.8mm, *L1*+*Ls*=21.4mm, *L*+*Ls*=33.8mm, *pxp*=*pxm*=10.4mm, *pym*=16.8mm, *pyp*=43.2mm).

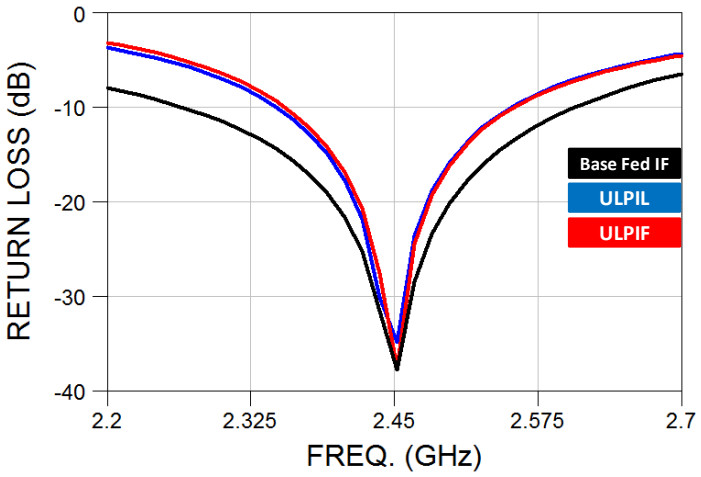

Fig. 4.2b. Return Loss characteristic of ULPIL (*h*=10mm, *pxp*=*pxm*=15mm, *pym*=10mm, *pyp*=50mm) ULPIF (*h*=10mm, *Ls*=6.8mm, *pxp*=*pxm*=15mm, *pym*=16.8mm, *pyp*=43.2mm) and Base Fed IF antenna (*h*=10mm, *Ls*=6.8mm, *L1*+*Ls*=21.4mm, *L*+*Ls*=33.8mm, *pxp*=*pxm*=10.4mm, *pym*=16.8mm, *pyp*=43.2mm).

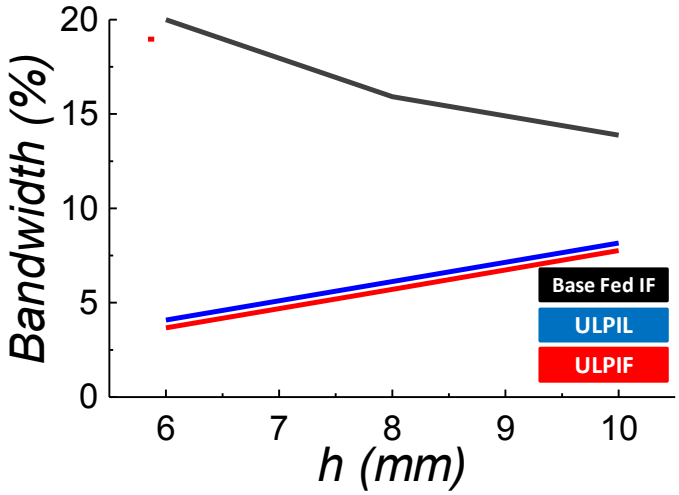

Fig. 4.2c. Comparison the return loss bandwidth between ULPIL, ULPIF and Base Fed IF antenna with different *h* at 2.45 GHz.

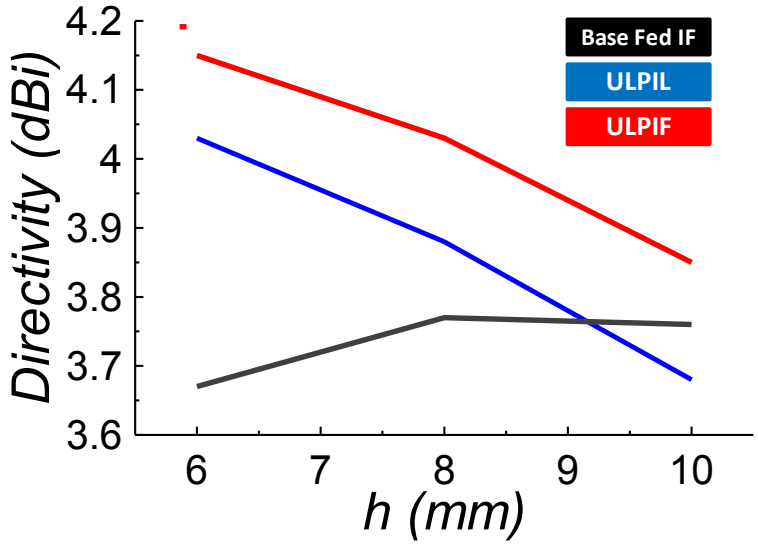

Fig. 4.2d. Comparison the directive gain between ULPIL, ULPIF and Base Fed IF antenna with different *h* at 2.45 GHz.

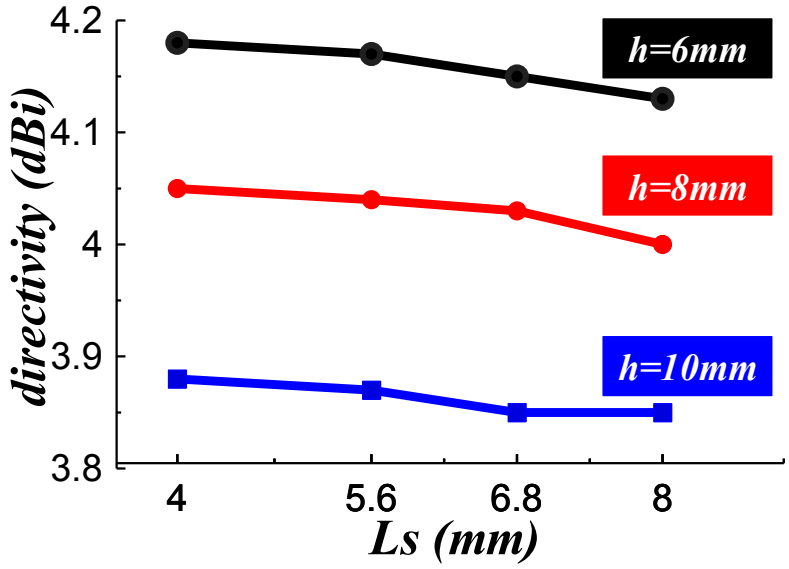

Fig.4.3. The directive gain of ULPIF at 4.25GHz (*pxp*=*pxm*=15mm, *pym*=16.8mm, *pyp*=43.2mm) with different *Ls*.

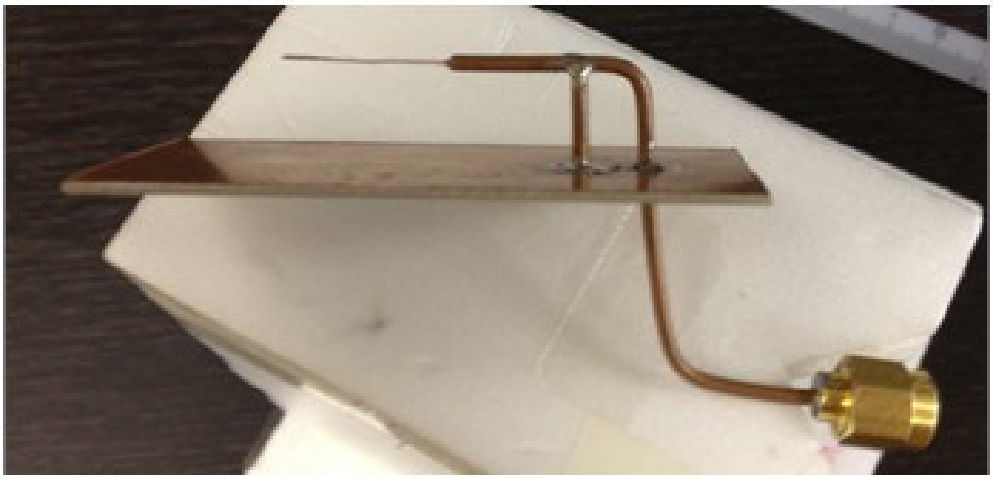

Fig. 4.4a. The photograph of fabricated ULPIF antenna (h=10mm, Ls=6.6mm, $L1$+Ls=17.1mm, L+Ls=34.1mm, pxp=pxm=15mm, pym=16.8mm, pyp=43.2mm).

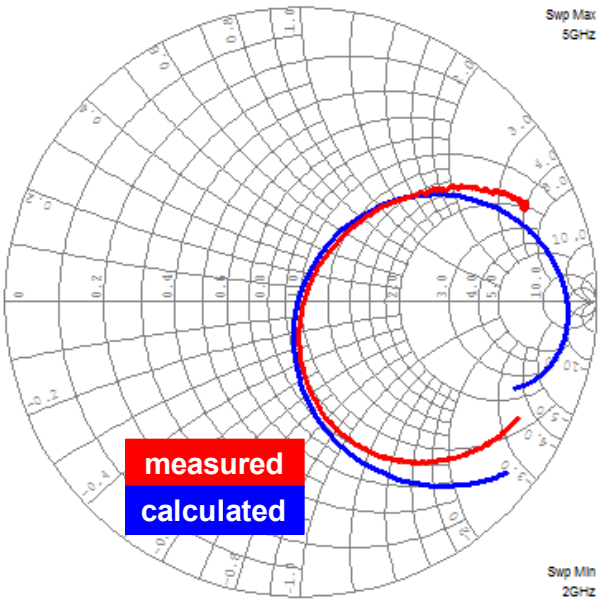

Fig. 4.4b. Input Impedance characteristic of ULPIF (Calculation; h=10mm, Ls=6.8mm, $L1$+Ls=17.9mm, L+Ls=34.6mm, pxp=pxm=15mm, pym=16.8mm, pyp=43.2mm) and (Measurement; h=10mm, Ls=6.6mm, $L1$+Ls=17.1mm, L+Ls=34.1mm, pxp=pxm=15mm, pym=16.8mm, pyp=43.2mm).

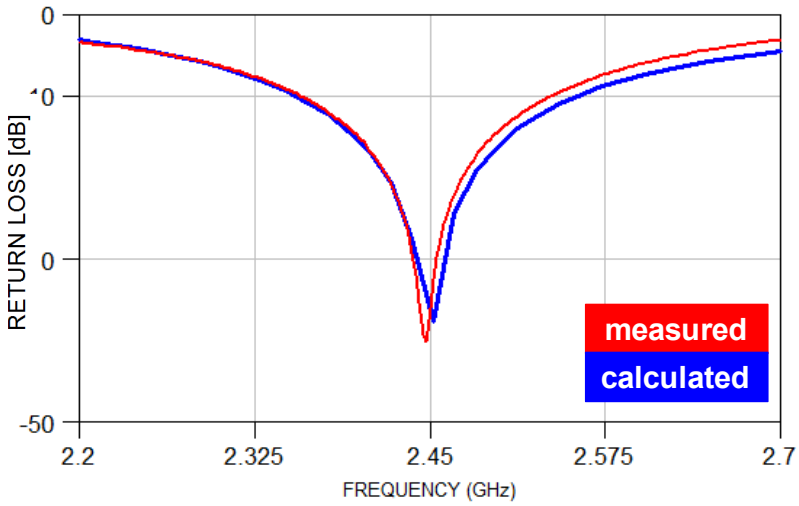

Fig. 4.4c. Return Loss characteristic of ULPIF (Calculation; *h*=10mm, *Ls*=6.8mm, *L1*+*Ls*=17.9mm, *L*+*Ls*=34.6mm, *pxp*=*pxm*=15mm, *pym*=10mm, *pyp*=50mm) and (Measurement; *h*=10mm, *Ls*=6.6mm, *L1*+*Ls*=17.1mm, *L*+*Ls*=34.1mm, *pxp*=*pxm*=15mm, *pym*=16.8mm, *pyp*=43.2mm).

4.4 Conclusion

The ULPIF antenna on a rectangular conducting plane has been proposed. The return loss and the directive gain of this antenna have been compared with those of the base fed inverted F antenna and the ULPIL antenna. The d irective gain of proposed antenna is higher than that of base fed inverted F antenna. When the size of conducting plane is 0.245 λ by 0.49 λ and antenna height is λ/20, the return loss bandwidth less than -10 dB becomes 3.67 % and the directive gain is 4.15 dBi. The measurement results are agree well with the calculation results. This ULPIF antenna may be promising as the base station antenna or mobile terminal antenna of the wireless communication system.

References Chapter - IV

[1] Douglas B. Miron, *"Small Antenna Design*", Communication Engineering Series, pp. 2-5, Elsevier Inc. Burlington, USA 2006.

[2] Y. Rahmat-Samii and Z. Li, Handset communication antenna, including human interactions, in *Wireless Network: From Physical Layer to Communication, Computing, Sensing and Control*, G. Franceschetti and S. Stonelli (Eds.), Academic Press, New York, 2006.

[3] Y. X. Guo, M. Y. W Chia, and Z. N. Chia, "Miniature built-in multiband antennas for mobile handset", *IEEE Trans. on Antennas Propagation,* vol. 52, pp 1936-1944. August 2004.

[4] G. Y. Lee and K. L. Wong, " Very low profile bent planar monopole antenna for GSM/ DCS dual-band mobile phone", *Microwave and Optical Technology Letters*, Vol. 34, No. 6 September, 2002.

[5] D. Liu and B. P. Gaucher, The inverted-F antenna height effects on bandwidth, *Proc. IEEE Antenna Propag. Symp.*, Vol. 2A, pp. 367-370, July 2005.

[6] C. Rowell, A brief survey of internal antennas in GSM phones: 1998 to 2004, Proc. *UNSC/URS/National Radio Science Meeting*, July 2005.

[7] K. Fujimoto, A. Henderson, K. Hirasawa and J. R. James, *Small Antennas*, pp.116-151, Research Studies Press, Letchworth, 1987.

[8] T. Yamashita and M. Taguchi, "*Ultra Low Profile Inverted L Antenna on a Finite Conducting Plane"*, Proc. International Sympoisum on Antennas and Propagation, pp.361-364, Oct.2009.

[9] S. Schulteis, C. Waldschmidt, C. Kuhnert and W. Wiesbeck, " *Design of a Capacitively Loaded Inverted F Antenna* ***for.*** *Wireless-LAN Applications***"**' Proc. International ITG-Conference on Antennas, Berlin, 178:187-190, Sept.2003.

[10] WIPL-D d.o.o.: http://www.wipl-d.com/

V. Two Low Profile Unbalanced Fed Inverted L Elements on Square Conducting Plane for MIMO Applications

5.1. Introduction

The demand for high data rate and large channel capacity of users in recent mobile communication systems drives the MIMO systems as the subject of investigation for several years [1]. A practical MIMO antenna should have a low signal correlation between antenna elements and good impedance matching characteristics [2] [3]. The mutual coupling is an important factor when antennas have been used for MIMO applications [4] [5]. Higher mutual coupling may result in lower antenna efficiencies and higher correlation coefficients. The effect of mutual coupling on the capacity of MIMO wireless channel was studied in [6]. One of the most critical parameter affecting mutual coupling and correlation is the spacing between antenna elements. Analytical studies have shown that the distance between typical antenna elements such as dipole antenna needs to be at least half wavelengths for minimal or no mutual coupling [7]. However, since the distance is limited due to the small area which the elements are placed, especially at the portable MIMO-enabled devices, the MIMO antennas should be designed as small as possible. This is more conspicuous when MIMO antennas will be used in small terminal devices and more effort will be devoted to devising new MIMO antenna elements with compact and reasonable antenna characteristics [8]-[10]. The authors have proposed the unbalanced fed, ultra low profile inverted L antenna on a rectangular conducting plane for mobile terminal devices [11] [12]. When the size of conducting plane is 0.245 λ (λ: wavelength) by 0.49 λ and the antenna height is λ/30, and the length of horizontal element is around a quarter wavelength, the input impedance of this antenna is matched to 50 Ω and its directivity becomes more than 4 dBi. In this antenna, the electromagnetic field is strongly excited between the inverted L element and the conducting plane. Therefore even though two inverted L antennas are closely located, the mutual coupling may be weak.

Several other designs of MIMO antenna satisfy for the requirement of MIMO systems; unfortunately these antennas have limitation of size for practical MIMO application. Also in general, MIMO antennas consist of complicated structures [13]-[18]. For example, in [17], two meandered monopoles with a gamma matching and a folded T-shaped stub between radiators are printed on an FR4 substrate with its size of 30 mm by 15 mm. Its directivity is less than 0 dBi. In this chapter, the very simple antenna composed of two unbalanced fed, ultra low profile inverted L antennas on a square conducting plane with its size of 55 mm is proposed as MIMO antenna applications [19]. In the numerical analysis, the electromagnetic simulator WIPL-D based on the Method of Moments is used [20].

5.2. Antenna Structure

Figure 5.1 shows the structure of the proposed antenna. Two identical low profile inverted L antenna elements with the height h = 4 mm are mounted on the square conducting plane with its size of 55 mm by 55 mm. The antenna size corresponds to 0.45 λ by 0.45 λ by 0.03 λ at the design frequency of 2.45 GHz. The antenna elements are composed of the semi rigid coaxial cable with outer and inner radius 1.095 mm and 0.255 mm, respectively. The inner conductor of the coaxial cable is extended from the end of outer conductor, that is, each antenna element is excited at the end of outer conductor. The distance d between two antenna elements are investigated in order to reduce the mutual coupling. Furthermore the distance is challenged to be less than half wavelength. Both the distance *pym* between the vertical element to the back edge of the ground plane and distance *pyp* between the vertical element to the front edge are fixed as 10 mm and 45 mm, respectively. In each case of the distance between two antennas, the length of horizontal elements L and $L1$ are optimized to achieve impedance matching at the center frequency of 2.45 GHz. Figure 5.2 shows other arrangements of antenna elements.

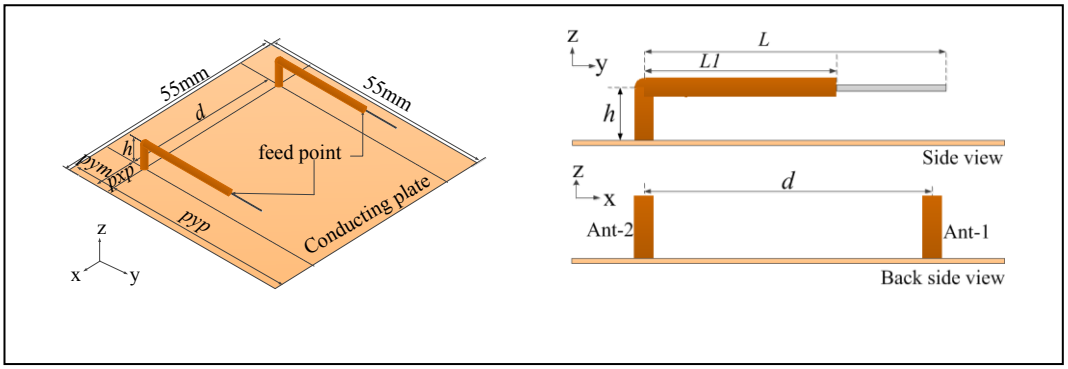

Figure 5.1. The structure of proposed antenna; arrangement-1 (*pym* = 10 mm, *pyp* = 45 mm, *h*=4mm).

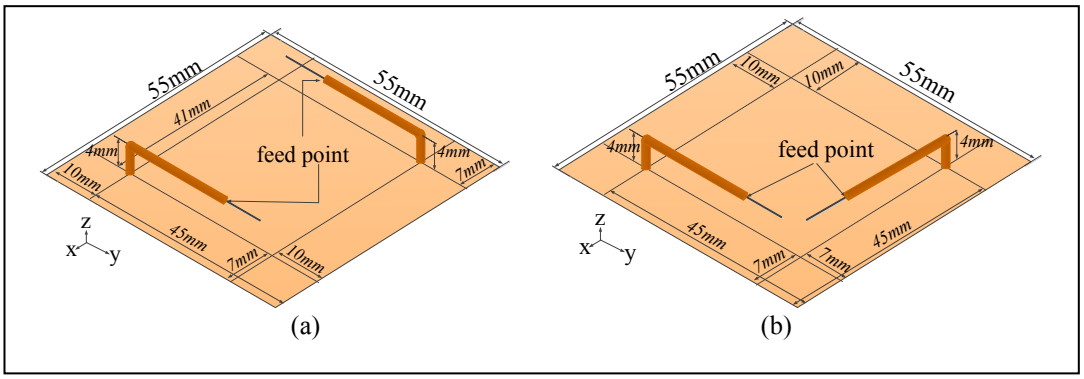

Figure. 5.2 (a) Arangement-2; opposite parallel and (b) arrangement-3; face to face perpendicullar arrangents.

5.3. Results and Discussion

In the calculation, the distance *d* between two inverted L antennas is changed from 30 mm to 45 mm. Table 5.1 shows the calculated return loss bandwidth larger than 10 dB, S21 and the directive gain in the z direction at 2.45 GHz for the different distance *d* between two inverted L elements. Figure 5.3 shows calculated S parameters of the optimized proposed MIMO antenna arrangement-1 for different distance *d* between two antenna elements. S21 becomes smaller than -20 dB as the distance d become longer than 41 mm.

Table 5.1. Calculated return loss bandwidth, S21 and directivity for different distance between two antennas *d* (arrangement-1).

h=4 mm, *pym*=10 mm, *pyp*=45 mm [mm]			Return loss bandwidth		S21 at 2.45 GHz	Dir. Gain at 2.45 GHz
d / *pxp*	*L*	*L1*	[MHz]	[%]	[dB]	[dBi]
30/12.5	30.7	22.7	50	2.04	-14.83	3.79
35/10	30.9	22.2	60	2.45	-17.86	3.98
41/7	31.2	21.4	90	3.67	-22.64	4.12
45/5	31.4	20.7	100	4.08	-25.28	4.17

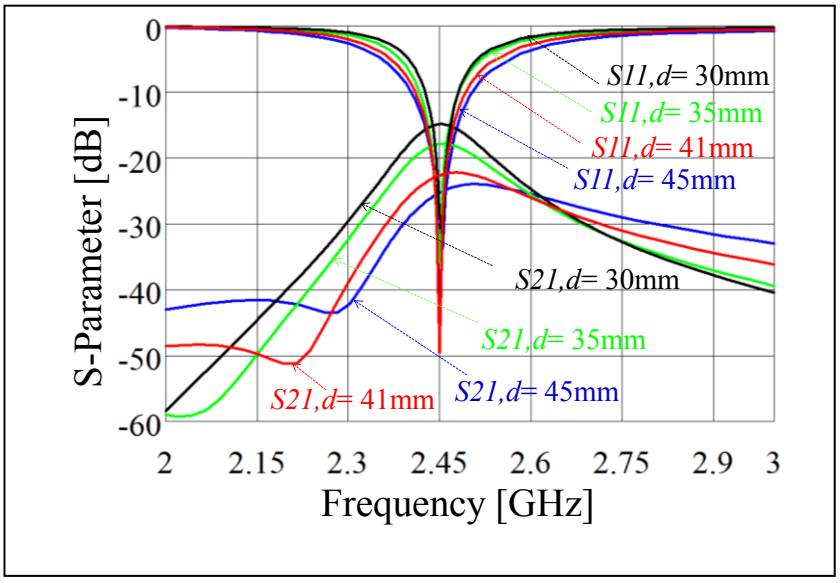

Figure 5.3. Calculated S parameters of proposed antenna for different *d* (arrangement-1, *h*=4mm, *pym*=10mm, *pyp*=45mm).

Table 5.2 shows the calculated return loss bandwidth, S21 and the directive gain in the z direction at 2.45 GHz for different antenna height *h*. When the height of antenna is increased, both the length of horizontal elements *L* and *L1* become shorter. This means that the resonant frequency is determined by the total length of horizontal and vertical elements. Figure 5.4 shows calculated S param-

eters of the proposed MIMO antenna arrangement-1 for different antenna height *h*. The return loss bandwidth and S21 become smaller as the antenna height *h* becomes smaller. As the antenna height becomes smaller, the electromagnetic field concentrates near the excited antenna element. Therefore the return loss bandwidth becomes narrower and the mutual coupling between two antennas becomes weak.

Table 5.2. Calculated return loss bandwidth and directivity for different antenna height *h* (arrangement-1)**.**

d=41mm, *pym*=10mm, *pyp*=45mm, *pxp*=7 mm [mm]			Return loss bandwidth		S21 at 2.45 GHz	Dir. gain at 2.45 GHz
h	*L*	*L1*	MHz	[%]	[dB]	[dBi]
3	31.9	23.9	50	2.04	-24.06	4.09
4	31.2	21.4	90	3.67	-22.64	4.12
5	30.6	19.1	120	4.90	-21.67	4.08
6	29.9	16.8	140	5.71	-20.98	4.05

Figure 5.5 shows the return loss bandwidth larger than 10 dB and the directive gain in the z direction at 2.45 GHz of the proposed MIMO antenna arrangement-1 for different distance *d* between two antenna elements and for different height *h* of antenna. Both the directive gain and the return loss bandwidth become larger by extending the distance between two antennas.

Figure 5.6 shows the directive gain in the z direction at the proposed MIMO antenna arrangement-1. Figure 5.7 shows the current distribution of proposed MIMO antenna arrangement-1 at 2.45 GHz. The inverted L element-1 is excited and the element-2 is terminated with 50 Ω load. The large surface current is induced near inverted L element-1, on the other hand weak surface current is induced on the element-2 at resonant frequency of 2.45 GHz. This means that the good isolation between two elements is achieved.

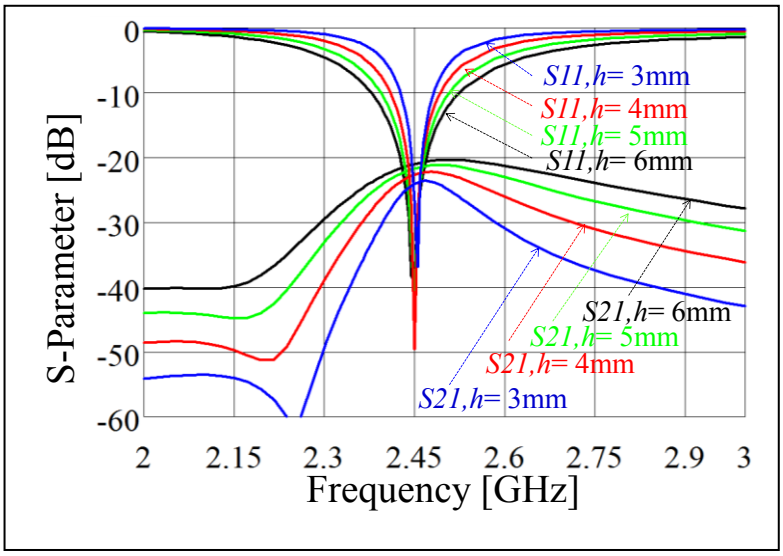

Figure 5.4. Calculated S parameters of proposed antenna for different *h* (arrangement-1, *d*=41mm, *pxp*=7mm, *pym*=10mm, *pyp*=45mm).

Figure 5.8 shows the electric field radiation patterns on zx plane, yz plane and xy plane of the proposed MIMO antenna arrangement-1 at 2.45 GHz when inverted L element-1 is fed and inverted L element-2 is terminated by the matching load 50 Ω. The peak gain of antenna-1 is 4.12 dBi. The current distribution on the inverted L antennas in the y direction and the surface on the conducting plane in the x and y directions contribute to the radiation. Therefore there are no deep nulls in any direction, although omnidirectional polarization antennas are used in general.

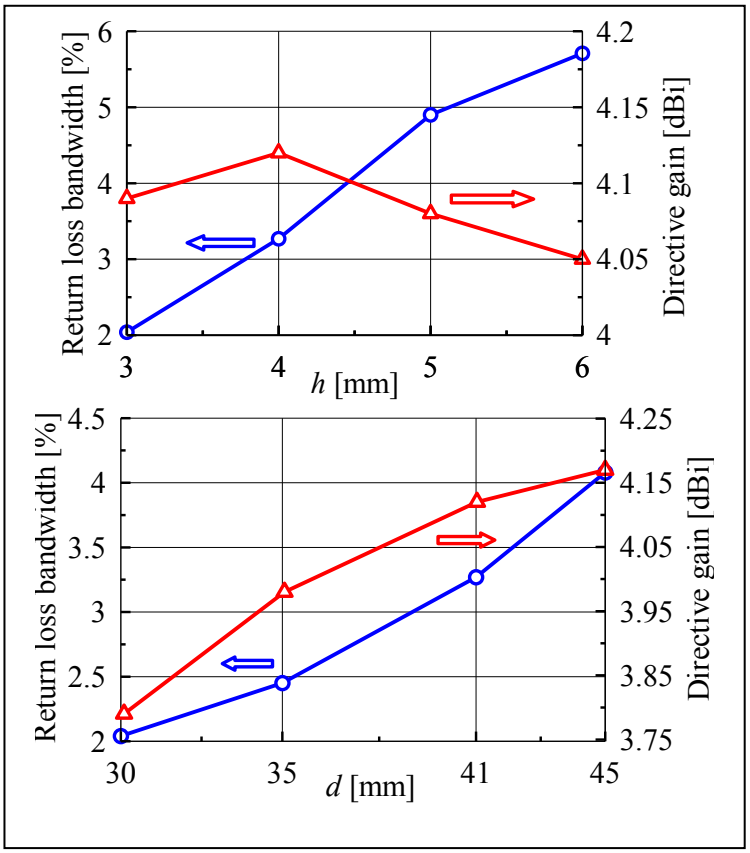

Figure 5.5. Return loss bandwidth and directive gain in z direction at 2.45 GHz (arrangement-1; *pxp*=7mm, *pym*=10mm, *pyp*=45mm).

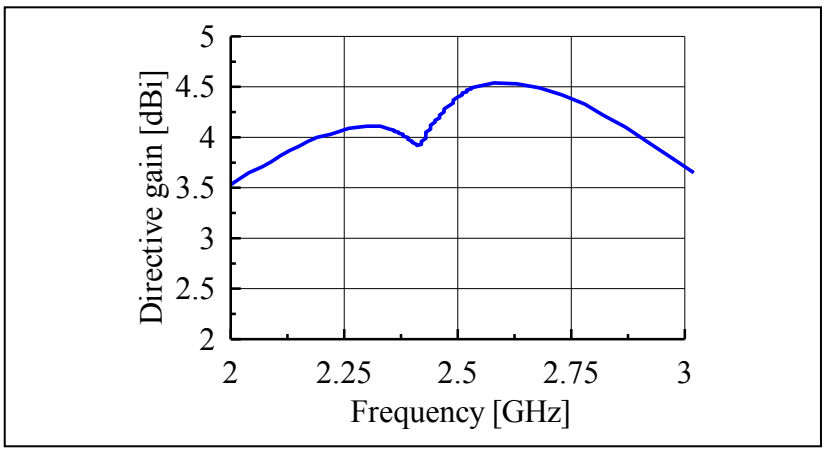

Figure 5.6. Calculated the directive gain at z direction (arrangemet-1; *pxp*=7mm, *pym*=10mm, *pyp*=45mm, *h*=4mm, *d*=41mm).

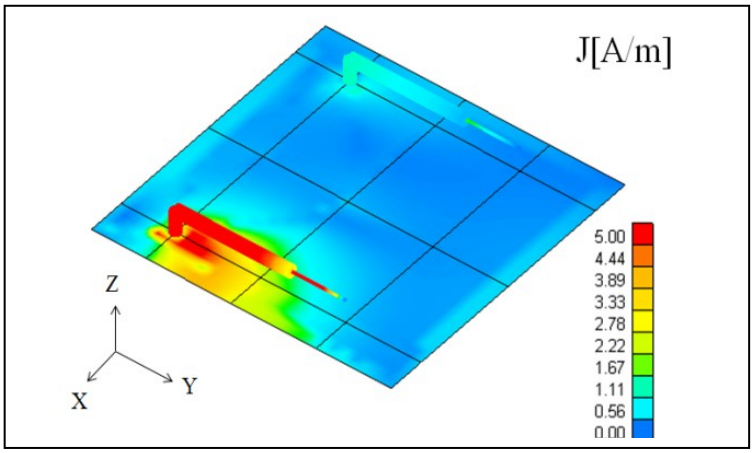

Figure 5.7. Calculated current distribution at frequency of 2.45 GHz (arrangement-1; *h*=4mm, *d*=41mm, *pxp*=7mm, *pym*=10mm, *pyp*=45mm, *L*=31.2mm, *L1*=21.4mm)**.**

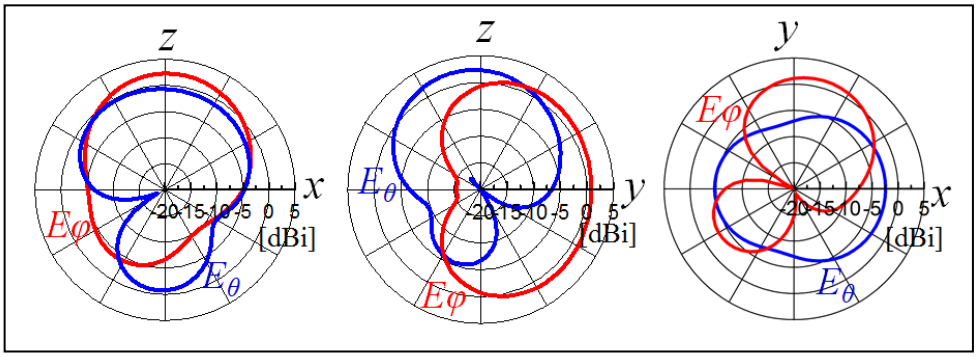

Figure 5.8. Simulated electric field radiation pattern of proposed antenna at 2.45 GHz (arrangement-1;*h*=4mm, d=41mm, *pxp*=7mm, *pym*=10mm, *pyp*=45mm, *L*=31.2mm, *L1*=21.4mm).

Figure 5.9 shows the near field distributions in the zx plane including feed points of arrangement-1, in the zx plane including the feed point of element1 of arrangement-2, and in the yz plane including feed point of element-2 of arrangement-3 at 2.45 GHz.

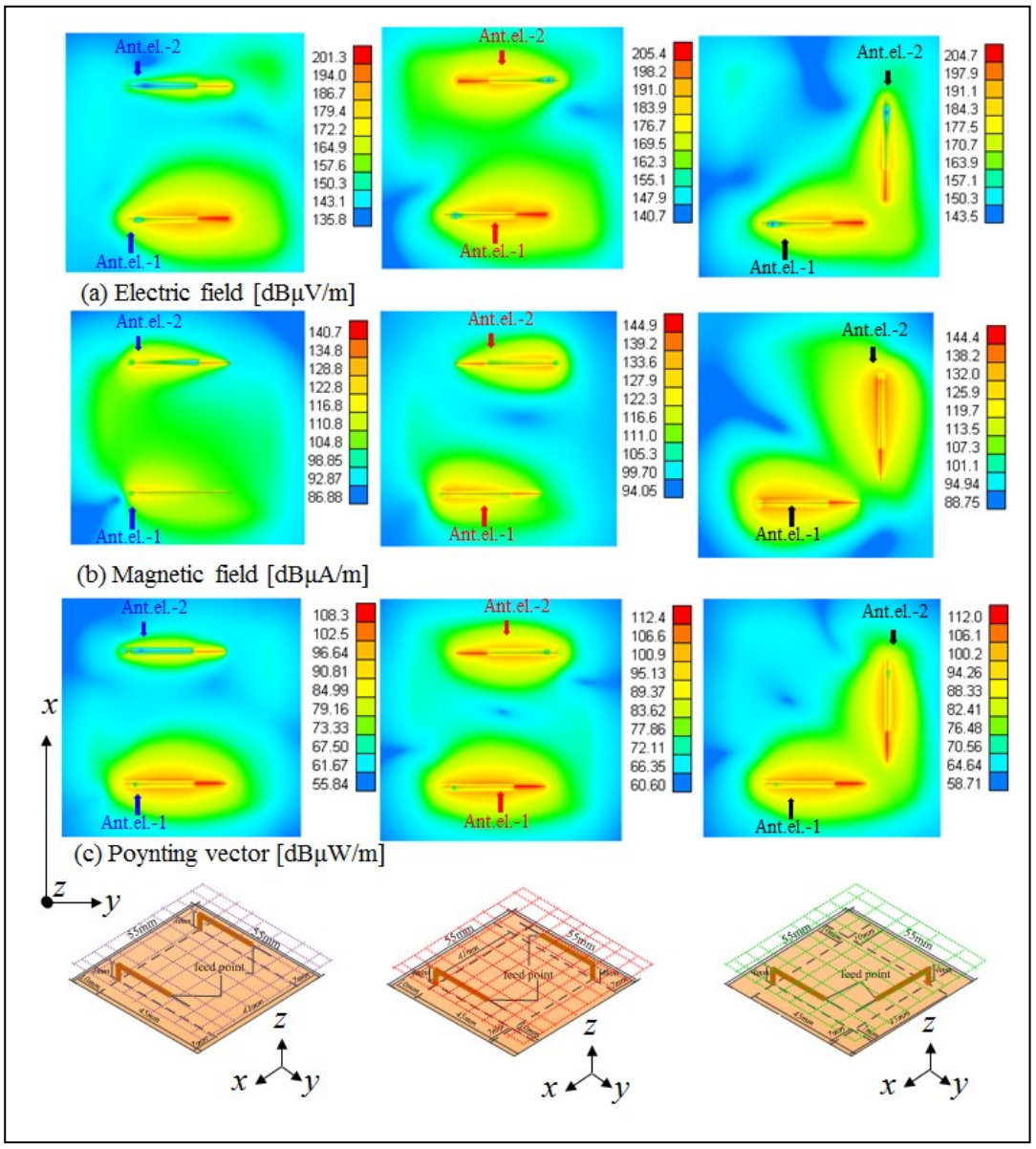

Figure 5.9. The near field distribution at 2.45 GHz (*h*=4mm, d=41mm, *pxp*=7mm, *pym*=10mm, *pyp*=45mm, *L*=31.2mm, *L1*=21.4mm).

Figure 5.10 shows the near field distributions in xy plane including horizontal elements of each arrangement at 2.45 GHz. The good isolation is achieved in the balanced structure as proposed MIMO arrangent-1. Whereas, it can be seen that two elements are highly coupled to each other at arrangement-2 and arrangement-3.

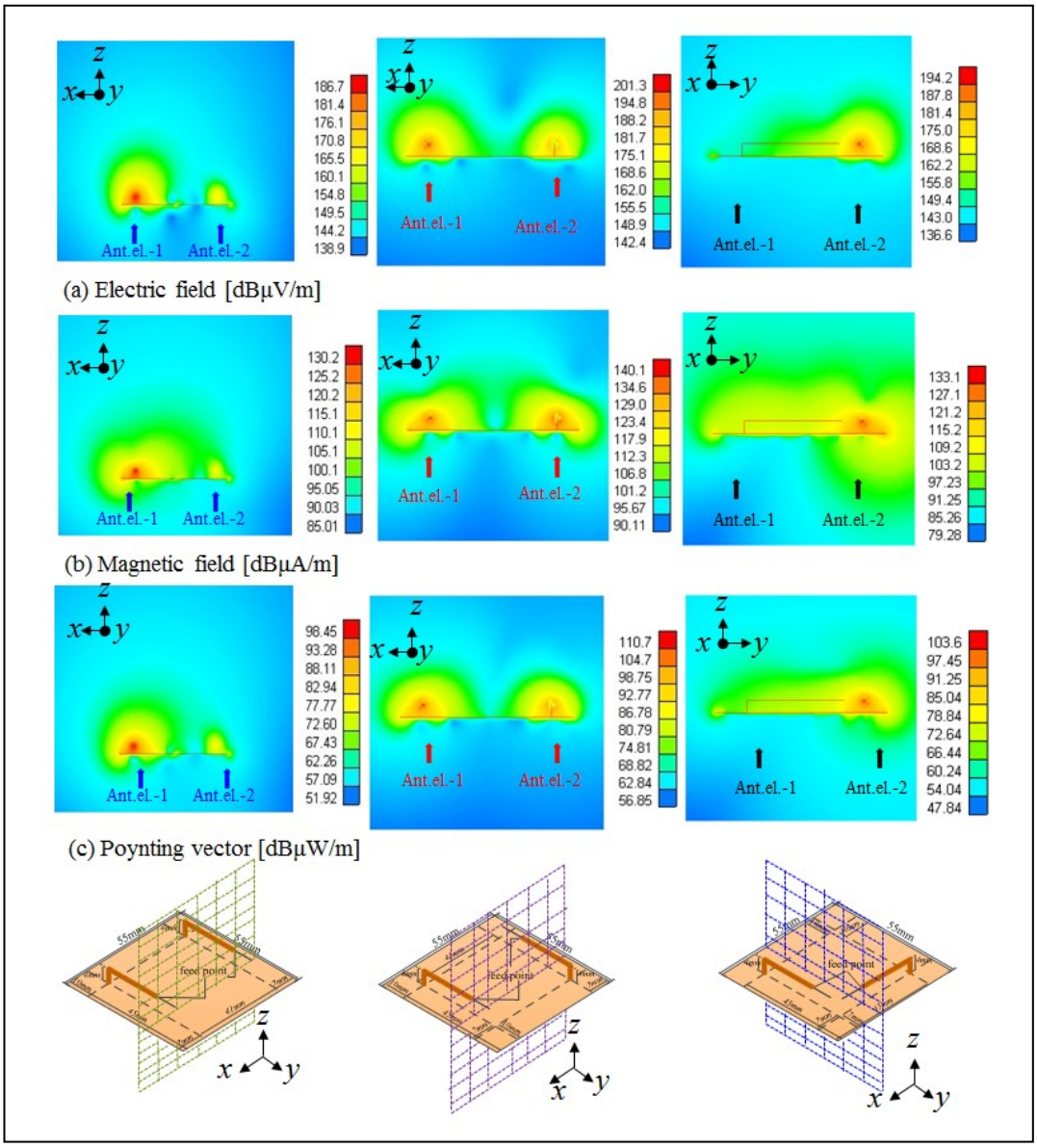

Figure 5.10. The near field distribution on horizontal elements of xy plane at 2.45 GHz (*h*=4mm, d=41mm, *pxp*=7mm, *pym*=10mm, *pyp*=45mm, *L*=31.2mm, *L1*=21.4mm)

From Figure 5.7, 5.9 and 5.10, in the case of proposed MIMO antenna arrangement-1, the surface current on the conducting plane between two antennas is small and the electromagnetic field becomes weak near the conducting plane between two antennas. This means that the mutual coupling is mainly not by the current flowing on the conducting plane but by the spatial coupling.

Figure 5.11 shows the reflection coefficients of three arrangements. The placement of inverted L elements as arrangement-1 obtains the best isolation between two elements.

Figure 5.12 shows the calculated and measured S parameters of proposed MIMO arrangement-1. The fairly good agreement between calculated and measured results is obtained.

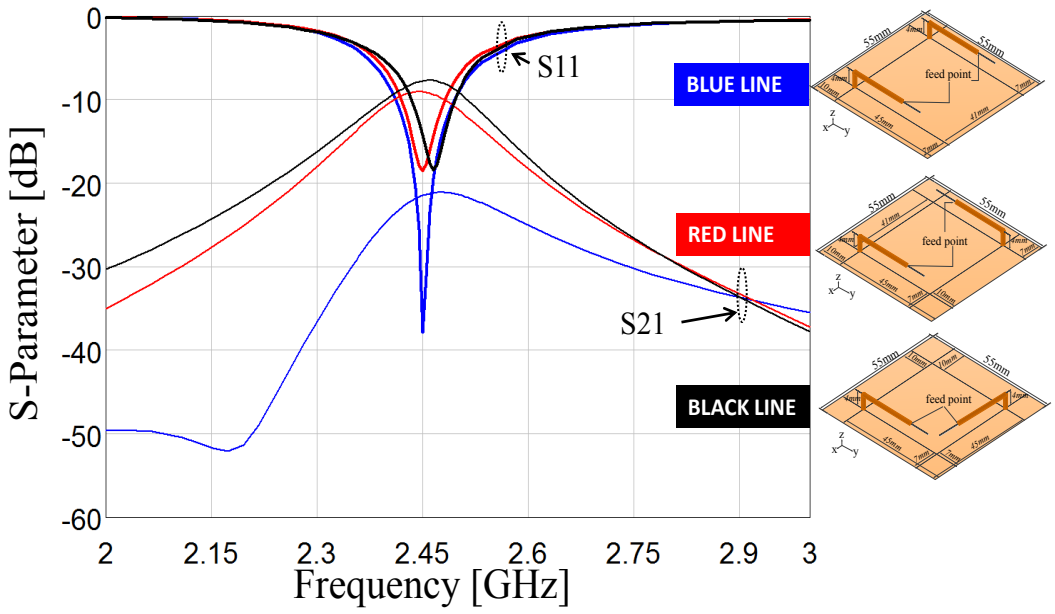

Figure 5.11. Reflection coefficients of proposed antenna with different arrangements (h=4mm, d=41mm, pxp=7mm, pym=10mm, pyp=45mm, L=31.2mm, $L1$=21.4mm).

The correlation coefficient of the proposed MIMO antenna is calculated through S parameter. The correlation coefficient ρ_e of a two element inverted L antenna system can be calculated by the following equation [21];

$$\rho_e = \frac{\left|S_{11}^{*}S_{12} + S_{21}^{*}S_{22}\right|^2}{(1-(\left|S_{11}\right|^2 + \left|S_{21}\right|^2))(1-(\left|S_{22}\right|^2 + \left|S_{12}\right|^2))} \tag{5-1}$$

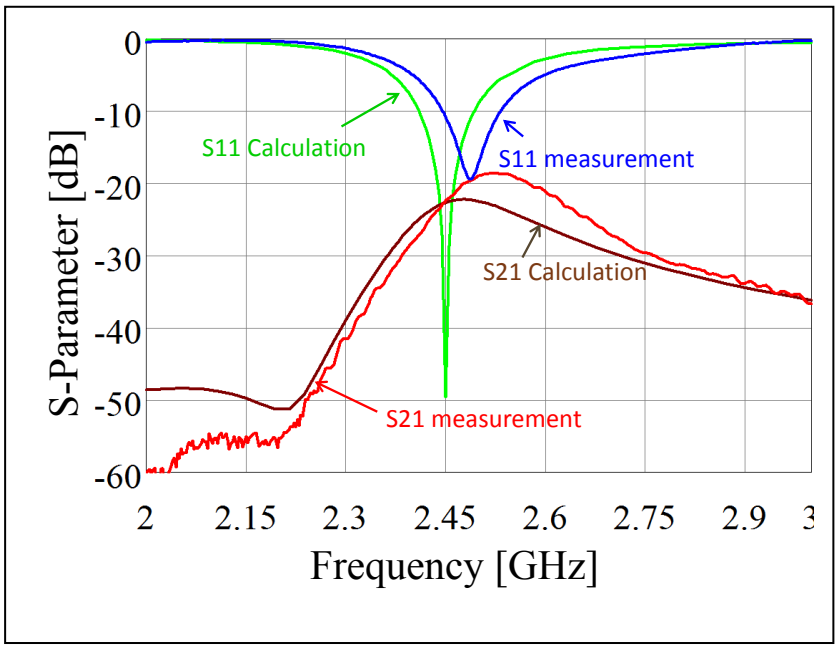

Figure 5.12. Calculated and measured S parameters of the proposed MIMO antenna (*pxp*=7mm, *pym*=10mm, *pyp*=45mm, *h*=4mm, *d*=41mm).

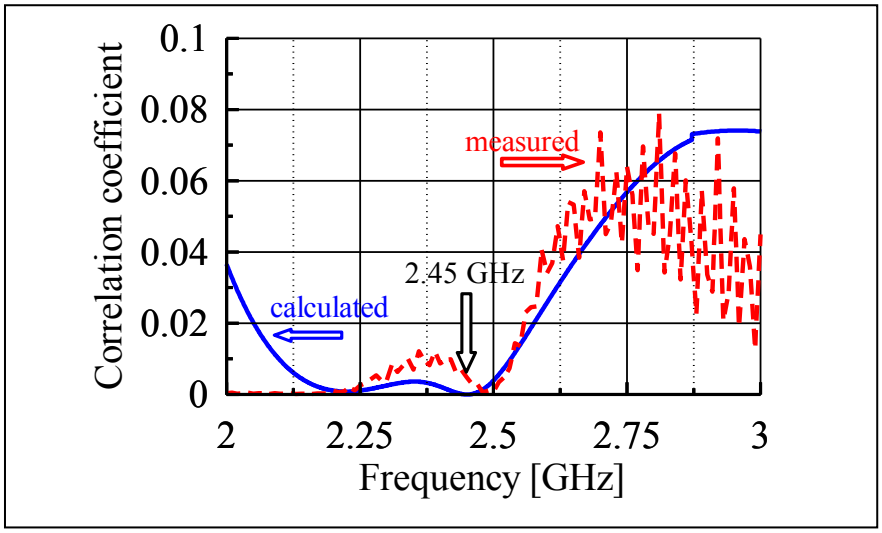

Figure 5.13. Calculated and measured correlation coefficient between two inverted L antennas (arrangemet-1; *pxp*=7mm, *pym*=10mm, *pyp*=45mm, *h*=4mm, *d*=41mm).

Figure 5.13 shows calculated and measured correlation coefficient of the proposed MIMO antenna arrangement-1. The correlation coefficient becomes

less than 0.02, which means that the proposed antenna has good diversity gain when antenna height and the distance between inverted L elements are 4 mm and 41 mm, respectively.

5.4. Conclusion

The MIMO antenna composed of two unbalanced fed, ultra low profile inverted L antenna elements has been proposed. Two inverted L elements are parallel located on the square conducting plane with its size of 045 λ by 0.45 λ. The height of inverted L antennas is 0.03 λ, and the distance between two inverted L antennas is 0.34 λ. With a very simple structure, the antenna has the good performances. The calculated and measured return loss bandwidths larger than 10 dB are 2.41 GHz to 2.50 GHz and 2.44 GHz to 2.53 GHz, respectively. The directive gain is 4.12 dBi. The proposed antenna is promising for MIMO application systems.

References Chapter - V

[1] Yu XH, Wang L, Wang HG, Wu XD, Shang YH, ”A novel multiport matching method for maximum capacity of an indoor MIMO system”. *Prog. Electromagn. Res*., Vol.130, pp.67-34, 2012. DOI:10.2528/PIER12040603 .

[2] Ding Y, Du Z, Gong K, Feng Z. ”A novel dula-band printed diversity antenna for mobile terminal”, IEEE Trans. Antenna Propagat., Vol. 55, pp.2088-2096, July 2007. DOI: 10.1109/TAP.2007.900249.

[3] Costa JR, Lima EB, Medeiros CR, Fernandes CA. ”Evaluation of a new wideband slot array for MIMO performance enhancement in indoor WLANs”, *IEEE Trans. Antenna Propagat*., Vol. 59, pp. 1200-1206, April 2011. DOI: 10.1109/TAP.2011.2109685.

[4] Karimian R., Soleimani M, Hashemi SM, ”Tri-band four elements MIMO antenna system for WLAN and WIMAX application”, *Journal of Electomagn. Waves and Application*, Vol. 26, Nos.17-18, pp. 2348-2357, Dec. 2012. DOI:10.1080/09205071.2012.734433.

[5] Cui S, Gong SX, Liu Y, Guan Y, ”Compact and low coupled monopole antennas for MIMO systems applications”, *Journal of Electomagn. Waves and Application*, Vol. 25, pp. 703-712, 2011. DOI: 10.1163/156939311794827221.

[6] Abouda, A.A. and S.G Hagman, ”Effect on mutual coupling capacity on MIMO wireless channels in high SNR scenario”, *Progress In Electromag., PIER*, Vol 65, pp. 27-40, 2006. doi:10.2528/PIER06072803

[7] Stutzman, W.L. and G.A. Thiele, Antenna Theory and Design, 2nd edition, Wiley, New Yoryk, pp.154-160, 1998.

[8] Foschini GJ, MJ Gans, ”On limits of wireless communications in fading environment when using multiple antennas”, *Wireless Pers. Commun*., Vol.6, pp.311-335, 1998.

[9] K. Fujimoto, A. Henderson, K. Hirasawa and J. R. James, ”Small Antennas”, *Research Studies Press, Letchworth*, pp. 116-151, 1987.

[10] K. Hirasawa, M. Haneishi,"Analysis, Design, and Measurement of Small and Low-Profile Antennas", Artech house, Inc., pp. 165-169, 1992.

[11] Yamashita and M. Taguchi, "Ultra Low Profile Inverted L Antenna on a Finite Conducting Plane", *Proc. International Sympoisum on Antennas and Propag*., pp.361-364, 2009.

[12] E. Rohadi and M. Taguchi, "Ultra Low Profile Antenna for 2.45 GHz Wireless Communications", *Proc. IEEE Int. Conf. on Communication and Satellite (Comnetsat)*, pp. 103-107, 2012. DOI: 10.1109/ComNetSat.2012.6380786.

[13] Votis C., Tatis G., Kostarakis P., "Envelope Correlation Parameter Measurements in a MIMO Antenna Array Conficguration", *Int. Journal Comm., Network and System Science*, Vol. 3, pp. 350-354, 2010. DOI: 10.4236/ijcns.2010.34044.

[14] Ahn S.B., Choo H.S., "Design of Vehicle of On-Glass 4x4 MIMO Antennas for WIBRO Applications", *Int. Journal of Automotive Tech*., Vol.14, pp. 731-737, 2013.

[15] Zeng Q., Yao Y., Liu S., Yu J. and Chen X.. "Tetraband Small-size printed Strip MIMO Antenna for Mobile Handset Application", *Research Article, Int. Journal of Antenna and Propag*.,Vol. 2012, ID 320582, 2012.

[16] Lee J.N, Lee K.C., Park N.H. and Park J.K., "Design of Dual-Band MIMO Antenna with High Isolation for Mobile terminal", ETRI Journal, Vo1.35, Pp. 177-187, 2013.

[17] Jin Z., Lim J. H. and Yun T.Y., "Small-Size and High-Isolation MIMO Antenna for WLAN", ETRI Journal, Vol.34, pp. 114-117, 2012.

[18] Kim S.H.,Jin Z.J., Chae Y. B.,and Yun T. Y., "Small Antenna Using Multiband, Wideband and High-Isolation MIMO Techniques", *ETRI Journal*, Vol. 35, pp. 51-57, 2013.

[19] E. Rohadi and M. Taguchi, "Two element ultra low profile inverted L antennas on finite conducting plate for MIMO applications", *Proc. IEEE Int. on Advanced Tech. for Comms. (ATC)*, pp. 74-77, 2013. DOI:

10.1109/ATC.2013.6698080.

[20] WIPL-D d.o.o.: http://www.wipl-d.com/, WIPL-D Pro v11.0, 2013.

[21] Thaysen J, Jakobsen KB, ”Envelope correlation in (N,N) MIMO antenna array from scattering parameters”, *Microwave Opt. Tech. Letter*. Vol. 48, pp.832-834, 2006. DOI: 10.1002/mop.21.

VI. Dual Band MIMO Antenna Composed of Two Low Profile Unbalanced Fed Inverted L Antennas for Wireless Communication

6.1. Introduction

The dual band antennas have been investigated with the development of wireless communication systems in recent years [1]-[8]. Most of these dual or multiple band antennas have an omnidirectional radiation pattern. In some applications such as wireless base station or access point, the unidirectional radiation pattern is needed. In order to realize the unidirectional radiation pattern, the antenna size becomes larger [4], [6] and [8]. A higher order mode may be excited in such antenna and large ripples may exist in the radiation pattern at the upper frequency bands [4]-[6]. The interference and the antenna gain reduction may occur due to the large ripple for base station or access point applications. Therefore the compact dual band antenna with unidirectional radiation pattern is desired. The dual or multiple band MIMO antennas are widely used for wireless communication because they become as an effective solution to enhance the channel capacity [9], [10]. One of authors has proposed the dual band antenna composed of the unbalanced fed inverted L antenna for 1.4 GHz and 2.2 GHz bands [11]. In [11], the parasitic element was located above an unbalanced fed inverted L antenna for higher band excitation. This antenna is promising as the candidate of the dual band antenna because it provides two distinct resonant modes for achieving dual-band operation. Furthermore, the authors have studied the advantages of inverted L antennas for wireless communication systems [12]-[13], and proposed the simple design and low cost material antenna for single band MIMO antenna systems [14]-[15].

In this chapter, a dual band MIMO antenna composed of two parallel identical ultra low profile inverted L antennas located on square conducting plane. The proposed antenna has a simple design and works at frequency bands of 2.45 GHz and 5 GHz. In order to satisfy the MIMO antenna system requirements, the pro-

posed antenna is investigated on mutual coupling between two inverted L elements and diversity gain through correlation coefficient value [16]-[19]. The electromagnetic simulator WILP-D based on Method of Moments is used for numerical analysis for the reason of shorter computation time compared with other simulation methods [20]. Then its results are validated with the measurement.

6.2. Antenna Structure

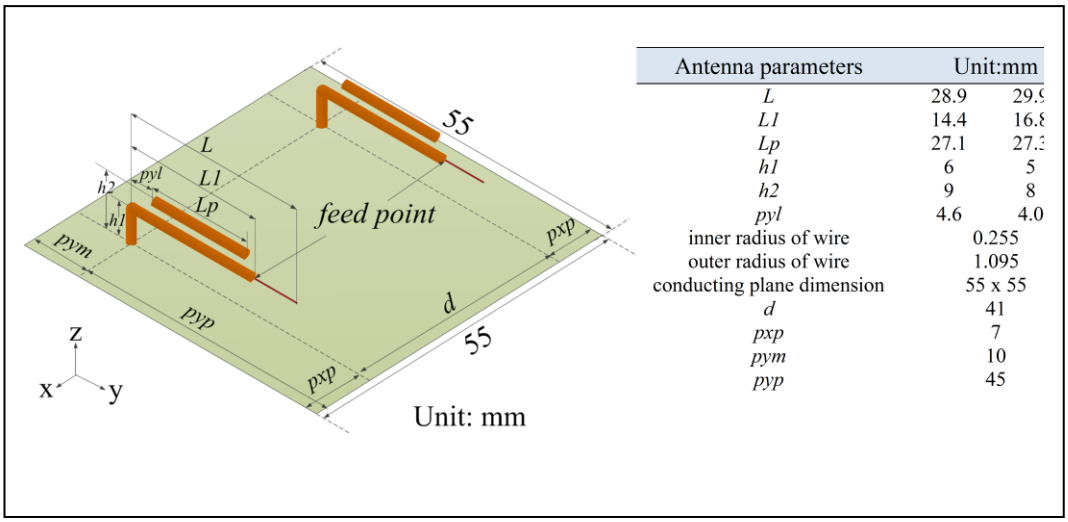

Antenna parameters	Unit:mm	
L	28.9	29.9
L1	14.4	16.8
Lp	27.1	27.3
h1	6	5
h2	9	8
pyl	4.6	4.0
inner radius of wire	0.255	
outer radius of wire	1.095	
conducting plane dimension	55 x 55	
d	41	
pxp	7	
pym	10	
pyp	45	

Fig. 6.1. The structure of proposed MIMO antenna.

Figure 6.1 shows the proposed dual band MIMO antenna. The proposed structure is configured by two low profile inverted L antennas located on finite conducting plate with dimension 55 mm by 55 mm (0.45 $\lambda_{2.45}$ by 0.45 $\lambda_{2.45}$). $\lambda_{2.45}$ is the wavelength at the frequency of 2.45 GHz. The parasitic element is placed above the horizontal element of low profile inverted L antenna. The feed points are located at the distance *L1* from the bend of horizontal elements of the inverted L antennas. Both the lengths of *L1* and *L* are adjusted to obtain the 50 Ohm impedance matching. In the calculation, the height of inverted *L* antenna *h1* is set as 5 mm or 6 mm. The length of parasitic elements *Lp* is determined so that the upper resonant frequency becomes to be 5 GHz. In the previous study in [12], the optimum distance between two inverted L antennas was 41mm in the case of the conducting plane was 55 mm by 55 mm. Therefore the distance between inverted

L antennas *d* is set to be 41 mm. The inverted L antenna is composed of the semi rigid coaxial cables with the radius of inner and outer conductors are 0.255 mm and 1.095 mm, respectively. The radius of parasitic elements is 1.095 mm. The distance between the vertical element of inverted L antennas and the edge on back-side *pym* is set as 10 mm. The distance between the vertical element of inverted L antennas and the edge on front side *pyp* is set as 45 mm. The distances between vertical element of inverted L antennas and outer edge on right and left side *pxp* are fixed as 7 mm.

6.3. Results and Discussion

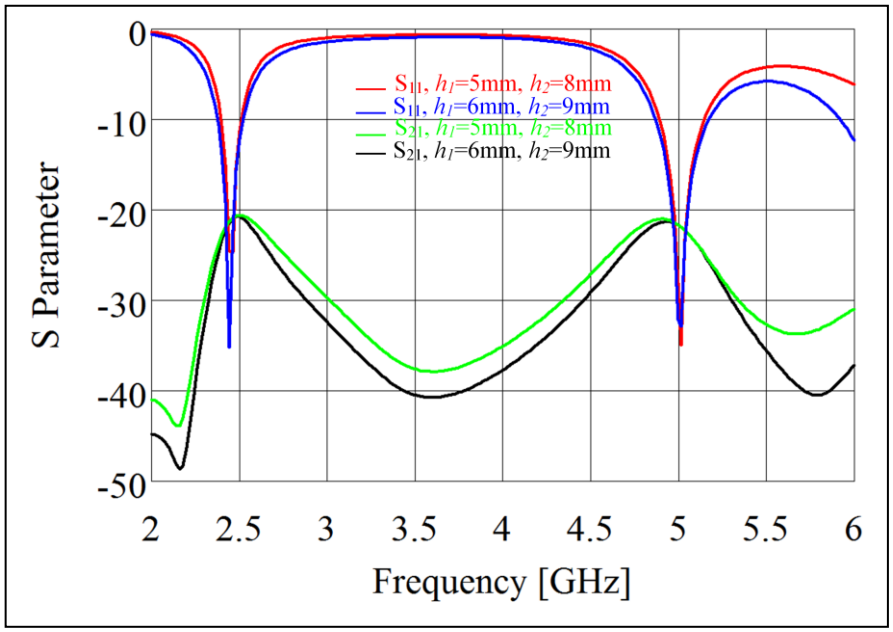

Fig. 6.2. Calculated scattering parameter of proposed antenna; *pyp*=45mm, *pxp*=7mm, *pym*=10mm, *d*=41mm.

Figure 6.2 show the calculated scattering parameters of proposed MIMO antenna. The S11 bandwidth less than -10dB of the proposed antenna are 5.71% (2.38 GHz - 2.52G Hz) for lower frequency band and 6% (4.87 GHz - 5.17GHz) for higher frequency band. The mutual coupling between two ports is less than -21 dB in the lower band and less than -23 dB in the higher one.

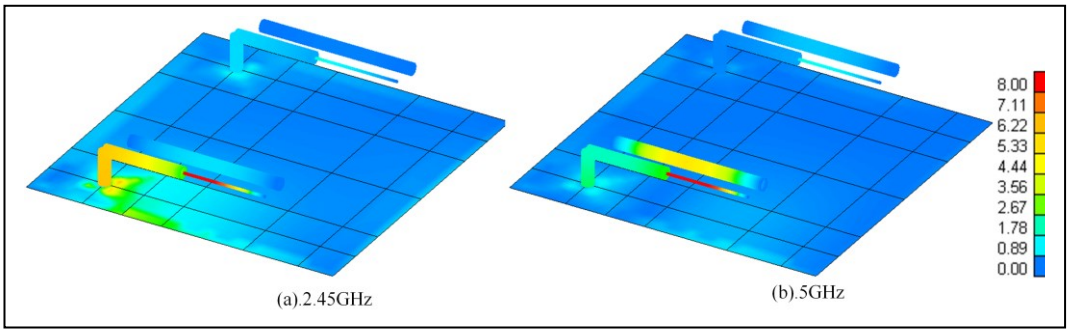

Fig. 6.3. The calculated current distributions of proposed antenna; *h1*=6mm, *h*2=9mm, *pyp*=45mm, *pxp*=7mm, *pym*=10mm, *d*=41mm.

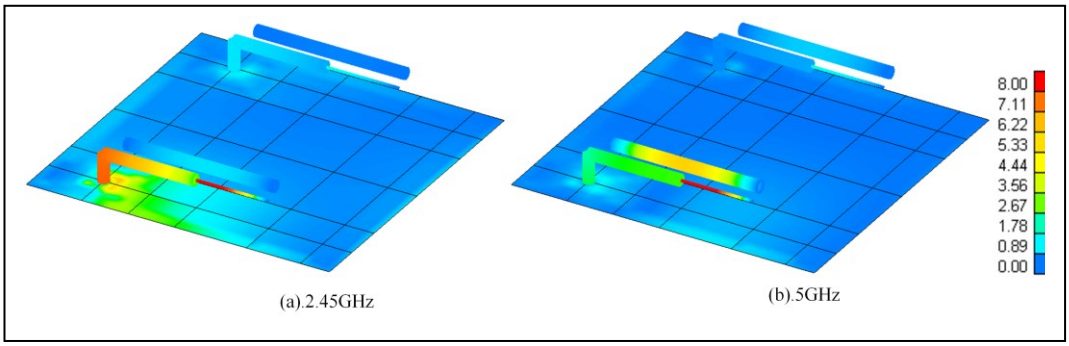

Fig. 6.4. The calculated current distributions of proposed antenna; *h1*=5mm, *h*2=8mm, *pyp*=45mm, *pxp*=7mm, *pym*=10mm, *d*=41mm.

Figure 6.3(a) and Figure 6.3(b) show the calculated current distributions at lower frequency of 2.45 GHz and higher frequency of 5 GHz. The height of inverted L antenna and parasitic element are *h1* = 6 mm and *h2* = 9 mm, respectively. Figure 6.4(a) and Figure 6.4(b) show the calculated current distributions when *h1* = 5 mm and *h2* = 8 mm. A surface current on the conducting plane between two inverted L antennas is small. This means that the proposed structure achieves a good isolation. When the height of inverted L antenna is 5 mm, a large surface current flows on the conducting plane under the inverted L antenna. Due to the strong mutual coupling between inverted L antenna and the conducting plane, the frequency bandwidth becomes slightly narrow.

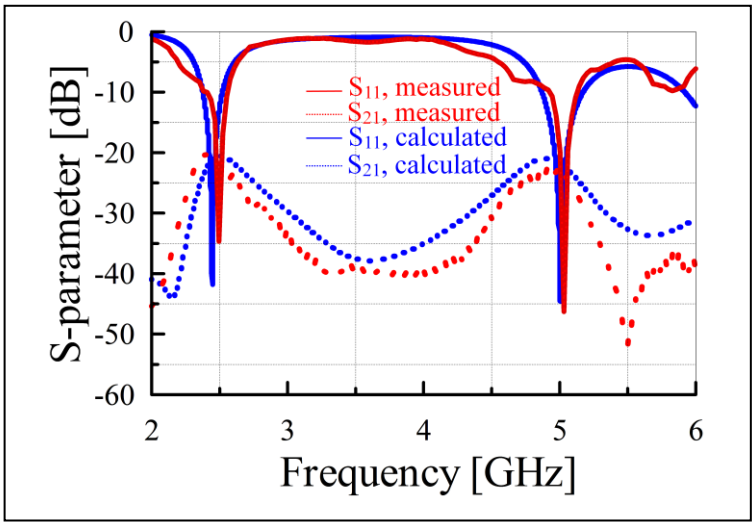

Fig. 6.5. Calculated and measured scattering parameter; *h1*=6mm, *h*2=9mm, *pyp*=45mm, *pxp*=7mm, *pym*=10mm, *d*=41mm.

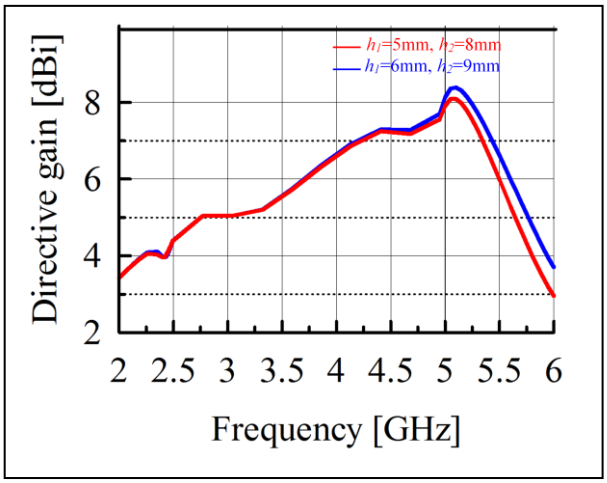

Fig. 6.6. The directive gain of the proposed antenna in z direction; *pyp*=45mm, *pxp*=7mm, *pym*=10mm, *d*=41mm.

Figure 6.5 show the comparison of calculated and measured scattering parameters of proposed MIMO antenna when the height of inverted L antenna and parasitic elements are *h1* =6 mm and *h2* = 9 mm, respectively. The scattering parameters are measured by the 6GHz board network analyzer R3760 by Advantest. The measured scattering parameters agree well with the calculated ones.

Figure 6.6 shows the directive gain of proposed MIMO antenna in the z direction. In both of cases of antenna height, the almost the same directive gain 4.11 dBi is obtained at 2.45 GHz. At 5 GHz, the current on the parasitic element is strongly excited. Since the equivalent size of antenna becomes large, the directive gain more than 8.11 dBi is obtained at this frequency.

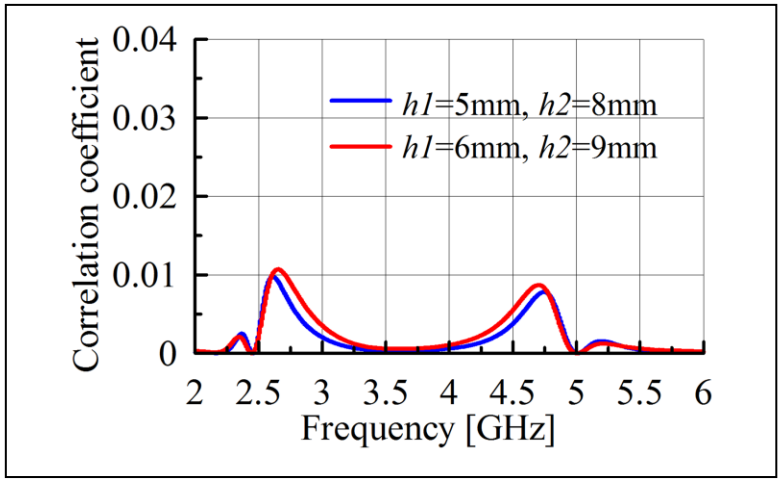

Fig. 6.7. Correlation coefficient; *pyp*=45mm, *pxp*=7mm, *pym*=10mm, *d*=41mm.

The MIMO antenna system correlation factor will be significantly degraded with high coupling levels. It can be calculated from the scattering parameters in isotropic/ uniform signal propagation [21]. The correlation coefficient ρ_e is important to achieve the required diversity gain of the MIMO antenna systems. When ρ_e becomes lower, the higher diversity gain is obtained. The value of ρ_e can be calculated by using [22];

$$\rho_e = \frac{\left|S_{11}^{*}S_{12} + S_{21}^{*}S_{22}\right|^2}{(1-(\left|S_{11}\right|^2+\left|S_{21}\right|^2))(1-(\left|S_{22}\right|^2+\left|S_{12}\right|^2))} \tag{6-1}$$

Figure 6.7 show the calculated correlation coefficients in two cases of antenna height. It is evident that the proposed antenna with enhanced isolation satisfies the MIMO requirements for spatial diversity with the value of ρ_e are less than 0.005 at both of lower and upper frequency bands. Figure 6.8 shows the calculated and measured correlation coefficient of the proposed MIMO antenna when the height of inverted antenna and the height of antenna elements are 6 mm

and 9 mm, respectively. A good agreement between calculated and measured results is obtained.

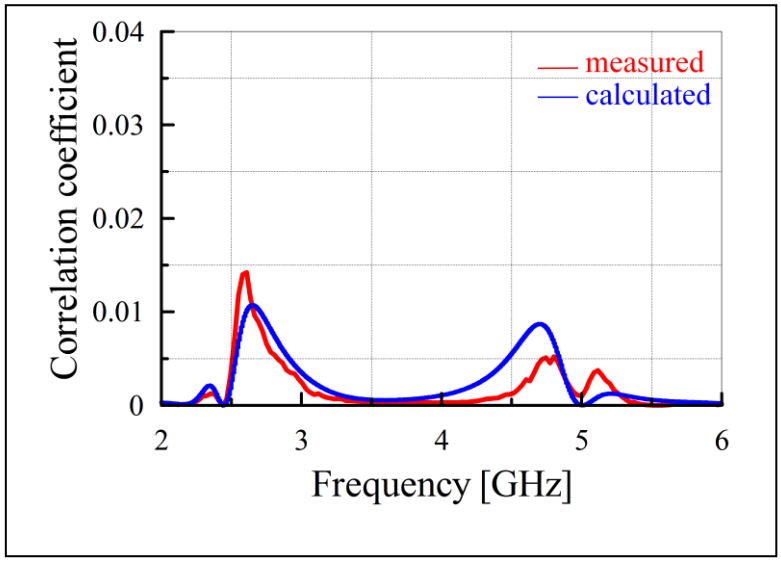

Fig. 6.8. Correlation coefficient; *h*1=6mm, *h*2=9mm, *pyp*=45mm, *pxp*=7mm, *pym*=10mm, *d*=41mm.

Figure 6.9 show the calculated electric field radiation pattern in xy-plane, xz-plane and yz-plane at 2.45 GHz and 5 GHz when the height of inverted L antenna is *h1=6* mm and height of parasitic element is *h2* = 9 mm, respectively. When the height of inverted of inverted L antenna is reduced to 5 mm, the calculated electric field radiation pattern are shown at Figure 6.10. As a result, the radiation patterns of the proposed antenna tends to cover complementary space region, which can provide pattern diversity to overcome the multipath fading problem and enhance the system performance.

Figure 6.11 shows the calculated near field distribution of the proposed antenna in xz-plane including the feed point in the case of *h1* = 6 mm and *h2* = 9 mm. The weak mutual coupling between two inverted L antennas is archived. It clearly illustrates that the spatial coupling is dominant at operation frequency bands since the small current are flowing on the conducting plane between two inverted L antennas.

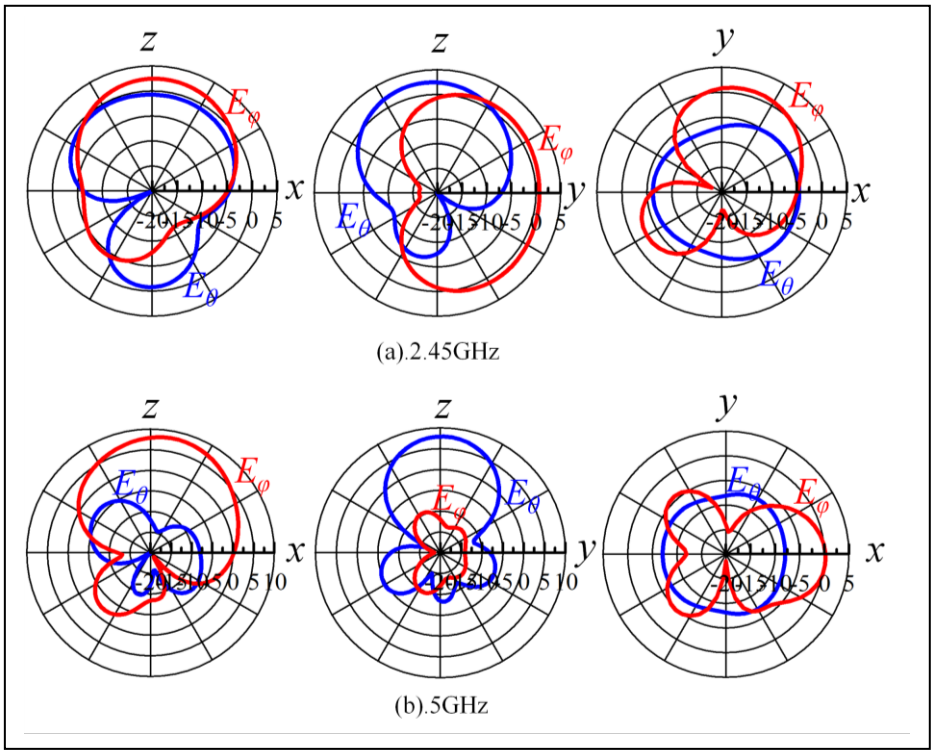

Fig. 6.9. Electric field radiation pattern; *h1*=6mm, *h*2=9mm, *pyp*=45mm, *pxp*=7mm, *pym*=10mm, *d*=41mm.

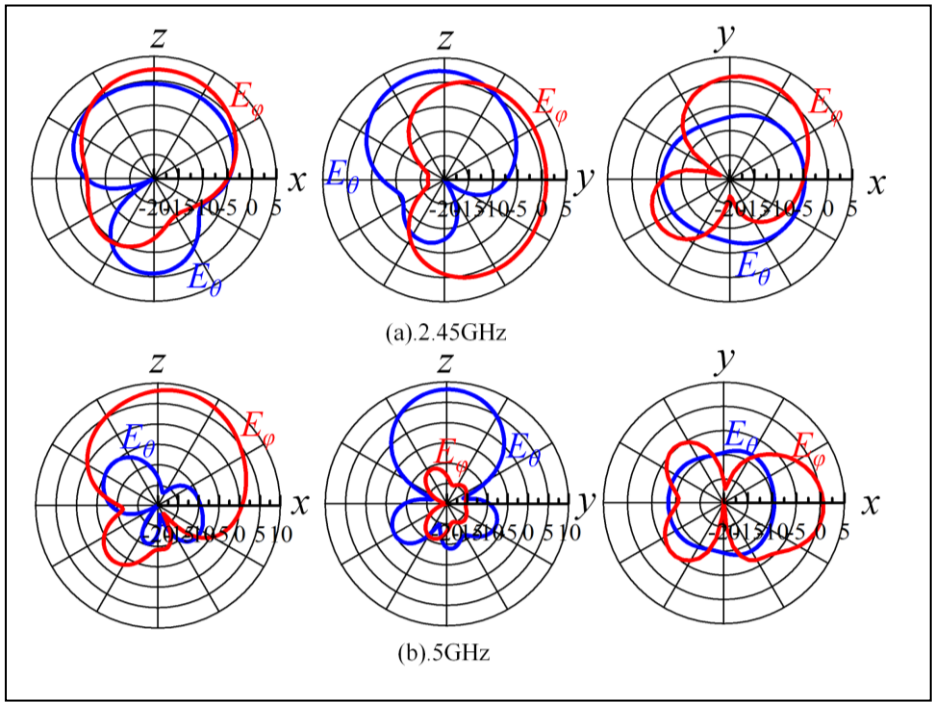

Fig. 6.10. Electric field radiation pattern; *h1*=5mm, *h*2=8mm, *pyp*=45mm, *pxp*=7mm, *pym*=10mm, *d*=41mm.

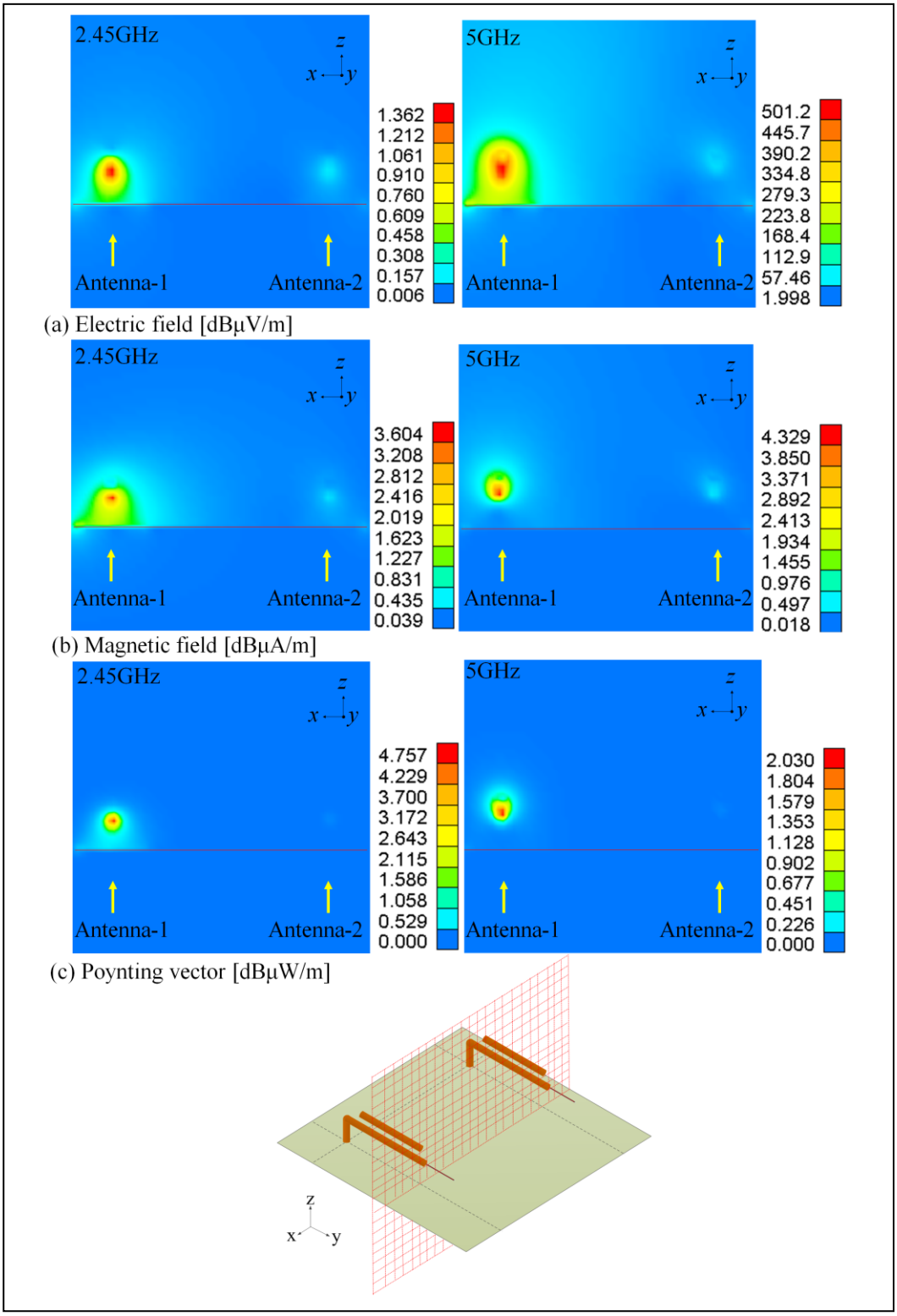

Figure 6.11 . The near field distribution at 2.45 GHz and 5 GHz. *h1*=6mm, *h2*=9mm, d=41mm, *pxp*=7mm, *pym*=10mm, *pyp*=45mm, *L*=28.9 mm, *L1*=14.2mm, *Lp*=27.1mm

6.4. Conclusion

In this chapter, a simple design and fabrication of dual band MIMO antenna composed of two ultra low profile inverted L antenna has been presented. The proposed antenna satisfies the MIMO system requirements with correlation coefficient less than 0.005 at both frequency bands. When the antenna size is 55 mm by 55 mm by 9 mm, the S11 bandwidth of 5.71% (140 MHz) at lower band of 2.45 GHz and 6 % (300MHz) at upper band of 5 GHz are obtained. The directive gains are 4.11 dBi at 2.45 GHz and 8.22 dBi at 5GHz. The good agreement of calculated and measured scattering parameters and the correlation coefficients are obtained. The presented design is suitable for MIMO communication applications.

References Chapter-VI

[1] Y.L. Kuo and K.L. Wong, ”Printed double-T monopole antenna for 2.4/5.2 GHz dual- band WLAN operations”, *IEEE Trans. Antennas Propagat.*, Vol. 51, no. 9, pp. 2187- 2192, Sept. 2003.

[2] Y. Ding , Z. Du ,K. Gong and Z. Feng . ”A novel dual-band printed diversity antenna for mobile terminal”, *IEEE Trans. Antenna Propagat*., Vol. 55, pp.2088-2096, July 2007. DOI: 10.1109/TAP.2007.900249.

[3] J.Y. Jan and L.C. Tseng, ”Small planar monopole antenna with a shorted parasitic inverted-L wire for wireless communications in the 2.4, 5.2, and 5.8-GHz bands”, *IEEE Trans. Antennas Propagat*., Vol. 52, no. 7, pp. 1903-1905, July, 2004.

[4] K.L. Wong, L.C. Chou and C.M. Su, ”Dual-band flate-plate antenna with a shorted parasitic element for laptop applications”, *IEEE Trans. Antennas Propagat.*, Vol. 53, no. 1, pp. 539-544, Jan. 2005.

[5] S.B. Chen, Y.C. Jiao, W. Wang and F.S. Zhang, ”Modified T-shaped planar monopole antennas for multiband operation”, *IEEE Transactions on Microwave Theory and Techniques*, Vol. 54, no. 8, pp. 3267-3270, Aug. 2006.

[6] L.C. Chou and K.L. Wong, ”Uni-Planar dual-band monopole antenna for 2.4/5 GHz WLAN operation in the laptop computer”, *IEEE Trans. Antennas Propagat.*, Vol. 55, no. 12, pp. 3739-3741, Dec. 2007.

[7] R. L. Li, B. Pan, J. Laskar, and M. M. Tentzeris, “A novel low-profile broadband dual- frequency planar antenna for wireless handsets”, *IEEE Trans. Antennas Propagat.*, Vol. 56, no. 4, pp. 1155-1162, April 2008.

[8] R. Li, T. Wu and M. Tentzeris, ”A Dual-Band Unidirectional Coplanar Antenna for 2.4-5-GHz Wireless Application”, *Proc. of The Asia-Pacific Microwave Conference 2008, APMC 2008,* pp. 1-4, December 2008.

[9] X.H. Yu, L. Wang, H.G. Wang, X.D. Wu and Y. H. Shang, “A novel multiport matching method for maximum capacity of an indoor MIMO system”, *Prog. Electromagn. Res*., Vol.130, pp.67-34, 2012. DOI:10.2528/PIER12040603.

[10] J. Zhang, J. O.Yang, K.Z. Zhang and F. Yang, ”A Novel Dual-Band MIMO Antenna with Lower Correlation Coefficient”, I*nt. Journal of Antenna Prop-*

agat., Vol. 2012, Article ID. 512975, 7 pages, Sept. 2011. DOI: 10.1155/2012/512975.

[11] S. Sato, and M. Taguchi, ”Dual band ultra low profile inverted L antenna ”, *Proc. Int.l Symposium on Antennas and Propagat. (ISAP)*, pp 1417 – 1420, Oct. 29 -Nov. 2, 2012.

[12] Yamashita and M. Taguchi, ”Ultra Low Profile Inverted L Antenna on a Finite Conducting Plane”, *Proc. International Sympoisum on Antennas and Propagat*., pp.361-364, 2009.

[13] E. Rohadi and M. Taguchi, ”Ultra Low Profile Antenna for 2.45 GHz Wireless Communications”, *Proc. IEEE Int. Conf. on Communication and Satellite (Comnetsat)*, pp. 103-107, 2012. DOI: 10.1109/ComNetSat.2012.6380786.

[14] E. Rohadi and M. Taguchi, ”Two element ultra low profile inverted L antennas on finite conducting plate for MIMO applications”, *Proc. IEEE Int. on Advanced Tech. for Comms. (ATC)*, pp. 74-77, 2013. DOI: 10.1109/ATC.2013.6698080.

[15] E. Rohadi and M. Taguchi, ”Two Low Profile Unbalanced Fed Inverted L Elements on Square Conducting Plane for MIMO Application”, *Wireless Engineering and Technology*, Vol.5, No.2, pp .34-43, April 2014. DOI: 10.4236/wet.2014.52005

[16] J.R. Costa, E.B. Lima, C.R. Medeiros and C.A. Fernandes, ”Evaluation of a new wideband slot array for MIMO performance enhancement in indoor WLANs”, *IEEE Trans. Antenna Propagat*., Vol. 59, pp. 1200-1206, April 2011. DOI: 10.1109/TAP.2011.2109685.

[17] S. Cui, S.X. Gong, Y. Liu and Y. Guan, ”Compact and low coupled monopole antennas for MIMO systems applications”, *Journal of Electomagn. Waves and Application*, Vol. 25, pp. 703-712, 2011. DOI: 10.1163/156939311794827221.

[18] A.A. Abouda and S.G. Hagman, ”Effect on mutual coupling capacity on MIMO wireless channels in high SNR scenario”, *Progress In Electromag., PIER*, Vol. 65, pp. 27-40, 2006. doi:10.2528/PIER06072803

[19] C. Votis, G. Tati and P. Kostarakis, ”Envelope Correlation Parameter Meas-

urements in a MIMO Antenna Array Conficguration", *Int. Journal Comm., Network and System Science*, Vol. 3, pp. 350-354, 2010. DOI:10.4236/ijsn.2010.34044.

[20] WIPL-D d.o.o.: http://www.wipl-d.com/, WIPL-D Pro v11.0, 2013.

[21] H. Paul, "The significance of radiation efficiencies when using S-parameter to calculate the received signal correlation from two antennas", *IEEE Antennas and Wireless Propagation Letters*, Vol. 4, No. 1, pp. 97-99, June 2005.

[22] J. Thaysen and K.B. Jakobsen, "Envelope correlation in (N,N) MIMO antenna array from scattering parameters", *Microwave Opt. Tech. Letter*. Vol. 48, pp.832-834, 2006. DOI: 10.1002/mop.21490.

VII. Summary of Publications

[i] Unbalanced Fed Ultra Low Profile Inverted L Antenna on a Rectangular Conducting Plane; Equivalent Circuit Expression

The characteristics of the unbalanced fed ultra low profile inverted L (ULPIL) antenna are compared with those of the base fed inverted F (BFIF) antenna. The mechanisms of impedance matching of two antennas are discussed. In the BFIF antenna, the short-circuited stub is connected in parallel with the base fed inverted L antenna. In the ULPIL antenna, the short-circuited stub seen to the base and the open-circuited stub seen to the antenna end are connected in series at the feed point. The input impedance of base fed inverted L antenna is compensated with two stubs. This means that the ULPIL antenna is the transmission line type antenna with a built-in automatic tuning circuit.

[ii] Dual Band MIMO Antenna Composed of Two Low Profile Unbalanced Fed Inverted L Antennas for Wireless Communications

A low profile dual-band multiple-input-multiple-output (MIMO) antenna system is proposed. The proposed MIMO antenna consists of two low profile unbalanced fed inverted L antennas with parasitic elements to resonate at 2.45 GHz and 5 GHz. The structure is uncomplicated by locating two ultra low profile inverted L antennas on the finite conducting plane. The proposed MIMO antenna is numerically and experimentally analyzed. When the size of conducting plane is 55 mm by 55 mm and the height of antenna is 9 mm, the directive gain of 4.11 dBi and the return loss bandwidth of 5.71% are achieved for lower frequency of 2.45 GHz. At the upper frequency of 5 GHz, the directive gain of 8.22 dBi and the return loss bandwidth of 6% are obtained. The proposed antenna has good diversity gain, shown by the correlation coefficient becomes less than 0.005 at the frequency of 2.45 GHz and 5 GHz band when the distance between inverted L elements is 41 mm. A good agreement between calculated and measured results is obtained. The results show the weak mutual coupling of the proposed antenna and

this feature enables it to cover the required bandwidths for WLAN operation at the 2.4 GHz band and 5 GHz band.

[iii] Two Low Profile Unbalanced Fed Inverted L Elements on Square Conducting Plane for MIMO Applications

Two ultra low profile inverted L antennas are located on the square conducting plane is numerically and experimentally analyzed as the multiple input multiple output (MIMO) antenna system. When the size of conducting plane is 0.45 λ by 0.45 λ and the height of antenna is 0.03 λ, the directive gain of 4.12 dBi and the return loss bandwidth of 3.67% are achieved. The proposed antenna has good diversity gain, shown by the correlation coefficient becomes less than 0.02 at the frequency of 2.45 GHz band when the distance between inverted L elements are 0.33 λ. The results show the weak mutual coupling of the proposed antenna and its performances are promising as MIMO antenna applications

[iv] Two element ultra low profile inverted L antennas on finite conducting plate for MIMO applications

As the multiple input multiple output (MIMO) antenna system, two ultra low profile inverted L antennas are located on the rectangular conducting plane is proposed and numerically analyzed. The directive gain of 4.12 dBi and the return loss bandwidth of 3.27% are achieved when the size of conducting plane is 0.45λ by 0.45 λ (λ: wavelength). The results show the weak mutual coupling of the proposed antenna and its characteristics are promising as MIMO antenna application

[v] Ultra Low Profile, Unbalanced FED Inverted F Antenna for 2.45 GHz Wireless Communication System

An ultra low profile unbalanced inverted antenna is proposed, which is analyzed numerically and its characteristics are compared with those ultra low profile inverted L antenna and conventional base fed inverted antenna then compared with its measured results. The design frequency is 2.45 GHz. When the size of

conducting plane is 0.245λby 0.49λand antenna height isλ/20, the return loss bandwidth less than -10 dB becomes 3.67 % and the directive gain is 4.15 dBi. In the numerical analysis, the electromagnetic simulator "WIPL-D" based on the method of moment is used.

[vi] Ultra Low Profile Antenna for 2.45 GHz Wireless Communication

The ultra low profile, conventional base fed F antenna is analyzed numerically and its characteristics are compared with those of the unbalanced fed, ultra low profile inverted L antenna. The design frequency is 2.45 GHz. When the size of conducting plane is 0.17 λ by 0.49 λ and the antenna height is 0.08 λ the return loss bandwidth less than -10 dB becomes 15.92 % and the directivity is 3.94 dBi. In the numerical analysis, the electromagnetic simulator "WIPL-D" based on the method of moment is used.

[vii] Ultra Low profile, Unbalanced Fed Inverted F Antenna on Finite Conducting Plane

The ultra low profile, unbalanced fed inverted F antenna is proposed and its characteristics are compared with those of the base fed inverted F antenna and the ultra low profile inverted L antenna. When the size of conducting plane is 0.245λby 0.49λand antenna height is l/30, the return loss bandwidth less than -10 dB becomes 2.45 % and the directivity is 4.35 dBi. In the numerical analysis, the electromagnetic simulator "WIPL-D" based on the method of moment is used.

VIII. General Conclusion

This thesis contributes to the advancement in design of dual band MIMO antenna at frequency band of 2.45 GHz and 5 GHz for wireless communication. Based on inverted L antenna structures, the proposed dual band MIMO are studied to obtain the good performances at the frequency bands. The base fed and unbalanced fed inverted F antennas are also studied. In diversity and MIMO performance evaluation, the studied antennas have been evaluated by measurements.

Moreover, dual band MIMO antennas for diversity need to be small, to be simple design, provides good impedance matching, low mutual coupling and envelope correlation between antennas.

Apart from the mentioned topics, future work should also consider the availability and current trends of advanced signal processing and developed triple or more bands MIMO antennas. Thus, many interesting challenges are waiting to be addressed in the near future.

Publications

Unbalanced Fed Ultra Low Profile Inverted L Antenna on a Rectangular Conducting Plane

Equivalent Circuit Expression

Mitsuo Taguchi
Graduate School of Engineering
Nagasaki University
Nagasaki, Japan
mtaguchi@nagasaki-u.ac.jp

Erfan Rohadi
Graduate School of Engineering
Nagasaki University
Nagasaki, Japan
bb52211281@cc.nagasaki-u.ac.jp

***Abstract*—The characteristics of the unbalanced fed ultra low profile inverted L (ULPIL) antenna are compared with those of the base fed inverted F (BFIF) antenna. The mechanisms of impedance matching of two antennas are discussed. In the BFIF antenna, the short-circuited stub is connected in parallel with the base fed inverted L antenna. In the ULPIL antenna, the short-circuited stub seen to the base and the open-circuited stub seen to the antenna end are connected in series at the feed point. The input impedance of base fed inverted L antenna is compensated with two stubs. This means that the ULPIL antenna is the transmission line type antenna with a built-in automatic tuning circuit.**

Keywords—low profile antenna; inverted L antenna; unbalanced feed; tuning circuit

I. INTRODUCTION

The input impedance of horizontal dipole located very close to a perfect conducting plane becomes low due to the existence of a metallic structure, and it approaches zero as the distance decreases toward zero [1 - 3]. An "ultra low profile dipole (ULPD) antenna", which is a horizontal dipole very closely located to an infinite conducting plane was proposed to solve the impedance matching issue [4]. A half wavelength dipole is excited at the offset points from its center, so that reasonable impedance can be obtained even with a conducting plane in proximity to the dipole. The maximum gain of 8.4 dBi, which is higher than that of a half-wave dipole with a quarter wavelength distance between the dipole and the reflector, is obtained. In order to realize ULPD, however, a 3 dB coupler and a 90° phase shifter are needed. The authors have applied the unbalanced feed to the ultra low profile inverted L antenna located very close on a rectangular conducting plane and analyzed numerically and experimentally [5]. We may call this antenna as "ULPIL antenna" for convenience.

As a low profile antenna, the base fed inverted F (BFIF) antenna is well known [6-12]. This antenna is composed of the base fed inverted L antenna and the short-circuited stub for impedance matching. In this paper, the characteristics of ULPIL antenna are compared with those of the BFIF antenna. The mechanisms of impedance matching of two antennas are compared. In the numerical analysis, the electromagnetic simulator WIPL-D based on the Method of Moments is used [13].

II. STRUCTURE OF PROPOSED ANTENNA

Fig. 1(a) shows the structure of the ULPIL antenna located on a rectangular conducting plane. The size of conducting plane is *pxp+pxm* by *pyp+pym*. The semi-rigid coaxial cable with the characteristic impedance of 50 Ω is mounted on the conducting plane. The radius of the outer conductor is 1.095 mm and that of the inner conductor is 0.255 mm, and the polytetrafluoroethylene is filled within a coaxial cable [14]. This antenna consists of a horizontal arm in the y-direction and a small leg in the z-direction. The coaxial cable is extended behind ground plane. The generator is connected to the bottom end of coaxial cable. The inner conductor of the coaxial cable is extended from the end of outer conductor, that is, this antenna is excited at the end of outer conductor in the numerical analysis. The height of horizontal element is *h*. Fig. 1(b) shows the conventional, base fed inverted F antenna. The design frequency is 2.45 GHz.

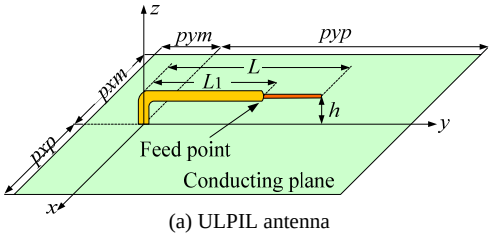

(a) ULPIL antenna

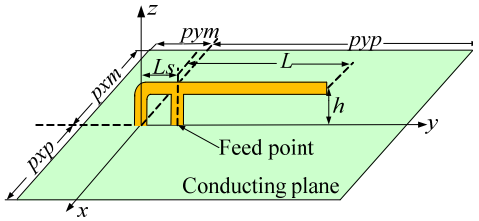

(b) BFIF antenna

Figure 1. ULPIL antenna and BFIF antenna on a rectangular conducting plane.

III. Results and Discussion

A. ULPIL antenna

The fixed antenna parameters are as follows; *pxp* = *pxm* = 15 mm, *pym* = 10 mm, *pyp* = 44 mm. Table 1 shows the return loss bandwidth and the directivity of ULPIL antenna for different antenna height *h*. The length of horizontal element *L* and the feed point position L_1 are optimized so that the resonant frequency becomes to be 2.45 GHz.

Fig. 2 shows the input impedance characteristics of ULPIL for different *L*. L_1 = 22.6 mm, *h* = 4mm are fixed. In the case of *L* = 31 mm, the resonant frequency becomes to be 2.45 GHz. In the figure, the input impedances at the design frequency of 2.45 GHz are indicated by "x". When *L* is 30 mm, the input reactance becomes capacitive. On the other hand, when *L* is 32 mm, the input reactance becomes inductive. This is easily explained by the transmission line theory [15]. The input reactance of the open-circuited parallel line becomes capacitive if its length becomes shorter than a quarter wavelength. Fig. 3 shows the reflection coefficient for different *L*. L_1 is optimized so that the S11 becomes smallest at the resonant frequency in each case. The resonant frequencies in the case of *L* = 30 mm, 31 mm, and 32 mm are 2.535 GHz, 2.45 GHz, and 2.375 GHz, respectively. The length of *L* becomes almost a quarter wavelength at each resonant frequency. This means that the resonant frequency can be adjusted by *L*.

TABLE I. Return Loss and Directivity of ULPIL Antenna for Differenet Antenna Height.

h	*L*	L_1	Return Loss Bandwidth			Directivity at 2.45GHz
(mm)	(mm)	(mm)	f_{low} (GHz)	f_{high} (GHz)	(%)	(dBi)
2	31.8	26.9	2.439	2.459	0.82	4.79
4	31.0	22.6	2.417	2.480	2.57	4.34
6	29.8	18.2	2.392	2.509	4.78	4.18
8	28.3	14.2	2.386	2.545	6.49	4.01
10	26.8	9.9	2.334	2.581	10.08	3.81

pxm = *pxp* = 15 mm, *pym* = 10 mm, *pyp* = 44 mm

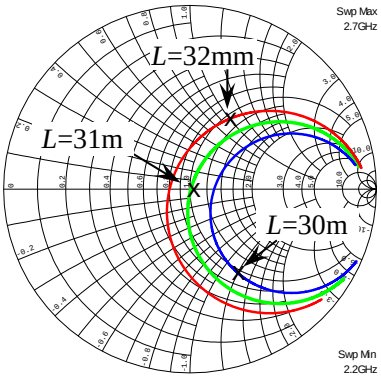

Figure 2. Input impedance characteristics of ULPIL antenna for different *L*. *h* = 4 mm, L_1 = 22.6 mm, *pxm* = *pxp* = 15 mm, *pym* = 10 mm, *pyp* = 44 mm.

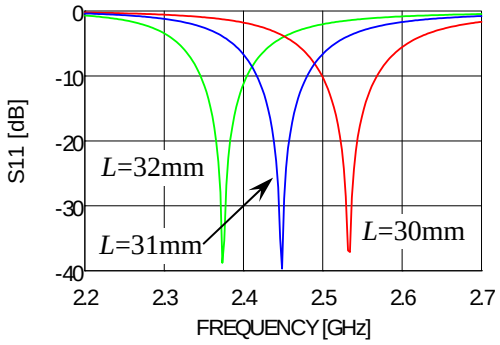

Figure 3. S11 characteristics of ULPIL antenna for different *L*. L_1 is optimized. *h* = 4 mm, *pxm* = *pxp* = 15 mm, *pym* = 10 mm, *pyp* = 44 mm.

Fig. 4 shows the calculated current distributions of ULPIL with L_1 = 22.6 mm and that of the base fed inverted L antenna. The input impedance is defined by the ratio of the impressed voltage and the feed point current. Therefore the input resistance becomes smaller, as L_1 becomes smaller. The input impedance is 50 Ω in the case of L_1 is 22.6 mm. That of base fed inverted L antenna is 4.06+j26.85 Ω. The directivity of ULPIL with L_1 = 22.6 mm and the base fed inverted L antenna are 4.34 dBi and 4.86 dBi, respectively. Since the input impedance of the base fed inverted L antenna is mismatched to 50 Ω, its actual gain becomes small.

B. BFIF antenna

The parameters of conducting plane are fixed as *pxp* = *pxm* = 15 mm, *pym* = 10 mm, and *pyp* = 44 mm. Table 2 shows the return loss bandwidth and the directivity of the BFIF antenna for different antenna height *h* in the case of the length of short stub L_s =3.3 mm. Fig. 5 shows the input impedance characteristics of the BFIF antenna for different *h*. In the BFIF antenna, the input impedance is adjusted by changing the element length *L* and short-circuited stub length L_s.

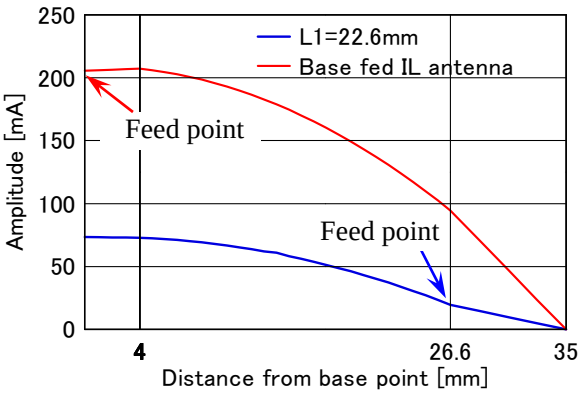

Figure 4. Calculated current distribution at 2.45 GHz for different L_1. *h* = 4 mm, *L* =31 mm, *pxm* = *pxp* = 15 mm, *pym* = 10 mm, *pyp* = 44 mm.

Fig. 6 shows the comparison of the return loss bandwidth between ULPIL antenna and BFIF antenna. When the height *h* of the BFIF antenna is less than 7 mm (about 0.05 λ), the return loss bandwidth larger than 10 dB is not satisfied even though the short stub is added. Therefore, in Fig. 6, data are not shown in the case of *h* is less than 7 mm.

C. Equivalent Circuits

The BFIF antenna is composed of the base fed inverted L antenna and the short-circuited stub. Fig. 7 shows the base fed inverted L antenna and the short-circuited stub. In order to evaluate the electrical length of vertical element of antenna, the monopole antenna with its height *h* shown in Fig. 7(c) is calculated. Fig. 8 shows the equivalent circuit of BFIF antenna. The input admittance of the base fed inverted L antenna is shown at A. The short-circuited stub is connected in parallel with the base fed inverted L antenna at the bend (B).

TABLE II. RETURN LOSS AND DIRECTIVITY OF BFIF ANTENNA FOR DIFFERENET ANTENNA HEIGHT.

Ls	***h***	***L***	**Return Loss Bandwidth**			**Directivity at 2.45GHz**
(mm)	**(mm)**	**(mm)**	f_{low} **(GHz)**	f_{high} **(GHz)**	**(%)**	**(dBi)**
3.3	7	26.2	2.388	2.520	5.39	4.02
3.3	8	25.6	2.353	2.556	8.29	3.92
3.3	9	24.9	2.334	2.587	10.33	3.80
3.3	10	24.3	2.312	2.610	12.16	3.69

pxm = *pxp* = 15 mm, *pym* = 10 mm, *pyp* = 44 mm

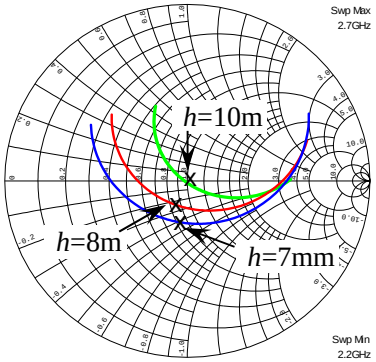

Figure 5. Input impedance characteristics of base fed inverted F antenna for different *h*.
pxm = *pxp* = 15 mm, *pym* = 10 mm, *pyp* = 44 mm, *Ls* = 3.3 mm.

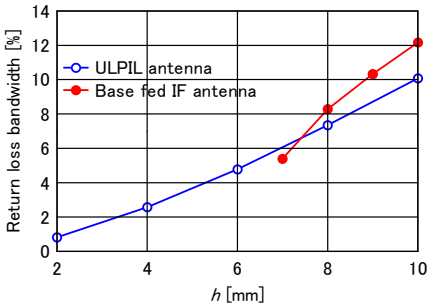

Figure 6. Comparison of return loss bandwidth between ULPIL antenna and base fed inverted F antenna.
pxm = *pxp* = 15 mm, *pym* = 10 mm, *pyp* = 44 mm, *Ls* = 3.3 mm.

Fig. 9 shows the how the short-circuited stub works as the matching circuit. The antenna height *h* is 6 mm, the length of short-circuited stub *Ls* is 3.3 mm. In this case, the return loss larger than 10 dB is not satisfied. The input admittances of base fed inverted L antenna and BFIF antenna at the design frequency of 2.45 GHz are indicated as A (Y_{BFIL}) and D (Y_{BFIF}), respectively. In the figure, the input admittances of base fed inverted L antenna at the frequency of 2.4 GHz and 2.5 GHz are indicated as $A_{2.4}$ and $A_{2.5}$, respectively. The input admittances of BFIF antenna are shown as $D_{2.4}$ and $D_{2.5}$. The input admittances of the short-circuited stub and the monopole antenna are shown as F (Y_{SS}) and G (Y_{Mono}), respectively. The short-circuited stub is connected at the bend of inverted L antenna. Therefore the observation point is moved from the feed point to the bend. Therefore, the phase shift from A to B on the Smith chart is considered corresponding to the length of antenna height. The normalized susceptance at B is *j*2.252. This susceptance is partially cancelled by the short-circuited stub. Consequently, the input admittance of BFIF antenna is shown at D. In order to match the input admittance, larger susceptance of short-circuited stub is needed as the antenna height becomes shorter. This is why the return loss larger than 10 dB is not satisfied in the case of *h* = 6 mm and *Ls* = 3.3 mm.

Next, the matching mechanism of the ULPIL antenna is discussed. Fig. 10 shows the base fed inverted L antenna. Fig. 11 shows the equivalent circuit of ULPIL antenna. The input impedance of base fed inverted L antenna (BFIL) is shown at A. The short-circuited stub seen to the base and the open-circuited stub seen to the antenna end are connected at the feed point B of ULPIL antenna. Therefore the observation point of the input impedance is moved from the base to the feed point.

(a) Base fed inverted L antenna (BFIL)

(b) Short-circuited stub (SS)

(c) Monopole antenna
Figure 7. Components of BFIF antenna.

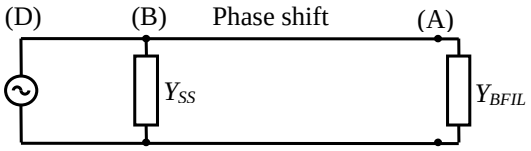

Figure 8. Equivalent circuit of BFIF antenna.

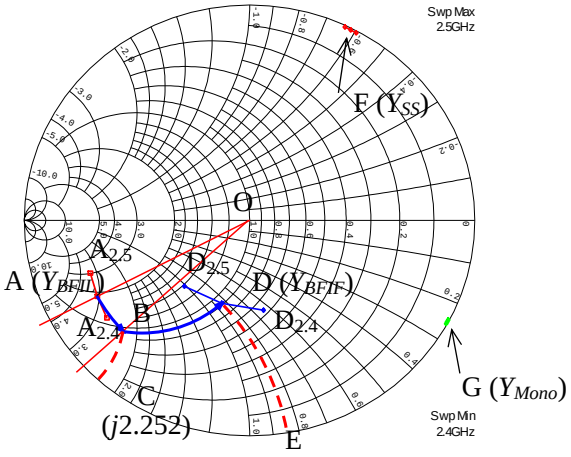

Figure 9. Impedance matching of BFIF antenna.
h=6mm, *L*=23.3mm, *Ls*=5mm, *pxp*=*pxm*=15mm, *pym*=10mm, *pyp*=44mm.

Figure 10. Base fed inverted L antenna (BFIL).

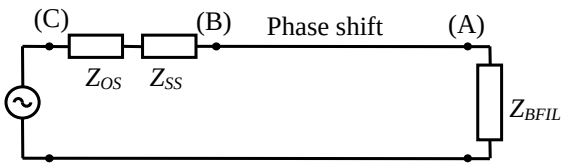

Figure 11. Equivalent circuit of ULPIL antenna.

Fig. 12 shows the how the input impedance is matched. The input impedance of base fed inverted L antenna and ULPIL antenna at the design frequency of 2.45 GHz are indicated as A and C, respectively. In the figure, the input impedances of base fed inverted L antenna at the frequency of 2.4 GHz and 2.5 GHz are indicated as $A_{2.4}$ and $A_{2.5}$, respectively. The input impedances of ULPIL antenna are also shown as $C_{2.4}$ and $C_{2.5}$. The phase shift from the base to the feed point of ULPIL antenna is shown as A to B in the Smith chart. At the feed point, the short-circuited stub and the open-circuited stub are connected in series. The input impedance of two stubs is almost opposite phase to the input capacitance at B. Therefore, the input capacitance at B is cancelled by the two stubs connected in series. As a result, the input impedance of ULPIL antenna is matched to 50 Ω at C.

IV. Conclusion

The ULPIL antenna has been analyzed numerically and its characteristics have been compared with those of the BFIF antenna. The mechanism of impedance matching of these two antennas have been discussed. In the BFIF antenna, the short-circuited stub is connected in parallel with the base fed inverted L antenna. As the antenna height becomes shorter, the short-circuited stub with shorter length is needed. On the other hand, in the ULPIL antenna, the short-circuited stub seen to the base and the open-circuited stub seen to the antenna end are connected in series at the feed point. The input impedance

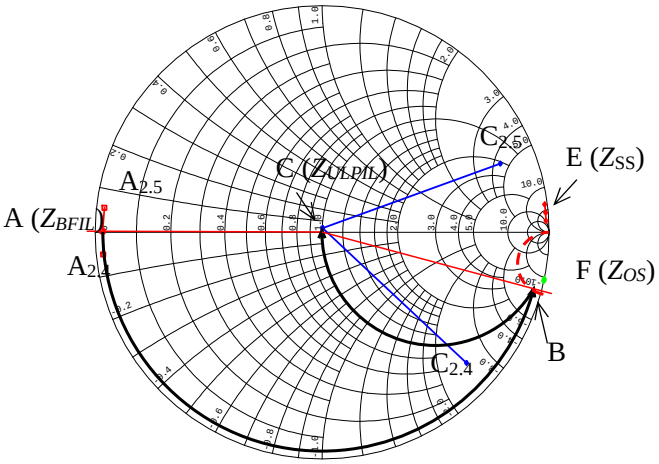

Figure 12. Impedance matching of ULPIL antenna.
h=2mm, *L*=31.8mm, L_1=26.9mm, *pxp*=*pxm*=15mm, *pym*=10mm, *pyp*=44mm

of base fed inverted L antenna is compensated with two stubs. This means that the ULPIL antenna has a built-in automatic tuning circuit.

References

[1] J. D. Kraus: Antennas. New York: McGraw-Hill, pp. 425–427 and 461-467, 1988.

[2] C. A. Balanis: Antenna Theory Analysis and Design. New York: Wiley, pp. 175–180, 1997.

[3] S. A. Schelkunoff and H. T. Friis: Antennas Theory and Practice. New York: Wiley, 1952.

[4] A. Thumvicit, T. Takano and Y. Kamata: "Characteristics verification of a half-wave dipole very close to a conducting plane with excellent impedance matching", IEEE Trans. on Antennas and Propagat., vol.55, no.1, pp.53-58, Jan.2007.

[5] T. Yamashita and M. Taguchi: "Ultra Low Profile Inverted L Antenna on a Finite Conducting Plane", Proc. 2009 International Symp. on Antennas and Propagation, pp.361-364, Oct.2009.

[6] H. Attia, M. M. Bait-Suwalian and O. M. Ramahi, "Enhanced Gain Planar Inverted-F Antenna with Metamaterial Superstrate for UMTS Applications", *Proc. PIERS.*, Cambridge, USA, pp. 494-497, 2010.

[7] Z. N. Chen, K. Hirasawa, "A New Inverted F Antenna with a Ring Dielectric Resonator", IEEE Trans. On Vehicular Technology, Vol. 48, No. 4, pp. 1029-1032, 1999.

[8] D. Liu and B. P. Gaucher, "The inverted-F antenna height effects on bandwidth", Proc. IEEE Antenna Propag. Symp., Vol. 2A, pp. 367-370, 2005.

[9] D. Liu and B. P. Gaucher, "A branched inverted-F antenna for dual band WLAN applications", Proc. IEEE Int. Symp. Antenna Propagations, Vol.3, pp. 2263-2626, 2004.

[10] E. Rohadi and M. taguchi M. Taguchi, "Ultra Low Profile Antenna for 2.45 GHz Wireless Communications", Proc. 2012 IEEE Int. Conf. on Communication and Networks and Satellite, pp. 103-107, 2012.

[11] S. Schulteis, C. Waldschmidt, C. Kuhnert and W. Wiesbeck, "Design of a Capacitively Loaded Inverted F Antenna **for** Wireless-LAN Applications", Proc. International ITG-Conference on Antennas, 178:187-190, 2003.

[12] K. Ito and T. Hose, "Study on the characteristics of planar inverted F antenna mounted in laptop computers for wireless LAN", Proc. IEEE Int. Symp. Antennas Propag., Vol. 2, pp. 22-25, 2003.

[13] "WIPL-D Pro v11.0 3D Electromagnetic Solver Professional Edition User's Manual", WIPL-D, 2013.

[14] http://www.coax.co.jp/english/semi/219.html.

[15] D. M. Pozar, "Microwave Engineering", Chapter 6, Addison-Wesley Publishing, Reading, MA, 1993.

Wireless Engineering and Technology, 2014, 5, 54-61
Published Online July 2014 in SciRes. http://www.scirp.org/journal/wet
http://dx.doi.org/10.4236/wet.2014.53007

Scientific Research

Dual Band MIMO Antenna Composed of Two Low Profile Unbalanced Fed Inverted L Antennas for Wireless Communications

Erfan Rohadi[1,2], Mitsuo Taguchi[1]

[1]Graduate School of Engineering, Nagasaki University, Nagasaki, Japan
[2]The State Polytechnic of Malang, Malang, Indonesia
Email: bb52211281@cc.nagasaki-u.ac.jp, erfanr@polinema.ac.id, mtaguchi@nagasaki-u.ac.jp

Received 18 April 2014; revised 21 May 2014; accepted 10 June 2014

Abstract

A low profile dual-band multiple-input-multiple-output (MIMO) antenna system is proposed. The proposed MIMO antenna consists of two low profile unbalanced fed inverted L antennas with parasitic elements to resonate at 2.45 GHz and 5 GHz. The structure is uncomplicated by locating two ultra low profile inverted L antennas on the finite conducting plane. The proposed MIMO antenna is numerically and experimentally analyzed. When the size of conducting plane is 55 mm by 55 mm and the height of antenna is 9 mm, the directive gain of 4.11 dBi and the S_{11} bandwidth of 5.71% are achieved for lower frequency of 2.45 GHz. At the upper frequency of 5 GHz, the directive gain of 8.22 dBi and the S_{11} bandwidth of 6% are obtained. The proposed antenna has good diversity gain, shown by the correlation coefficient becomes less than 0.005 at the frequency of 2.45 GHz and 5 GHz band when the distance between inverted L elements is 41 mm. A good agreement between calculated and measured results is obtained. The results show that the weak mutual coupling of the proposed antenna and this feature enables it to cover the required bandwidths for WLAN operation at the 2.4 GHz band and 5 GHz band.

Keywords

Dual Band MIMO, Inverted L Antenna, ILA, Low Profile Antenna, Parasitic Element, Correlation Coefficients, ISM, WCS

1. Introduction

The dual band antennas have been investigated with the development of wireless communication systems in re-

How to cite this paper: Rohadi, E. and Taguchi, M. (2014) Dual Band MIMO Antenna Composed of Two Low Profile Unbalanced Fed Inverted L Antennas for Wireless Communications. *Wireless Engineering and Technology*, **5**, 54-61.
http://dx.doi.org/10.4236/wet.2014.53007

cent years [1]-[8]. Most of these dual or multiple band antennas have an omnidirectional radiation pattern. In some applications such as wireless base station or access point, the unidirectional radiation pattern is needed. In order to realize the unidirectional radiation pattern, the antenna size becomes larger [4] [6] [8]. A higher order mode maybe excited in such antenna and large ripples may exist in the radiation pattern at the upper frequency bands [4]-[6]. The interference and the antenna gain reduction may occur due to the large ripple for base station or access point applications. Therefore the compact dual band antenna with unidirectional radiation pattern is desired. The dual or multiple band MIMO antennas are widely used for wireless communication because they become as an effective solution to enhance the channel capacity [9] [10]. One of authors has proposed the dual band antenna composed of the unbalanced fed inverted L antenna for 1.4 GHz and 2.2 GHz bands [11]. In [11], the parasitic element was located above an unbalanced fed inverted L antenna for higher band excitation. This antenna is promising as the candidate of the dual band antenna because it provides two distinct resonant modes for achieving dual-band operation. Furthermore, the authors have studied the advantages of inverted L antennas for wireless communication systems [12] [13], and proposed the simple design and low cost material antenna for single band MIMO antenna systems [14] [15].

In this paper, a dual band MIMO antenna composed of two parallel identical ultra low profile inverted L antennas located on square conducting plane. The proposed antenna has a simple design and works at frequency bands of 2.45 GHz and 5 GHz. In order to satisfy the MIMO antenna system requirements, the proposed antenna is investigated on mutual coupling between two inverted L elements and diversity gain through correlation coefficient value [16]-[19]. The electromagnetic simulator WILP-D based on the method of moments is used for numerical analysis for the reason of shorter computation time compared with other simulation methods [20]. Then its results are validated with the measurement.

2. Antenna Structure

Figure 1 shows the proposed dual band MIMO antenna. The proposed structure is configured by two low profile inverted L antennas located on finite conducting plate with dimension 55 mm by 55 mm (0.45 $\lambda_{2.45}$ by 0.45 $\lambda_{2.45}$). $\lambda_{2.45}$ is the wavelength at the frequency of 2.45 GHz. The parasitic element is placed above the horizontal element of low profile inverted L antenna. The feed points are located at the distance L_1 from the bend of horizontal elements of the inverted L antennas. Both the lengths of L_1 and L are adjusted to obtain the 50 Ohm impedance matching. In the calculation, the height of inverted L antenna h_1 is set as 5 mm or 6 mm. The length of parasitic elements L_p is determined so that the upper resonant frequency becomes to be 5 GHz. In the previous study in [12], the optimum distance between two inverted L antennas was 41 mm in the case of the conducting plane was 55 mm by 55 mm. Therefore the distance between inverted L antennas d is set to be 41 mm. The inverted L antenna is composed of the semi rigid coaxial cables with the radius of inner and outer conductors are 0.255 mm and 1.095 mm, respectively. The radius of parasitic elements is 1.095 mm. The distance between the vertical element of inverted L antennas and the edge on backside *pym* is set as 10 mm. The distance between the vertical element of inverted L antennas and the edge on front side *pyp* is set as 45 mm. The distances between vertical element of inverted L antennas and outer edge on right and left side *pxp* are fixed as 7 mm.

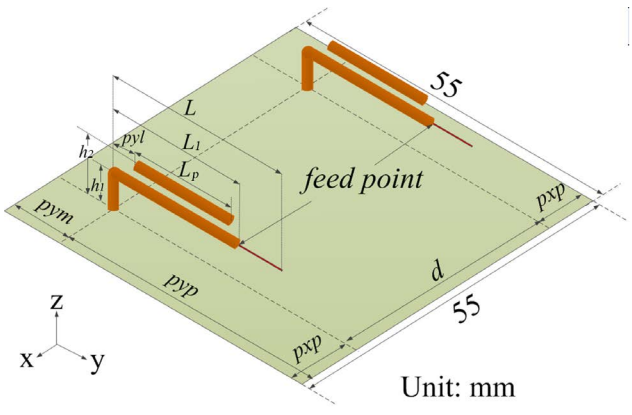

Antenna parameters	Unit:mm	
L	28.9	29.9
L_1	14.4	16.8
L_p	27.1	27.3
h_1	6	5
h_2	9	8
pyl	4.6	4.0
inner radius of wire	0.255	
outer radius of wire	1.095	
conducting plane dimension	55 x 55	
d	41	
pxp	7	
pym	10	
pyp	45	

Figure 1. The structure of proposed MIMO antenna.

3. Results and Discussion

Figure 2 show the calculated scattering parameters of proposed MIMO antenna. The S_{11} bandwidth less than −10 dB of the proposed antenna are 5.71% (2.38 - 2.52 GHz) for lower frequency band and 6% (4.87 - 5.17 GHz) for higher frequency band. The mutual coupling between two ports is less than −21 dB in the lower band and less than −23 dB in the higher one.

Figure 3(a) and **Figure 3(b)** show the calculated current distributions at lower frequency of 2.45 GHz and higher frequency of 5 GHz. The height of inverted L antenna and parasitic element are h_1 = 6 mm and h_2 = 9 mm, respectively. **Figure 4(a)** and **Figure 4(b)** show the calculated current distributions when h_1 = 5 mm and h_2 = 8 mm. A surface current on the conducting plane between two inverted L antennas is small. This means that the proposed structure achieves a good isolation. When the height of inverted L antenna is 5 mm, a large surface current flows on the conducting plane under the inverted L antenna. Due to the strong mutual coupling between inverted L antenna and the conducting plane, the frequency bandwidth becomes slightly narrow.

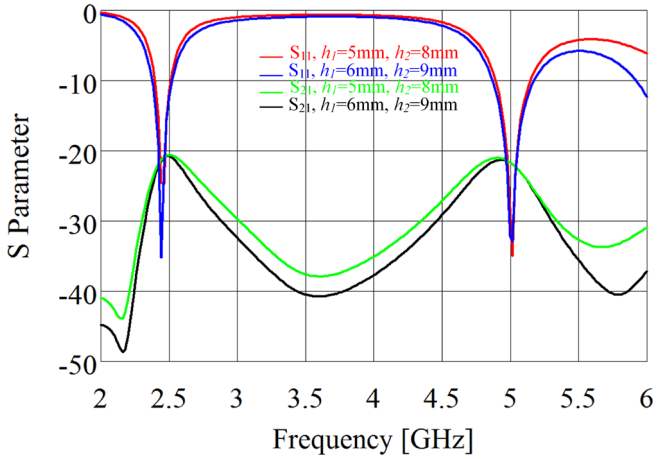

Figure 2. Calculated scattering parameter of proposed antenna. *pyp* = 45 mm, *pxp* = 7 mm, *pym* = 10 mm, *d* = 41 mm.

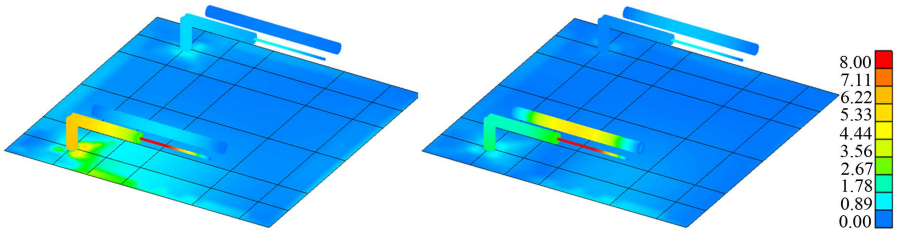

(a) (b)

Figure 3. Current distributions of proposed antenna. h_1 = 6mm, h_2 = 9 mm, *pyp* = 45 mm, *pxp* = 7 mm, *pym* = 10 mm, *d* = 41 mm. (a) 2.45 GHz; (b) 5 GHz.

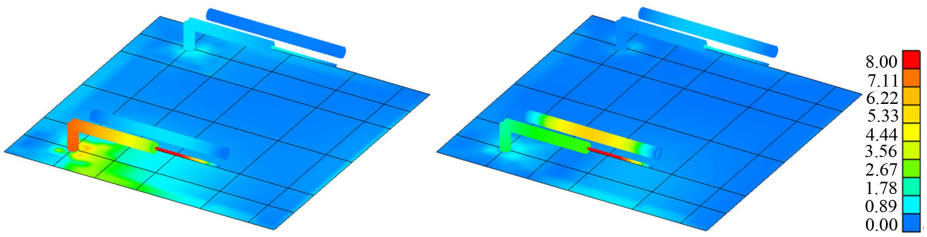

(a) (b)

Figure 4. The calculated current distributions of proposed antenna. h_1 = 5 mm, h_2 = 8 mm, *pyp* = 45 mm, *pxp* = 7 mm, *pym* = 10 mm, *d* = 41 mm. (a) 2.45 GHz; (b) 5 GHz.

Figure 5 show the comparison of calculated and measured scattering parameters of proposed MIMO antenna when the height of inverted L antenna and parasitic elements are h_1 = 6 mm and h_2 = 9 mm, respectively. The scattering parameters are measured by the 6 GHz board network analyzer R3760 by Advantest. The measured scattering parameters agree well with the calculated ones.

Figure 6 shows the directive gain of proposed MIMO antenna in the *z* direction. In both of cases of antenna height, the almost the same directive gain 4.11 dBi is obtained at 2.45 GHz. At 5 GHz, the current on the parasitic element is strongly excited. Since the equivalent size of antenna becomes large, the directive gain more than 8.11 dBi is obtained at this frequency.

The MIMO antenna system correlation factor will be significantly degraded with high coupling levels. It can be calculated from the scattering parameters in isotropic/uniform signal propagation [21]. The correlation coefficient ρ_e is important to achieve the required diversity gain of the MIMO antenna systems. When ρ_e becomes lower, the higher diversity gain is obtained. The value of ρ_e can be calculated by using [22];

$$\rho_e = \frac{\left|S_{11} * S_{12} + S_{21} * S_{22}\right|^2}{\left(1-\left(\left|S_{11}\right|^2 + \left|S_{21}\right|^2\right)\right)\left(1-\left(\left|S_{22}\right|^2 + \left|S_{12}\right|^2\right)\right)} \quad (1)$$

Figure 7 show the calculated correlation coefficients in two cases of antenna height. It is evident that the proposed antenna with enhanced isolation satisfies the MIMO requirements for spatial diversity with the value of ρ_e are less than 0.005 at both of lower and upper frequency bands. **Figure 8** shows the calculated and meas-

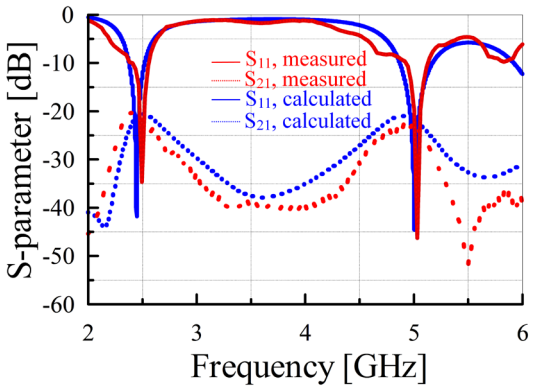

Figure 5. Calculated and measured scattering parameter. h_1 = 6 mm, h_2 = 9 mm, *pyp* = 45 mm, *pxp* = 7 mm, *pym* = 10 mm, *d* = 41 mm.

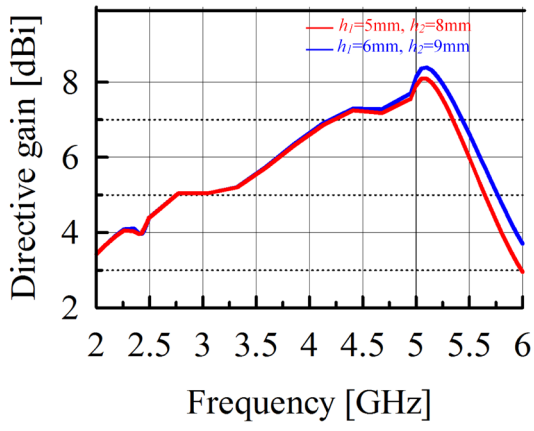

Figure 6. The directive gain of the proposed antenna in z direction. *pyp* = 45 mm, *pxp* = 7 mm, *pym* = 10 mm, *d* = 41 mm.

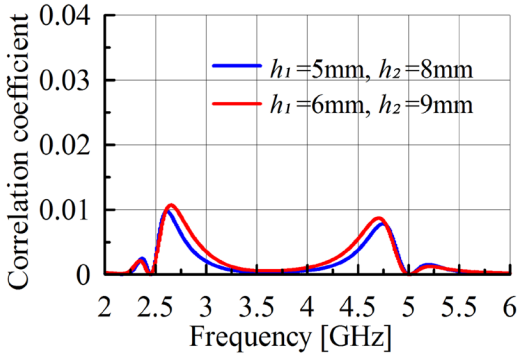

Figure 7. Correlation coefficient. *pyp* = 45 mm, *pxp* = 7 mm, *pym* = 10 mm, *d* = 41 mm.

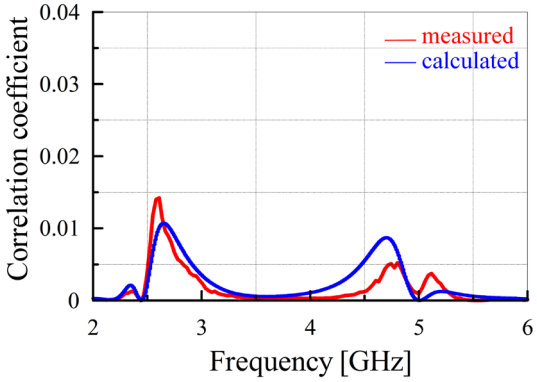

Figure 8. Correlation coefficient. h_1 = 6 mm, h_2 = 9 mm, *pyp* = 45 mm, *pxp* = 7 mm, *pym* = 10 mm, *d* = 41 mm.

ured correlation coefficient of the proposed MIMO antenna when the height of inverted antenna and the height of antenna elements are 6 mm and 9 mm, respectively. A good agreement between calculated and measured results is obtained.

Figure 9 show the calculated electric field radiation pattern in *xy*-plane, *xz*-plane and *yz*-plane at 2.45 GHz and 5 GHz when the height of inverted L antenna is h_1 = 6 mm and height of parasitic element is h_2 = 9 mm, respectively. When the height of inverted of inverted L antenna is reduced to 5 mm, the calculated electric field radiation pattern are shown at **Figure 10**.

As a result, the radiation patterns of the proposed antenna tends to cover complementary space region, which can provide pattern diversity to overcome the multipath fading problem and enhance the system performance.

Figure 11 shows the calculated near field distribution of the proposed antenna in *xz*-plane including the feed point in the case of h_1 = 6 mm and h_2 = 9 mm. The weak mutual coupling between two inverted L antennas is archived. It clearly illustrates that the spatial coupling is dominant at operation frequency bands since the small current are flowing on the conducting plane between two inverted L antennas.

4. Conclusion

In this paper, a simple design and fabrication of dual band MIMO antenna composed of two ultra low profile inverted L antenna has been presented. The proposed antenna satisfies the MIMO system requirements with correlation coefficient less than 0.005 at both frequency bands. When the antenna size is 55 mm by 55 mm by 9 mm, the S_{11} bandwidth of 5.71% (140 MHz) at lower band of 2.45 GHz and 6% (300 MHz) at upper band of 5 GHz are obtained. The directive gains are 4.11 dBi at 2.45 GHz and 8.22 dBi at 5 GHz. The good agreement of calculated and measured scattering parameters and the correlation coefficients are obtained. The presented design is suitable for MIMO communication applications.

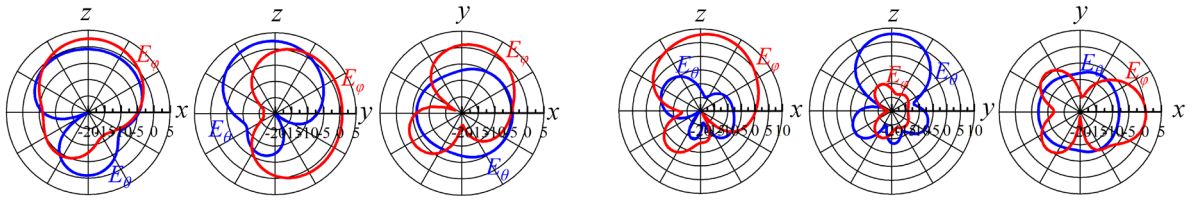

Figure 9. Electric field radiation pattern. h_1 = 6 mm, h_2 = 9 mm, *pyp* = 45 mm, *pxp* = 7 mm, *pym* = 10 mm, *d* = 41 mm. (a) 2.45 GHz; (b) 5 GHz.

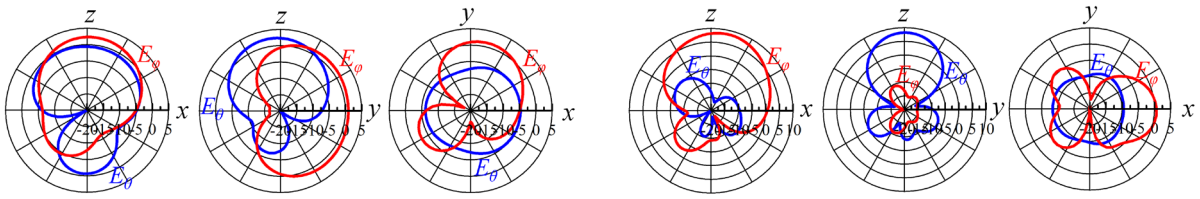

Figure 10. Electric field radiation pattern. h_1 = 5 mm, h_2 = 8 mm, *pyp* = 45 mm, *pxp* = 7 mm, *pym* = 10 mm, *d* = 41 mm. (a) 2.45 GHz; (b) 5 GHz.

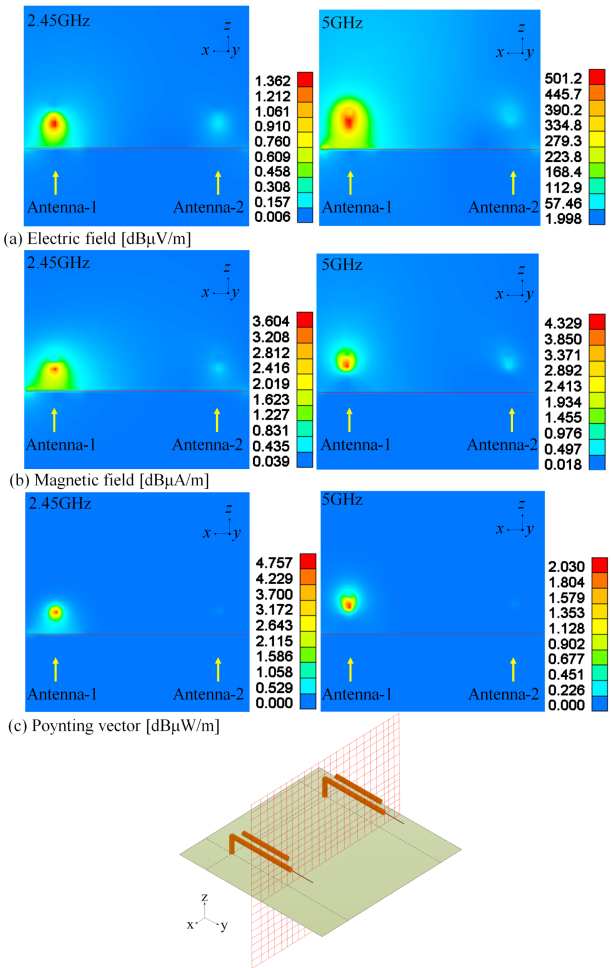

Figure 11. The near field distribution at 2.45 GHz and 5 GHz (h_1 = 6 mm, h_2 = 9 mm, d = 41 mm, *pxp* = 7 mm, *pym* = 10 mm, *pyp* = 45 mm, *L* = 28.9 mm, L_1 = 14.2 mm, L_p = 27.1 mm).

Acknowledgements

ErfanRohadi would like to thank to the General of Higher Education, Ministry Education and Culture of Republic Indonesia for providing the scholarship of the doctoral course program.

References

[1] Kuo, Y.L. and Wong, K.L. (2003) Printed Double-T Monopole Antenna for 2.4/5.2 GHz Dual-Band WLAN Operations. *IEEE Transactions on Antennas and Propagation*, **51**, 2187-2192. http://dx.doi.org/10.1109/TAP.2003.816391

[2] Ding, Y., Du, Z., Gong, K. and Feng, Z. (2007) A Novel Dual-Band Printed Diversity Antenna for Mobile Terminal. *IEEE Transactions on Antennas and Propagation*, **55**, 2088-2096. http://dx.doi.org/10.1109/TAP.2007.900249

[3] Jan, J.Y. and Tseng, L.C. (2004) Small Planar Monopole Antenna with a Shorted Parasitic Inverted-L Wire for Wireless Communications in the 2.4, 5.2, and 5.8-GHz Bands. *IEEE Transactions on Antennas and Propagation*, **52**, 1903-1905. http://dx.doi.org/10.1109/TAP.2004.831370

[4] Wong, K.L., Chou, L.C. and Su, C.M. (2005) Dual-Band Flate-Plate Antenna with a Shorted Parasitic Element for Laptop Applications. *IEEE Transactions on Antennas and Propagation*, **53**, 539-544. http://dx.doi.org/10.1109/TAP.2004.838754

[5] Chen, S.B., Jiao, Y.C., Wang, W. and Zhang, F.S. (2006) Modified T-Shaped Planar Monopole Antennas for Multiband Operation. *IEEE Transactions on Microwave Theory and Techniques*, **54**, 3267-3270. http://dx.doi.org/10.1109/TMTT.2006.877811

[6] Chou, L.C. and Wong, K.L. (2007) Uni-Planar Dual-Band Monopole Antenna for 2.4/5 GHz WLAN Operation in the Laptop Computer. *IEEE Transactions on Antennas and Propagation*, **55**, 3739-3741. http://dx.doi.org/10.1109/TAP.2007.910501

[7] Li, R.L., Pan, B., Laskar, J. and Tentzeris, M.M. (2008) A Novel Low-Profile Broadband Dual-Frequency Planar Antenna for Wireless Handsets. *IEEE Transactions on Antennas and Propagation*, **56**, 1155-1162. http://dx.doi.org/10.1109/TAP.2008.919171

[8] Li, R., Wu, T. and Tentzeris, M. (2008) A Dual-Band Unidirectional Coplanar Antenna for 2.4 - 5-GHz Wireless Application. *Proceedings of the Asia-Pacific Microwave Conference*, December 2008, 1-4. http://dx.doi.org/10.1109/APMC.2008.4958537

[9] Yu, X.H., Wang, L., Wang, H.G., Wu, X.D. and Shang, Y.H. (2012) A Novel Multiport Matching Method for Maximum Capacity of an Indoor MIMO System. *Progress in Electromagnetics Research*, **130**, 67-34. http://dx.doi.org/10.2528/PIER12040603

[10] Zhang, J., Yang, J.O., Zhang, K.Z. and Yang, F. (2012) A Novel Dual-Band MIMO Antenna with Lower Correlation Coefficient. *International Journal of Antennas and Propagation*, **2012**, Article ID: 512975. http://dx.doi.org/10.1155/2012/512975

[11] Sato, S. and Taguchi, M. (2012) Dual Band Ultra Low Profile Inverted L Antenna. *Proceedings of International Symposiumon Antennas and Propagat*, 29 October-2 November, 1417-1420.

[12] Yamashita, T. and Taguchi, M. (2009) Ultra Low Profile Inverted L Antenna on a Finite Conducting Plane. *Proceedings of International Symposiumon Antennas and Propagat*, Bangkok, 20-23 October, 361-364.

[13] Rohadi, E. and Taguchi, M. (2012) Ultra Low Profile Antenna for 2.45 GHz Wireless Communications. *Proceedings of IEEE International Conferece on Communication and Satellite* (*Comnetsat*), 103-107.

[14] Rohadi, E. and Taguchi, M. (2013) Two Element Ultra Low Profile Inverted L Antennas on Finite Conducting Plate for MIMO Applications. *Proceedings of IEEE International Conference on Advanced Technologies for Communications* (*ATC*), Ho Chi Minh City, 16-18 October 2013, 74-77.

[15] Rohadi, E. and Taguchi, M. (2014) Two Low Profile Unbalanced Fed Inverted L Elements on Square Conducting Plane for MIMO Application. *Wireless Engineering and Technology*, **5**, 34-43. http://dx.doi.org/10.4236/wet.2014.52005

[16] Costa, J.R., Lima, E.B., Medeiros, C.R. and Fernandes, C.A. (2011) Evaluation of a New Wideband Slot Array for MIMO Performance Enhancement in Indoor WLANs. *IEEE Transactions on Antennas and Propagation*, **59**, 1200-1206. http://dx.doi.org/10.1109/TAP.2011.2109685

[17] Cui, S., Gong, S.X., Liu, Y. and Guan, Y. (2011) Compact and Low Coupled Monopole Antennas for MIMO Systems Applications. *Journal of Electromagnetic Waves and Applications*, **25**, 703-712. http://dx.doi.org/10.1163/156939311794827221

[18] Abouda, A.A. and Hagman, S.G. (2006) Effect on Mutual Coupling Capacity on MIMO Wireless Channels in High SNR Scenario. *Progress in Electromagnetic*, **65**, 27-40. http://dx.doi.org/10.2528/PIER06072803

[19] Votis, C., Tati, G. and Kostarakis, P. (2010) Envelope Correlation Parameter Measurements in a MIMO Antenna Array Conficguration. *International Journal of Computer Science and Communication Networks*, **3**, 350-354.

[20] WIPL-D d.o.o. (2013) WIPL-D Pro v11.0. http://www.wipl-d.com/

[21] Paul, H. (2005) The Significance of Radiation Efficiencies When Using S-Parameter to Calculate the Received Signal Correlation from Two Antennas. *IEEE Antennas and Wireless Propagation Letters*, **4**, 97-99. http://dx.doi.org/10.1109/LAWP.2005.845913

[22] Thaysen, J. and Jakobsen, K.B. (2006) Envelope Correlation in (N,N) MIMO Antenna Array from Scattering Parameters. *Microwave and Optical Technology Letters*, **48**, 832-834. http://dx.doi.org/10.1002/mop.21490

Scientific Research Publishing (SCIRP) is one of the largest Open Access journal publishers. It is currently publishing more than 200 open access, online, peer-reviewed journals covering a wide range of academic disciplines. SCIRP serves the worldwide academic communities and contributes to the progress and application of science with its publication.

Other selected journals from SCIRP are listed as below. Submit your manuscript to us via either submit@scirp.org or Online Submission Portal.

Wireless Engineering and Technology, 2014, 5, 34-43
Published Online April 2014 in SciRes. http://www.scirp.org/journal/wet
http://dx.doi.org/10.4236/wet.2014.52005

Two Low Profile Unbalanced Fed Inverted L Elements on Square Conducting Plane for MIMO Applications

E. Rohadi[1,2], M. Taguchi[1]

[1]Graduate School of Engineering, Nagasaki University, Nagasaki, Japan
[2]The State Polytechnic of Malang, Malang, Indonesia
Email: bb52211281@cc.nagasaki-u.ac.jp, erfanr@polinema.ac.id, mtaguchi@nagasaki-u.ac.jp

Received 27 January 2014; revised 2 March 2014; accepted 19 March 2014

Abstract

Two ultra low profile inverted L antennas located on the square conducting plane are numerically and experimentally analyzed as the multiple input multiple output (MIMO) antenna system. When the size of conducting plane is 0.45 λ by 0.45 λ and the height of antenna is 0.03 λ, the directive gain of 4.12 dBi and the return loss bandwidth of 3.67% are achieved. The proposed antenna has good diversity gain shown by the correlation coefficient, and becomes less than 0.02 at the frequency of 2.45 GHz band when the distance between inverted L elements is 0.33 λ. The results show the weak mutual coupling of the proposed antenna and its performances are promising as MIMO antenna applications.

Keywords

Low Profile Antenna, Inverted L Antenna, MIMO Antenna, Correlation Coefficient, WIPL-D

1. Introduction

The demand for high data rate and large channel capacity of users in recent mobile communication systems drives the MIMO systems as the subject of investigation for several years [1]. A practical MIMO antenna should have a low signal correlation between antenna elements and good impedance matching characteristics [2] [3]. The mutual coupling is an important factor when antennas have been used for MIMO applications [4] [5]. Higher mutual coupling may result in lower antenna efficiencies and higher correlation coefficients. The effect of mutual coupling on the capacity of MIMO wireless channel was studied in [6]. One of the most critical parameter affecting mutual coupling and correlation is the spacing between antenna elements. Analytical studies

How to cite this paper: Rohadi, E. and Taguchi, M. (2014) Two Low Profile Unbalanced Fed Inverted L Elements on Square Conducting Plane for MIMO Applications. *Wireless Engineering and Technology*, **5**, 34-43.
http://dx.doi.org/10.4236/wet.2014.52005

have shown that the distance between typical antenna elements such as dipole antenna needs to be at least half wavelengths for minimal or no mutual coupling [7]. However, since the distance is limited due to the small area which the elements are placed, especially at the portable MIMO-enabled devices, the MIMO antennas should be designed as small as possible. This is more conspicuous when MIMO antennas will be used in small terminal devices and more effort will be devoted to devising new MIMO antenna elements with compact and reasonable antenna characteristics [8]-[10]. The authors have proposed the unbalanced fed, ultra low profile inverted L antenna on a rectangular conducting plane for mobile terminal devices [11] [12]. When the size of conducting plane is 0.245 λ (λ: wavelength) by 0.49 λ and the antenna height is λ/30, and the length of horizontal element is around a quarter wavelength, the input impedance of this antenna is matched to 50 Ω and its directivity becomes more than 4 dBi. In this antenna, the electromagnetic field is strongly excited between the inverted L element and the conducting plane. Therefore even though two inverted L antennas are closely located, the mutual coupling may be weak.

Several other designs of MIMO antenna satisfy for the requirement of MIMO systems; unfortunately these antennas have limitation of size for practical MIMO application. Also in general, MIMO antennas consist of complicated structures [13]-[18]. For example, in [17], two meandered monopoles with a gamma matching and a folded T-shaped stub between radiators are printed on an FR4 substrate with its size of 30 mm by 15 mm. Its directivity is less than 0 dBi. In this paper, the very simple antenna composed of two unbalanced fed, ultra low profile inverted L antennas on a square conducting plane with its size of 55 mm is proposed as MIMO antenna applications [19]. In the numerical analysis, the electromagnetic simulator WIPL-D based on the Method of Moments is used [20].

2. Antenna Structure

Figure 1 shows the structure of the proposed antenna. Two identical low profile inverted L antenna elements with the height h = 4 mm are mounted on the square conducting plane with its size of 55 mm by 55 mm. The antenna size corresponds to 0.45 λ by 0.45 λ by 0.03 λ at the design frequency of 2.45 GHz. The antenna elements are composed of the semi rigid coaxial cable with outer and inner radius 1.095 mm and 0.255 mm, respectively. The inner conductor of the coaxial cable is extended from the end of outer conductor, that is, each antenna element is excited at the end of outer conductor. The distance d between two antenna elements are investigated in order to reduce the mutual coupling. Furthermore the distance is challenged to be less than half wavelength. Both the distance *pym* between the vertical element to the back edge of the ground plane and distance *pyp* between the vertical element to the front edge are fixed as 10 mm and 45 mm, respectively. In each case of the distance between two antennas, the length of horizontal elements L and $L1$ are optimized to achieve impedance matching at the center frequency of 2.45 GHz. **Figure 2** shows other arrangements of antenna elements.

3. Results and Discussion

In the calculation, the distance d between two inverted L antennas is changed from 30 mm to 45 mm. **Table 1** shows the calculated return loss bandwidth larger than 10 dB, S21 and the directive gain in the z direction at 2.45 GHz for the different distance d between two inverted L elements. **Figure 3** shows calculated S parameters of the optimized proposed MIMO antenna arrangement-1 for different distance d between two antenna elements. S21 becomes smaller than −20 dB as the distance d become longer than 41 mm.

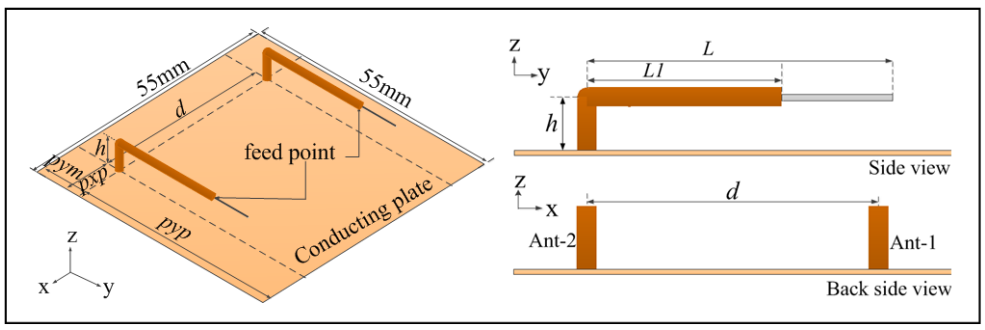

Figure 1. The structure of proposed antenna; arrangement-1 (*pym* = 10 mm, *pyp* = 45 mm, *h* = 4 mm).

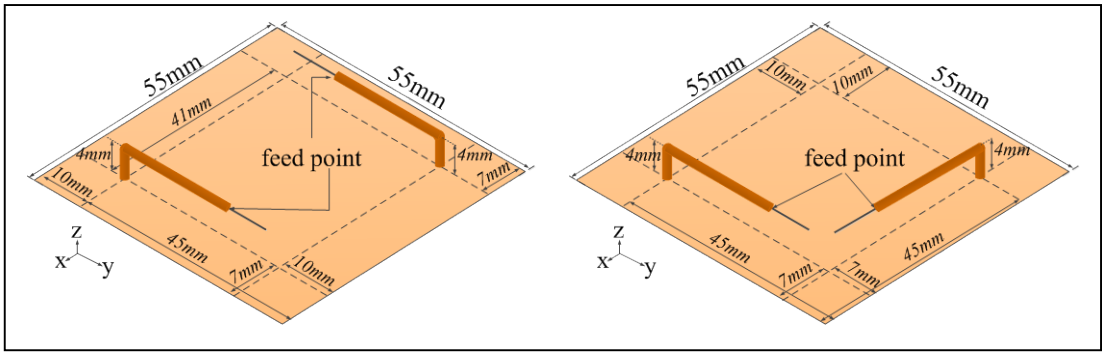

(a) (b)

Figure 2. (a) Arangement-2; opposite parallel and (b) arrangement-3; face to face perpendicular arrangements.

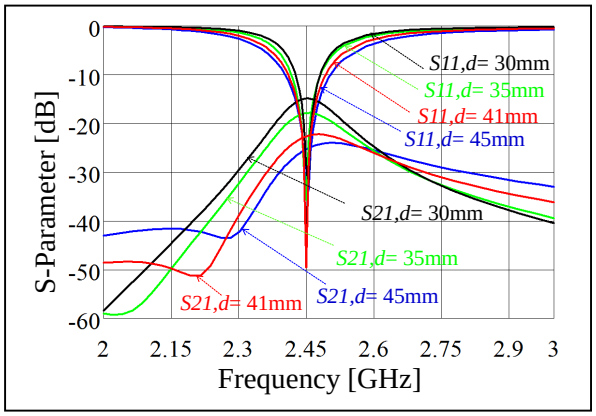

Figure 3. Calculated S parameters of proposed antenna for different *d* (arrangement-1, *h* = 4 mm, *pym* = 10 mm, *pyp* = 45 mm).

Table 1. Calculated return loss bandwidth, S21 and directivity for different distance between two antennas *d* (arrangement-1).

h = 4 mm, *pym* = 10 mm, *pyp* = 45 mm [mm]			Return loss bandwidth		S21 at 2.45 GHz	Dir. Gain at 2.45 GHz
d/pxp	*L*	*L*1	[MHz]	[%]	[dB]	[dBi]
30/12.5	30.7	22.7	50	2.04	−14.83	3.79
35/10	30.9	22.2	60	2.45	−17.86	3.98
41/7	31.2	21.4	90	3.67	−22.64	4.12
45/5	31.4	20.7	100	4.08	−25.28	4.17

Table 2 shows the calculated return loss bandwidth, S21 and the directive gain in the z direction at 2.45 GHz for different antenna height *h*. When the height of antenna is increased, both the length of horizontal elements *L* and *L*1 become shorter. This means that the resonant frequency is determined by the total length of horizontal and vertical elements. **Figure 4** shows calculated S parameters of the proposed MIMO antenna arrangement-1 for different antenna height *h*. The return loss bandwidth and S21 become smaller as the antenna height *h* becomes smaller. As the antenna height becomes smaller, the electromagnetic field concentrates near the excited antenna element. Therefore the return loss bandwidth becomes narrower and the mutual coupling between two antennas becomes weak.

Table 2. Calculated return loss bandwidth and directivity for different antenna height *h* (arrangement-1).

d = 41 mm, *pym* = 10 mm, *pyp* = 45 mm, *pxp* = 7 mm [mm]			Return loss bandwidth		S21 at 2.45 GHz	Dir. Gain at 2.45 GHz
h	*L*	*L*1	MHz	[%]	[dB]	[dBi]
3	31.9	23.9	50	2.04	−24.06	4.09
4	31.2	21.4	90	3.67	−22.64	4.12
5	30.6	19.1	120	4.90	−21.67	4.08
6	29.9	16.8	140	5.71	−20.98	4.05

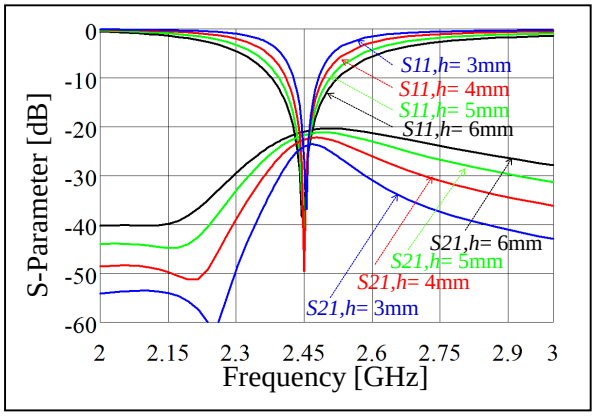

Figure 4. Calculated S parameters of proposed antenna for different *h* (arrangement-1, *d* = 41 mm, *pxp* = 7 mm, *pym* = 10 mm, *pyp* = 45 mm).

Figure 5 shows the return loss bandwidth larger than 10 dB and the directive gain in the z direction at 2.45 GHz of the proposed MIMO antenna arrangement-1 for different distance *d* between two antenna elements and for different height *h* of antenna. Both the directive gain and the return loss bandwidth become larger by extending the distance between two antennas.

Figure 6 shows the directive gain in the z direction at the proposed MIMO antenna arrangement-1. **Figure 7** shows the current distribution of proposed MIMO antenna arrangement-1 at 2.45 GHz. The inverted L element-1 is excited and the element-2 is terminated with 50 Ω load. The large surface current is induced near inverted L element-1, on the other hand weak surface current is induced on the element-2 at resonant frequency of 2.45 GHz. This means that the good isolation between two elements is achieved.

Figure 8 shows the electric field radiation patterns on zx plane, yz plane and xy plane of the proposed MIMO antenna arrangement-1 at 2.45 GHz when inverted L element-1 is fed and inverted L element-2 is terminated by the matching load 50 Ω. The peak gain of antenna-1 is 4.12 dBi. The current distribution on the inverted L antennas in the y direction and the surface on the conducting plane in the x and y directions contribute to the radiation. Therefore there are no deep nulls in any direction, although omnidirectional polarization antennas are used in general.

Figure 9 shows the near field distributions in the zx plane including feed points of arrangement-1, in the zx plane including the feed point of element1 of arrangement-2, and in the yz plane including feed point of element-2 of arrangement-3 at 2.45 GHz.

Figure 10 shows the near field distributions in xy plane including horizontal elements of each arrangement at 2.45 GHz. The good isolation is achieved in the balanced structure as proposed MIMO arrangent-1. Whereas, it can be seen that two elements are highly coupled to each other at arrangement-2 and arrangement-3.

From **Figure 7**, **Figure 9** and **Figure 10**, in the case of proposed MIMO antenna arrangement-1, the surface current on the conducting plane between two antennas is small and the electromagnetic field becomes weak near

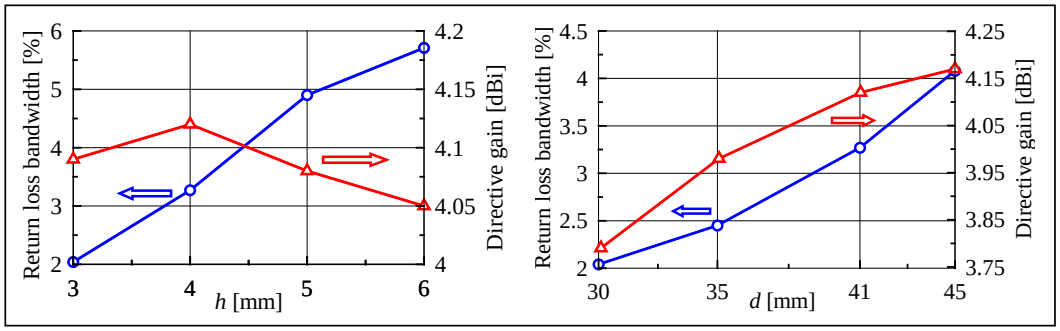

Figure 5. Return loss bandwidth and directive gain in z direction at 2.45 GHz (arrangement-1; *pxp* = 7 mm, *pym* = 10 mm, *pyp* = 45 mm).

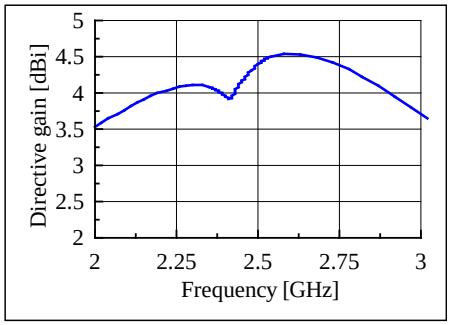

Figure 6. Calculated directive gain at z direction (arrangemet-1; *pxp* = 7 mm, *pym* = 10 mm, *pyp* = 45 mm, *h* = 4 mm, *d* = 41 mm).

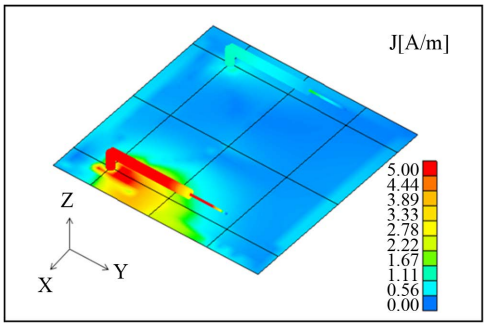

Figure 7. Calculated current distribution at frequency of 2.45 GHz (arrangement-1; *h* = 4 mm, *d* = 41 mm, *pxp* = 7 mm, *pym* = 10 mm, *pyp* = 45 mm, *L* = 31.2 mm, *L*1 = 21.4 mm).

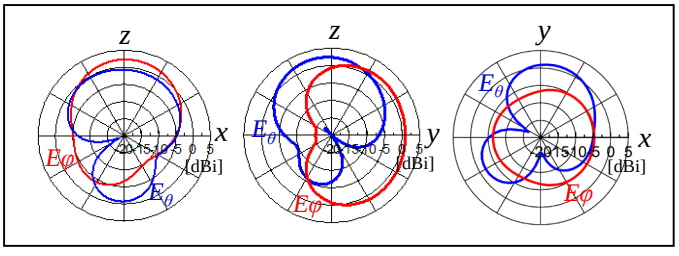

Figure 8. Simulated electric field radiation pattern of proposed antenna at 2.45 GHz (arrangement-1; *h* = 4 mm, d = 41 mm, *pxp* = 7 mm, *pym* = 10 mm, *pyp* = 45 mm, *L* = 31.2 mm, *L*1 = 21.4 mm).

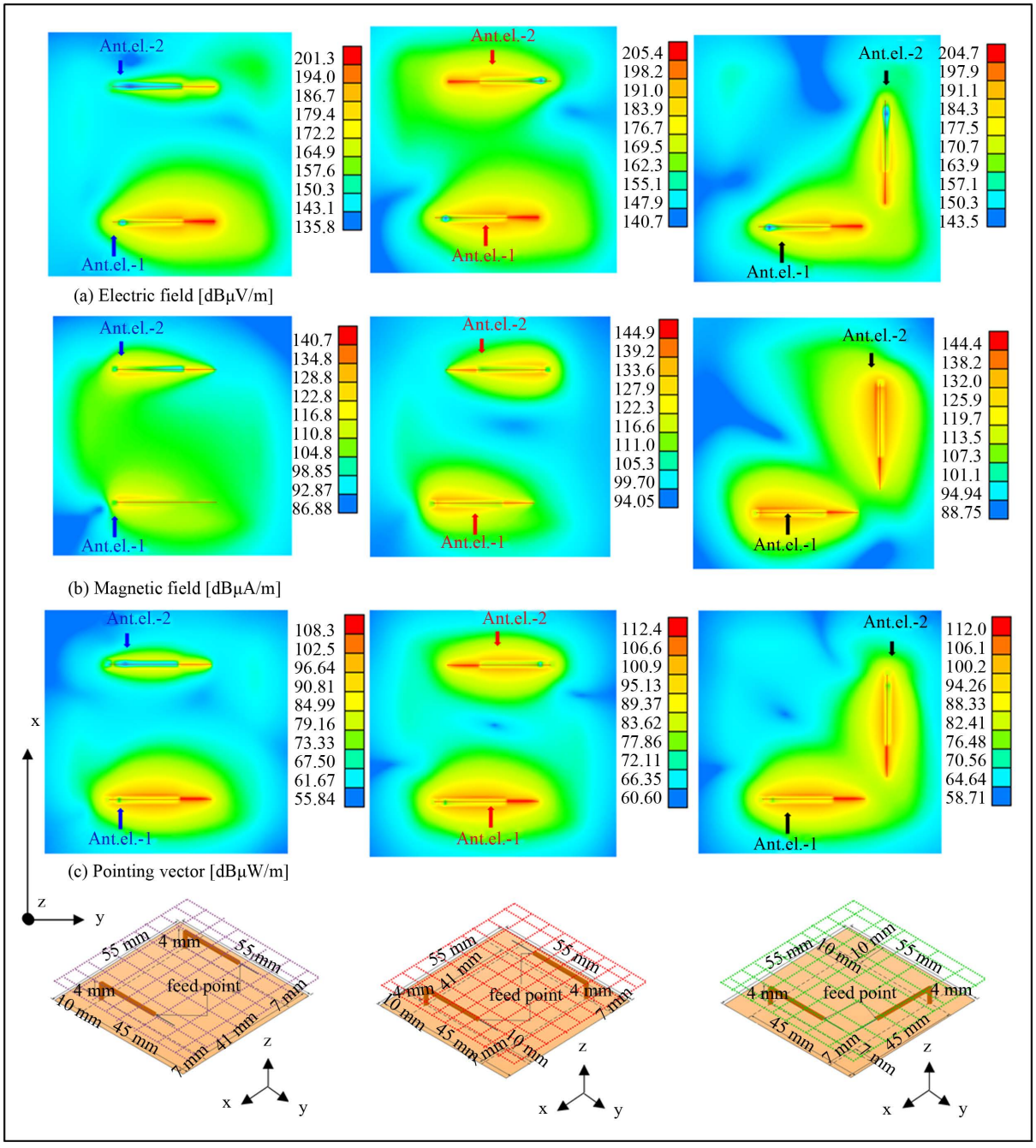

Figure 9. The near field distribution at 2.45 GHz (h = 4 mm, d = 41 mm, pxp = 7 mm, pym = 10 mm, pyp = 45 mm, L = 31.2 mm, $L1$ = 21.4 mm).

the conducting plane between two antennas. This means that the mutual coupling is mainly not by the current flowing on the conducting plane but by the spatial coupling.

Figure 11 shows the reflection coefficients of three arrangements. The placement of inverted L elements as arrangement-1 obtains the best isolation between two elements.

Figure 12 shows the calculated and measured S parameters of proposed MIMO arrangement-1. The fairly good agreement between calculated and measured results is obtained.

The correlation coefficient of the proposed MIMO antenna is calculated through S parameter. The correlation coefficient ρ_e of a two element inverted L antenna system can be calculated by the following equation [21];

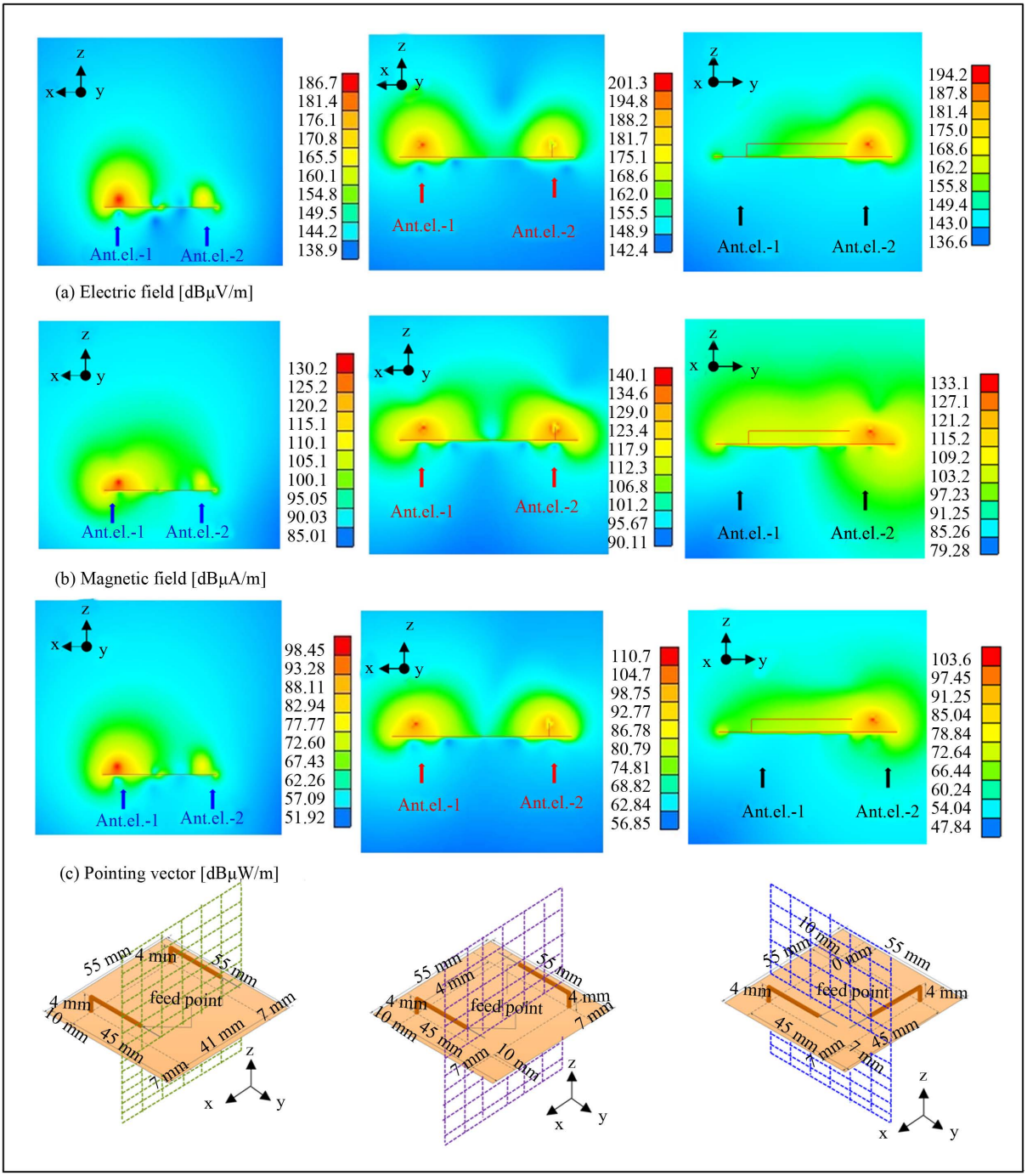

Figure 10. The near field distribution on horizontal elements of xy plane at 2.45 GHz (h = 4 mm, d = 41 mm, pxp = 7 mm, pym = 10 mm, pyp = 45 mm, L = 31.2 mm, $L1$ = 21.4 mm).

$$\rho_e = \frac{\left|S_{11} * S_{12} + S_{21} * S_{22}\right|^2}{\left(1-\left(\left|S_{11}\right|^2 + \left|S_{21}\right|^2\right)\right)\left(1-\left(\left|S_{22}\right|^2 + \left|S_{12}\right|^2\right)\right)} \quad (1)$$

Figure 13 shows calculated and measured correlation coefficient of the proposed MIMO antenna arrangement-1. The correlation coefficient becomes less than 0.02, which means that the proposed antenna has good

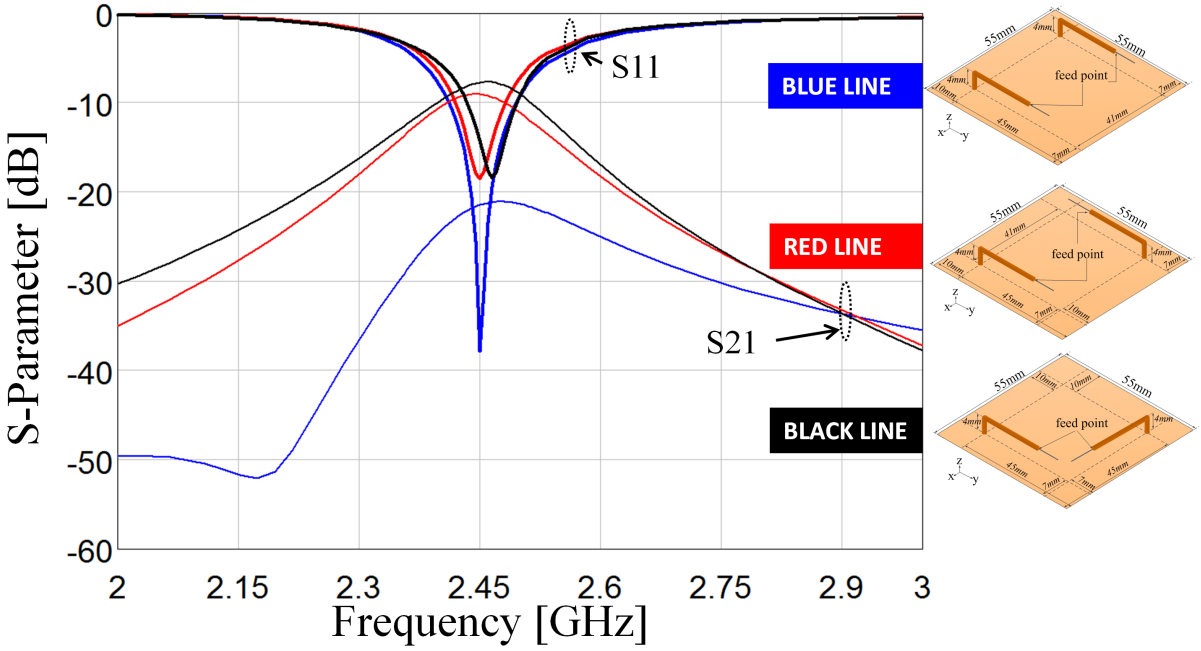

Figure 11. Reflection coefficients of proposed antenna with different arrangements (h = 4 mm, d = 41 mm, pxp = 7 mm, pym = 10 mm, pyp = 45 mm, L = 31.2 mm, $L1$ = 21.4 mm).

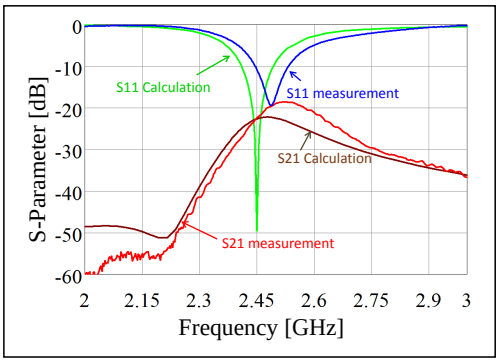

Figure 12. Calculated and measured S parameters of the proposed MIMO antenna (pxp = 7 mm, pym = 10 mm, pyp = 45 mm, h = 4 mm, d = 41 mm).

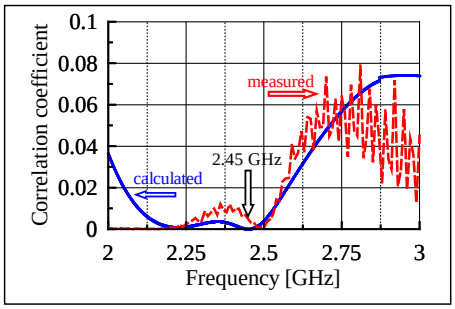

Figure 13. Calculated and measured correlation coefficient between two inverted L antennas (arrangemet-1; pxp = 7 mm, pym = 10 mm, pyp = 45 mm, h = 4 mm, d = 41 mm).

diversity gain when antenna height and the distance between inverted L elements are 4 mm and 41 mm, respectively.

4. Conclusion

The MIMO antenna, composed of two unbalanced fed, ultra low profile inverted L antenna elements, has been proposed. Two inverted L elements are parallel located on the square conducting plane with its size of 045 λ by 0.45 λ. The height of inverted L antennas is 0.03 λ, and the distance between two inverted L antennas is 0.34 λ. With a very simple structure, the antenna has the good performances. The calculated and measured return loss larger than 10 dB is 2.41 to 2.50 GHz and 2.44 to 2.53 GHz, respectively. The directive gain is 4.12 dBi. The proposed antenna is promising for MIMO application systems.

Acknowledgements

Erfan Rohadi would like to thank to the General of Higher Education, Ministry Education and Culture of Republic Indonesia for providing the scholarship of the doctoral course program.

References

[1] Yu, X.H., Wang, L., Wang, H.G., Wu, X.D. and Shang, Y.H. (2012) A Novel Multiport Matching Method for Maximum Capacity of an Indoor MIMO System. *Progress in Electromagnetics Research*, **130**, 67-34. http://dx.doi.org/10.2528/PIER12040603

[2] Ding, Y., Du, Z., Gong, K. and Feng, Z. (2007) A Novel Dula-Band Printed Diversity Antenna for Mobile Terminal. *IEEE Transactions on Antennas and Propagations*, **55**, 2088-2096. http://dx.doi.org/10.1109/TAP.2007.900249

[3] Costa, J.R., Lima, E.B., Medeiros, C.R. and Fernandes, C.A. (2011) Evaluation of a New Wideband Slot Array for MIMO Performance Enhancement in Indoor WLANs. *IEEE Transactions on Antennas and Propagations*, **59**, 1200-1206. http://dx.doi.org/10.1109/TAP.2011.2109685

[4] Karimian, R., Soleimani, M. and Hashemi, S.M. (2012) Tri-Band four Elements MIMO Antenna System for WLAN and WIMAX Application. *Journal of Electromagnetic Waves and Applications*, **26**, 2348-2357. http://dx.doi.org/10.1080/09205071.2012.734433

[5] Cui, S., Gong, S.X., Liu, Y. and Guan, Y. (2011) Compact and Low Coupled Monopole Antennas for MIMO Systems Applications. *Journal of Electromagnetic Waves and Applications*, **25**, 703-712. http://dx.doi.org/10.1163/156939311794827221

[6] Abouda, A.A. and Hagman, S.G. (2006) Effect on Mutual Coupling Capacity on MIMO Wireless Channels in High SNR Scenario. *Progress in Electromagnetics Research Symposium*, **65**, 27-40.

[7] Stutzman, W.L. and Thiele, G.A. (1998) Antenna Theory and Design. 2nd Edition, Wiley, New York, 154-160.

[8] Foschini G.J. and Gans, M.J. (1998) On Limits of Wireless Communications in Fading Environment When Using Multiple Antennas. *Wireless Personal Communications*, **6**, 311-335. http://dx.doi.org/10.1023/A:1008889222784

[9] Fujimoto, K., Henderson, A., Hirasawa, K. and James, J.R. (1987) Small Antennas. Research Studies Press, Letchworth, 116-151.

[10] Hirasawa, K. and Haneishi, M. (1992) Analysis, Design, and Measurement of Small and Low-Profile Antennas. Artech House Inc., Norwood, 165-169.

[11] Yamashita, T. and Taguchi, M. (2009) Ultra Low Profile Inverted L Antenna on a Finite Conducting Plane. *International Sympoisum on Antennas and Propagation*, Bangkok, 20-23 October 2009, 361-364.

[12] Rohadi, E. and Taguchi, M. (2012) Ultra Low Profile Antenna for 2.45 GHz Wireless Communications. *IEEE International Conference on Communication, Networks and Satellite* (*ComNetSat*), Bali, 12-14 July 2012, 103-107.

[13] Votis, C., Tatis, G. and Kostarakis, P. (2010) Envelope Correlation Parameter Measurements in a MIMO Antenna Array Configuration. *International Journal of Communications, Network and System Sciences*, **3**, 350-354. http://dx.doi.org/10.4236/ijcns.2010.34044

[14] Ahn, S.B. and Choo, H.S. (2013) Design of Vehicle of On-Glass 4 × 4 MIMO Antennas for WIBRO Applications. *International Journal of Automotive Technology*, **14**, 731-737.

[15] Zeng, Q., Yao, Y., Liu, S., Yu, J. and Chen, X. (2012) Tetraband Small-Size Printed Strip MIMO Antenna for Mobile Handset Application. *International Journal of Antennas and Propagation*, **2012**, 320582. http://dx.doi.org/10.1155/2012/320582

[16] Lee, J.N, Lee, K.C., Park, N.H. and Park, J.K. (2013) Design of Dual-Band MIMO Antenna with High Isolation for

Mobile Terminal. *ETRI Journal*, **35**, 177-187. http://dx.doi.org/10.4218/etrij.13.0112.0250

[17] Jin, Z., Lim, J.H. and Yun, T.Y. (2012) Small-Size and High-Isolation MIMO Antenna for WLAN. *ETRI Journal*, **34**, 114-117. http://dx.doi.org/10.4218/etrij.12.0211.0083

[18] Kim, S.H., Jin, Z.J., Chae, Y.B. and Yun, T.Y. (2013) Small Antenna Using Multiband, Wideband and High-Isolation MIMO Techniques. *ETRI Journal*, **35**, 51-57. http://dx.doi.org/10.4218/etrij.13.0112.0183

[19] Rohadi, E. and Taguchi, M. (2013) Two Element Ultra Low Profile Inverted L Antennas on Finite Conducting Plate for MIMO Applications. *International Conference on Advanced Technologies for Communications* (*ATC*), Ho Chi Minh City, 16-18 October 2013, 74-77.

[20] WIPL-D d.o.o. (2013) WIPL-D Pro v11.0. http://www.wipl-d.com

[21] Thaysen, J. and Jakobsen, K.B. (2006) Envelope Correlation in (N,N) MIMO Antenna Array from Scattering Parameters. *Microwave and Optical Technology Letters*, **48**, 832-834. http://dx.doi.org/10.1002/mop.21490

Two element ultra low profile inverted L antennas on finite conducting plate for MIMO applications

Erfan Rohadi
Graduate School of Engineering
Nagasaki University
14-1 Bunkyo-machi, Nagasaki, 852-8521 Japan
bb52211281@cc.nagasaki-u.ac.jp

Mitsuo Taguchi
Graduate School of Engineering
Nagasaki University
14-1 Bunkyo-machi, Nagasaki, 852-8521 Japan
mtaguchi@nagasaki-u.ac.jp

***Abstract*—As the multiple input multiple output (MIMO) antenna system, two ultra low profile inverted L antennas are located on the rectangular conducting plane is proposed and numerically analyzed. The directive gain of 4.12 dBi and the return loss bandwidth of 3.27% are achieved when the size of conducting plane is 0.45 λ by 0.45 λ (λ: wavelength). The results show the weak mutual coupling of the proposed antenna and its characteristics are promising as MIMO antenna application.**

Keywords—low profile anetnna; inveted L antenna; MIMO; WIPL-D

I. INTRODUCTION

The demand for high data rate and large channel capacity of users in recent mobile communication systems drives the MIMO systems as the subject of investigation for several years [1]. A practical MIMO antenna should have a low signal correlation between antenna elements and good impedance matching characteristics [2, 3]. The mutual coupling is an important factor when antennas have been used for MIMO applications [4, 5]. Due to the limited space, especially at the portable MIMO-enabled devices, the MIMO antennas should be designed as small as possible. This is more conspicuous when MIMO antennas will be used in small terminal devices and more effort will be devoted to devise new MIMO antenna elements with compact and reasonable antenna characteristics [6-8]. The authors have proposed the unbalanced fed, ultra low profile inverted L antenna on a rectangular conducting plane for mobile terminal devices [9, 10]. When the size of conducting plane is 0.245 λ (λ: wavelength) by 0.49 λ and the antenna height is λ/30, and the length of horizontal element is around a quarter wavelength, the input impedance of this antenna is matched to 50 Ω and its directivity becomes more than 4 dBi. In this antenna, the electromagnetic field is strongly excited between the inverted L element and the conducting plane. Therefore if two inverted L antennas are located closely, the mutual coupling may be weak.

In this paper, the MIMO antenna composed of two ultra law profile inverted L antennas is proposed. In the numerical analysis, the electromagnetic simulator WIPL-D based on method of moment is used [11].

II. ANTENNA STRUCTURE

Fig. 1 shows the structure of the proposed antenna. Two identical low profile inverted L antenna elements with the height h = 4 mm are mounted on the square conducting plane with its size of 55 mm by 55 mm. The antenna size is 0.45 λ by 0.45 λ by 0.03 λ at the design frequency of 2.45 GHz. The antenna elements are composed of the semi rigid coaxial cable with outer and inner radius 1.095 mm and 0.255 mm, respectively. The feed points are located at the edge of the outer conductor on each antenna elements. The distance d between two antenna elements are investigated in order to reduce the mutual coupling. Both the distance *pym* between vertical element to back edge of the ground plane and distance *pyp* between vertical element to the front edge are fixed as 10 mm and 45 mm, respectively. In each case of the distance

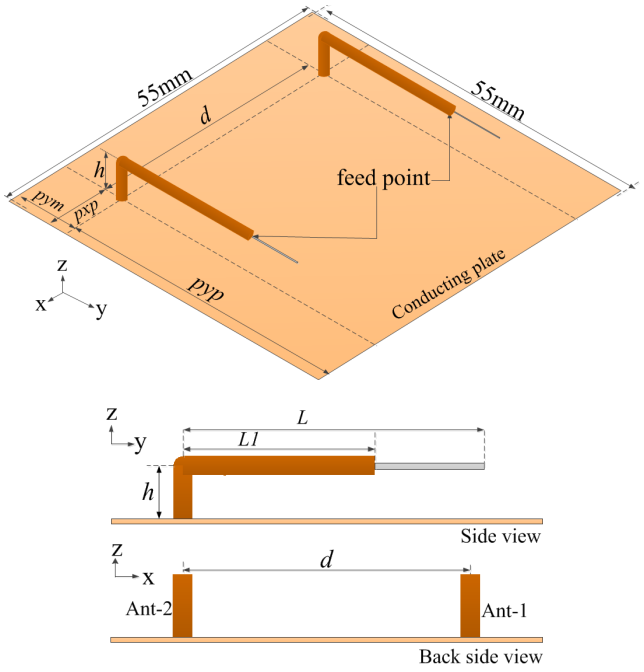

Fig. 1. The structure of proposed antenna.
pym = 10 mm, *pyp* = 45 mm, *h* = 4 mm

between two antennas, the length of horizontal elements L and $L1$ are optimized to achieve impedance matching and the mutual couplings are examined.

III. Results and Discussion

In the calculation, the distance d between two inverted L antennas is changed from 30 mm to 45 mm. Table I shows the simulated return loss bandwidth larger than 10 dB and the directive gain in the z direction at 2.45 GHz for the different distance d between two antenna elements. The length of horizontal elements L becomes longer when the distance d is increased, on the other hand, $L1$ becomes shorter. Fig. 2 shows simulated S parameters and input impedance characteristics of the proposed antenna for different distance d between two antenna elements. S21 becomes smaller than -20 dB as the distance d become longer than 41 mm.

Table II shows the simulated return loss bandwidth and the directive gain in the z direction at 2.45 GHz for different antenna height h. Fig. 3 shows simulated S parameter of the proposed antenna and input impedance characteristics for different antenna height h. The return loss bandwidth and S21 become smaller as the antenna height h becomes smaller. As the antenna height becomes smaller, the electromagnetic field concentrates near the excited antenna element. Therefore the mutual coupling between two antennas becomes weak.

Fig. 4 shows the return loss bandwidth and the directive gain in the z direction at 2.45 GHz for different distance d between two antenna elements and for different height h of antenna. Both the directive gain and the return loss bandwidth become larger by extending the distance between two antennas. Fig. 5 shows the simulated current distribution of the proposed antenna at 2.45 GHz in the case of the distance d between antennas is 41 mm. Fig. 6 shows the electric field radiation pattern on xz-plane, yz-plane and xy-plane at 2.45 GHz when inverted L antenna-1 is fed and inverted L antenna-2 is terminated by the matching load 50Ω. The peak gain of antenna-1 is 4.12 dBi. The current distribution on the inverted L antennas in the y direction and the surface current on the

TABLE I. CALCULATED RETURN LOSS BANDWIDTH AND DIRECTIVITY FOR DIFFERENT DISTANCE BETWEEN TWO ANTENNAS

h=4, pym=10, pyp=45 (mm)				Return loss bandwidth		Dir. Gain at 2.45 GHz
L	*L1*	*pxp*	*d*	MHz	%	dBi
30.7	22.7	12.5	30	50	2.04	3.79
30.9	22.2	10	35	60	2.45	3.98
31.2	21.4	7	41	80	3.27	4.12
31.4	20.7	5	45	100	4.08	4.17

TABLE II. CALCULATED RETURN LOSS BANDWIDTH AND DIRECTIVITY FOR DIFFERENT ANTENNA HEIGHT

pym=10, pyp=45, pxp=7 (mm)				Return loss bandwidth		Dir. Gain at 2.45 GHz
L	*L1*	*h*	*d*	MHz	%	dBi
31.9	23.9	3	41	50	2.04	4.09
31.2	21.4	4	41	80	3.27	4.12
30.6	19.1	5	41	120	4.90	4.08
29.9	16.8	6	41	140	5.71	4.05

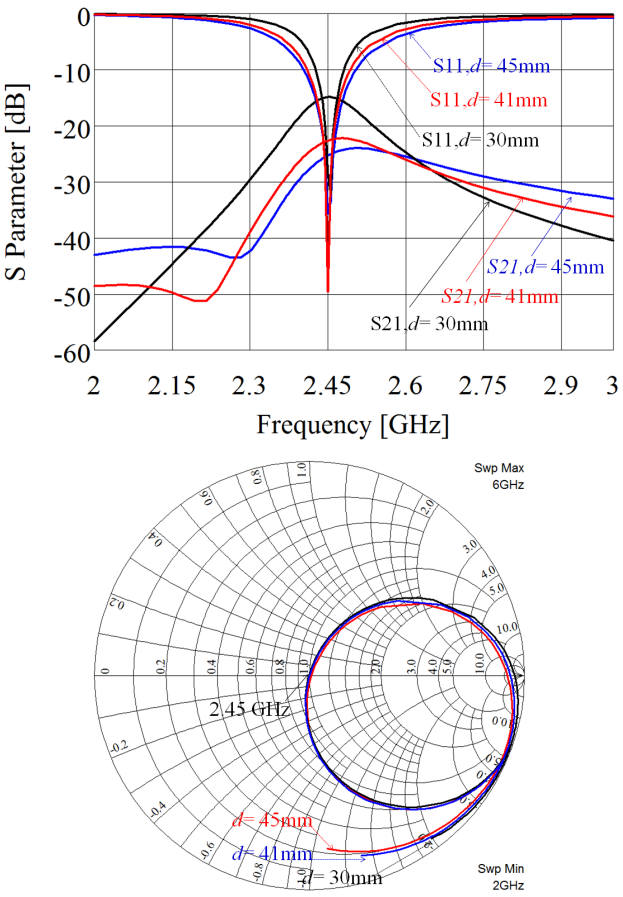

Fig. 2. Simulated S parameters and input impedance characteristics of proposed antenna with d variation.
h=4mm, pym=10mm, pyp=45mm

conducting plane in the x and y directions contribute to the radiation. Therefore there are no deep nulls in any direction, although omnidirectional polarization antennas are used in general.

Fig. 7 shows the near field distributions of the proposed antenna. From Fig. 5 and 7, the surface current on the conducting plane between two antennas is small and the electromagnetic field becomes weak near the conducting plane between two antennas. This means that the mutual coupling is mainly not by the current flowing on the conducting plane but by the spatial coupling.

The correlation coefficient of the proposed MIMO antenna is calculated through S parameter. The correlation coefficient ρ_e of a two element inverted L antenna system can be determined by the following equation [12];

$$\rho_e = \frac{\left|S_{11}^{*}S_{12}+S_{21}^{*}S_{22}\right|^2}{(1-(|S_{11}|^2+|S_{21}|^2))(1-(|S_{22}|^2+|S_{12}|^2))} \quad (1)$$

Fig. 8 shows the correlation coefficient of the proposed antenna. The correlation coefficient becomes less than 0.02, which means that the proposed antenna has good diversity gain.

Fig. 9 shows the calculated and measured impedance characteristics of the proposed antenna in the case of antenna

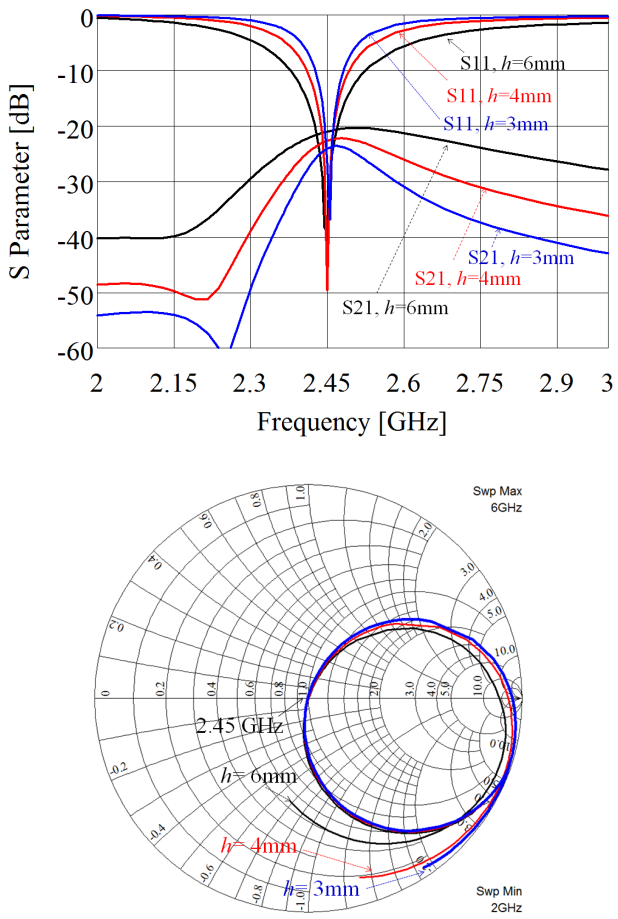

Fig. 3. Simulated of the S parameter and input impedance characteristics of proposed antenna with *h* variation.
d=41mm, *pxp*=7mm, *pym*=10mm, *pyp*=45mm

height is 4 mm and distance between two elements is 41mm. The measured results agree with the calculation results.

I. CONCLUSION

A new type of MIMO antennas composed of two ultra low profile inverted L antennas has been presented. The good performance of gain is achieved at design frequency of 2.45 GHz band. The proposed MIMO antenna has small dimension. The height of inverted L antennas is 0.03 λ and the size of square conducting plane is 045 λ by 0.45 λ. When the distance between two inverted L antennas is 0.34 λ, the directive gain and return loss bandwidth are 4.12 dBi and 3.27 %, respectively. The proposed antenna is promising for MIMO application systems.

ACKNOWLEDGMENT

Erfan Rohadi would like to thank to the General of Higher Education, Ministry Education and Culture of Republic Indonesia for providing the scholarship on the doctoral course program.

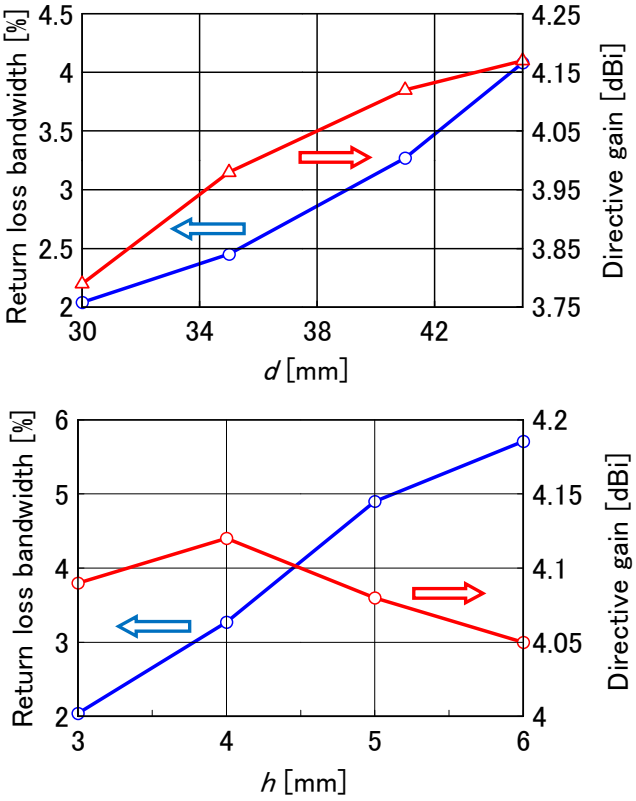

Fig. 4. Return loss bandwidth and directive gain in z direction at 2.45 GHz. *pxp*=7mm, *pym*=10mm, *pyp*=45mm

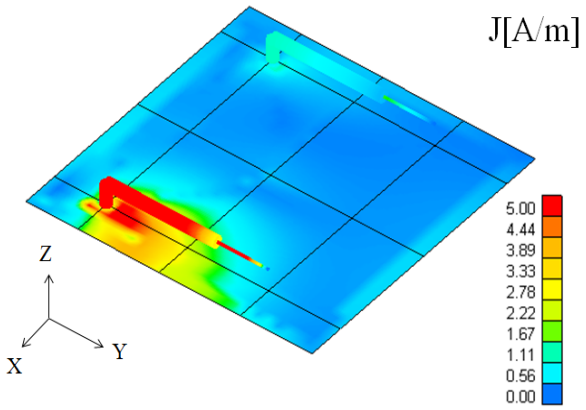

Fig. 5. Simulation of current distribution at frequency of 2.45 GHz. *h*=4mm, *d*=41mm, *pxp*=7mm, *pym*=10mm, *pyp*=45mm, *L*=31.2mm,

REFERENCES

[1] Yu XH, Wang L, Wang HG, Wu XD, Shang YH, 'A novel multiport matching method for maximum capacity of an indoor MIMO system'. Prog. Electromagn. Res. vol.130, pp.67-34, 2012.

[2] Ding Y, Du Z, Gong K, Feng Z.'A novel dula-band printed diversity antenna for mobile terminal', IEEE Trans. Antenna Propagat., vol. 55, pp.2088-2096, July 2007.

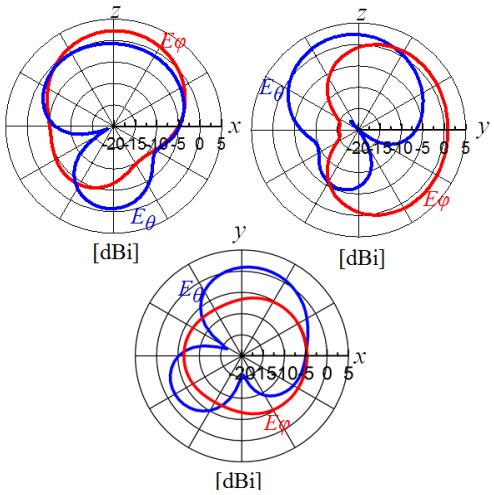

Fig. 6 Simulated electric field radiation pattern of proposed antenna at 2.45 GHz.
h=4mm, d=41mm, *pxp*=7mm, *pym*=10mm, *pyp*=45mm, *L*=31.2mm, *L1*=21.4mm

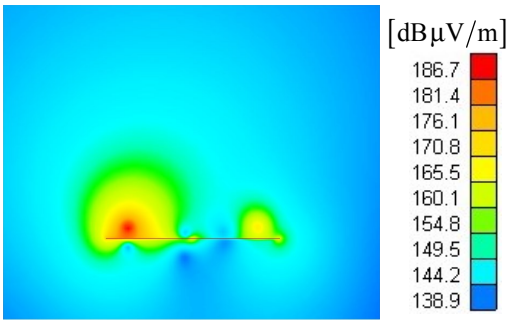

(a) Electric field

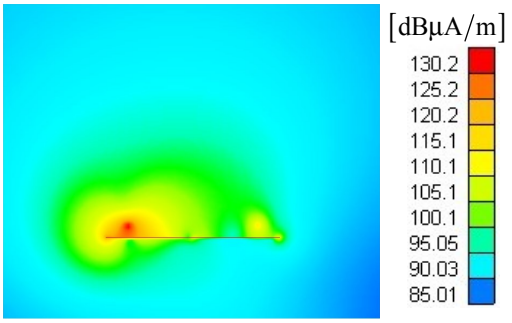

(b) Magnetic field

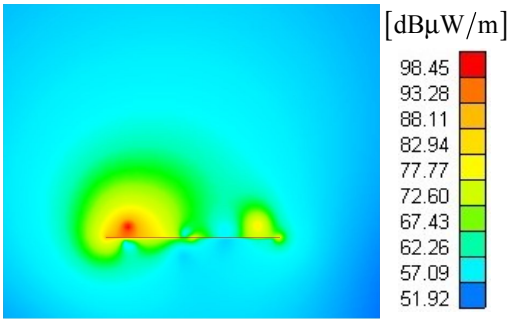

(c) Poynting vector

Fig. 7 The near field distribution at 2.45 GHz.
h=4mm, d=41mm, *pxp*=7mm, *pym*=10mm, *pyp*=45mm, *L*=31.2mm, *L1*=21.4mm

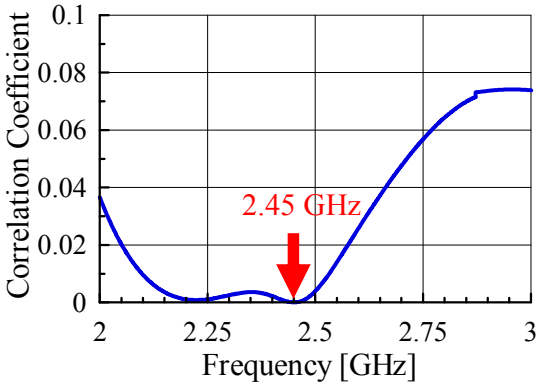

Fig. 8. Calculated correlation coefficient between two inverted L antenns.
pxp=7mm, *pym*=10mm, *pyp*=45mm, *h*=4mm, *d*=41mm.

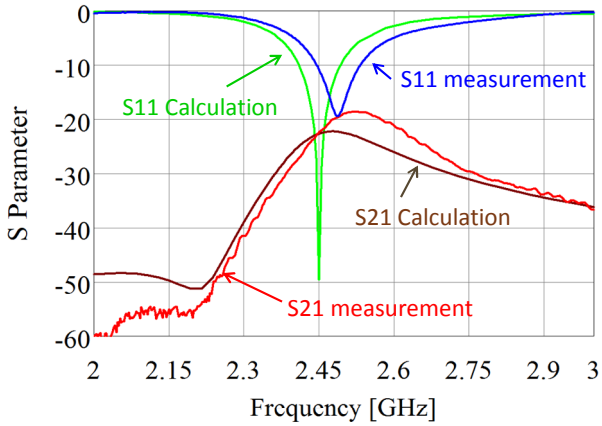

Fig. 9. Calculated and measured S parameters of the proposed MIMO antenna.
pxp=7mm, *pym*=10mm, *pyp*=45mm, *h*=4mm, *d*=41mm.

[3] Costa JR, Lima EB, Medeiros CR, Fernandes CA. 'Evaluation of a new wideband slot array for MIMO performance enhancement in indoor WLANs', IEEE Trans. Antenna Propagat., vol. 59, pp. 1200-1206, April 2011.

[4] Karimian R., Soleimani M, Hashemi SM, 'Tri-band four elements MIMO antenna system for WLAN and WIMAX application', Journal of Electomagn. Waves and Application, Vol 26, Nos.17-18, pp. 2348-2357, Dec. 2012.

[5] Cui S, Gong SX, Liu Y, Guan Y, 'Compact and low coupled monopole antennas for MIMO systems applications', Journal of Electomagn. Waves and Application, vol 25, pp. 703-712, 2011.

[6] Foschini GJ, MJ Gans, 'On limits of wireless communications in fading environment when using multiple antennas', Wireless Pers. Commun., vol.6, pp.311-335, 1998.

[7] K. Fujimoto, A. Henderson, K. Hirasawa and J. R. James, "Small Antennas", Research Studies Press, Letchworth, pp. 116-151, 1987.

[8] K. Hirasawa, M. Haneishi,"Analysis, Design, and Measurement of Small and Low-Profile Antennas", Artech house, Inc., pp. 165-169, 1992.

[9] Yamashita and M. Taguchi, "Ultra Low Profile Inverted L Antenna on a Finite Conducting Plane", *Proc. International Sympoisum on Antennas and Propag.*, pp.361-364, 2009.

[10] E. Rohadi and M. Taguchi, "Ultra Low Profile Antenna for 2.45 GHz Wireless Communications", *Proc. IEEE Int. Conf. on Communication and Satellite (Comnetsat)*, pp. 103-107, 2012.

[11] WIPL-D d.o.o.: http://www.wipl-d.com/, WIPL-D Pro v7.0, 2008.

[12] Thaysen J, Jakobsen KB, "*Envelope correlation in (N,N) MIMO antenna array from scattering parameters*", Microwave Opt. Tech. Letter. Vol. 48, pp.832-834, 2006.

Ultra Low Profile, Unbalanced Fed Inverted F Antenna for 2.45 GHz Wireless Communication System

Erfan Rohadi [#1], Mitsuo Taguchi [*2]

[#] *Graduate School of Engineering, Nagasaki University*
14-1 Bunkyou-machi, Nagasaki-Shi 852-8521, JAPAN
[1] bb52211281@cc.nagasaki-u.ac.jp

[*] *Graduate School of Engineering, Nagasaki University*
14-1 Bunkyou-machi, Nagasaki-Shi, 852-8521, JAPAN
[2] mtaguchi@nagasaki-u.ac.jp

Abstract—**An ultra low profile unbalanced inverted antenna is proposed, which is analyzed numerically and its characteristics are compared with those ultra low profile inverted L antenna and conventional base fed inverted antenna then compared with its measured results. The design frequency is 2.45 GHz. When the size of conducting plane is 0.245 λ by 0.49 λ and antenna height is λ/20, the return loss bandwidth less than -10 dB becomes 3.67 % and the directive gain is 4.15 dBi. In the numerical analysis, the electromagnetic simulator "WIPL-D" based on the method of moment is used.**

I. Introduction

The small and low-profile antenna for the miniaturization of communication equipment is needed for mobile communication systems. The low profile antennas do not extend very far from the surface they are mounted on.The well known low profile antenna is inverted F antenna for its abilities to allow a simplify impedance matching and to controlling both the return loss bandwidth and directive gain [1]. The inverted F antenna possesses good properties as required for wireless local area network application and mobile applications and it also provide a fairly return loss bandwidth. For further information refer to [2], [3], [4], [5] and [6]. In this paper, the ultra low profile, unbalanced fed inverted F antenna is proposed and its characteristics are compared with the previous proposed low profile unbalanced inverted L antenna which is located very close on a rectangular conducting plane [7] and [8]. Measured trough the fabrication is needed to validate its calculation characteristics. The proposed ultra low profile, unbalanced inverted F antenna, and then we called ULPIF for the convenience. In the numerical analysis, the electromagnetic simulator "WIPL-D" is used [9].

II. Analytical Model

The unbalanced fed inverted F antenna is identical to a transmission line antenna of length $h + L + Ls \approx \lambda/4$. Alternately, the configuration is treated as a small loop inductor, consisting of the feed probe and the inverted L element behind the feed point, resonated with the capacitance of a horizontal wire above a ground plane, shown by Fig. 1. The sum of horizontal elements, *L, Ls* and the height antenna effects to the resonant frequency of the antenna. If the antenna height h is low, a capacitive coupling between conducting plane and the upper part of antenna occurs; hence the total length of horizontal element can be reduced. The length of short stub *Ls* has no effect onto the resonant frequency but to the input Impedance [10].

Fig. 1 shows the structure of the proposed ULPIF antenna located on a rectangular conducting plane (*pxp+pxm* by *pyp+pym*) and its size is fixed as *pxp=pxm*=15mm, *pyp*=43.2mm and *pym*=16.8mm when the length of short stub *Ls* is 6.8mm. The coaxial radiator is mounted on the conducting plane. The radius of the outer conductor is 0.8 mm and that of the inner conductor is 0.16 mm. The inner conductor of the coaxial cable is extended from the end of outer conductor. Therefore, this antenna is excited at the end of outer conductor. The height of horizontal element is *h*. The design frequency is 2.45 GHz. The wavelength λ at 2.45 GHz is 122.45 mm.

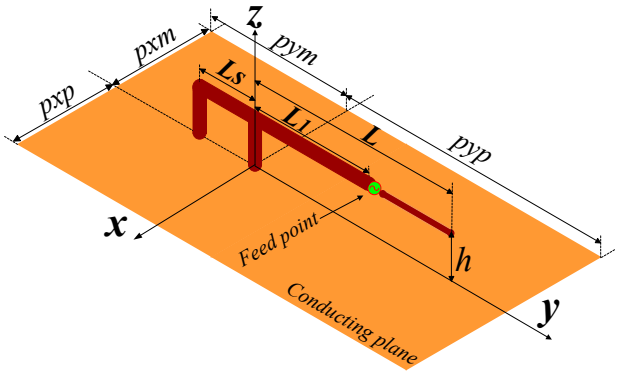

Fig. 1. Structure of the proposed ULPIF

III. Results and Discussion

The ULPIF antenna is analyzed by adjusting the antenna height *h*. The limitation maximum h is 1/10 λ (wavelength). The heights *h* are 6mm, 8mm and 10 mm for the calculation analysis. The length of short stub *Ls* is adjusted in order to enhance the antenna gain even though it has limitation when the horizontal antenna very closed to the conducting plane. The length of horizontal antenna *L1* is adjusted in order to tune at the frequency design, on the other hand other horizontal *L* is adjusted due to impedance matching 50 Ohm. The length of horizontal elements *L* and *L1* are increased by reducing the antenna height.

Table 1 shows the calculated return loss bandwidth and the directive gains in the z direction of ULPIL antenna, ULPIF antenna and low profile conventional base fed inverted F (Base Fed IF) antenna for different antenna height *h*. The directive gain of ULPIF antenna is larger than that of ULPIL antenna. This may be due to that the total length of horizontal element of the ULPIF antenna *L+L1 + Ls* is a little bit longer than that of ULPIL antenna. When the height h is 0.08λ, the total length element of ULPIF and ULPIL are 0.34 λ and 0.3λ, respectively. The base fed IF antenna has wider the bandwidth antenna and smaller gain than the ULPIF. Increasing the antenna height decreases the total of horizontal element. The calculation results indicate the antenna return loss bandwidth increases nearly linearly with the antenna height; on the other hand the directivity reduces.

TABLE I
Return Loss Bandwidth and Directive Gain of ULPIL and ULPIF Antenna for Different height of Antenna at 2.45 GHz

h	*L*	*L1*	Return Loss Bandwidth			Directive Gain at 2.45 GHz [dBi]
[mm]			f-low [GHz]	f-high [GHz]	%	
ULPIL						
6	29.7	18.3	2.40	2.50	4.08	4.03
8	28.4	14.2	2.38	2.53	6.12	3.88
10	26.8	10.0	2.35	2.55	8.16	3.68
ULPIF, *Ls*=6.8 mm						
6	30.0	19.2	2.41	2.50	3.67	4.15
8	29.1	15.2	2.38	2.52	5.71	4.03
10	27.8	11.1	2.46	2.55	7.76	3.85
Base Fed IF, *Ls*=6.8 mm						
6	29.0	17.2	2.15	2.64	20.00	3.67
8	28.1	15.8	2.22	2.61	15.92	3.76
10	27.0	14.6	2.27	2.61	13.88	3.76

Table 2 shows the calculated return loss bandwidth of ULPIF antenna and the directive gain in the z direction for different length of short stub *Ls* and antenna height *h* when the size conducting plane *pxp=pxp*=15mm by *pym*=16.8mm + *pyp*=42.2 mm at 2.45 GHz The length of short stub *Ls* can be reduced due to the antenna gain enhancement, on the other hand the bandwidth antenna little bit becomes narrower. The Ls adjustment almost doesn't affect on the length of horizontal elements *L* and *L1*.

TABLE 2
Return Loss Bandwidth and Directive Gain of ULPIF Antenna for Different height and Length Short Stub of Antenna at 2.45 GHz

Ls	*L*	*L1*	Return Loss Bandwidth			Directive Gain at 2.45 GHz [dBi]
[mm]			f-low [GHz]	f-high [GHz]	%	
h=6mm						
4	30.4	18.8	2.40	2.50	4.08	4.18
5.6	30.1	19.0	2.40	2.50	4.08	4.17
6.8	30.0	19.2	2.41	2.50	3.67	4.15
8	29.9	19.2	2.41	2.50	3.67	4.13
h=8mm						
4	29.1	15.0	2.38	2.53	6.12	4.05
5.6	29.1	15.0	2.38	2.53	6.12	4.04
6.8	29.1	15.2	2.38	2.52	5.71	4.03
8	29	15.5	2.38	2.52	5.71	4.00
h=10mm						
4	27.8	10.9	2.35	2.56	8.57	3.88
5.6	27.8	11.0	2.36	2.56	8.16	3.87
6.8	27.8	11.1	2.36	2.55	7.76	3.85
8	27.7	11.3	2.36	2.55	7.76	3.82

Figure 2a and Figure 2b show the calculated input impedance and return loss characteristics result between ULPIF (*h*=10mm, *Ls*=6.8mm, *pxp=pxm*=15mm, *pym*=16.8mm, *pyp*=43.2mm), ULPIL (*h*=10mm, *pxp=pxm*=15mm, *pym*=10mm, *pyp*=50mm) and Base Fed IF antenna (*h*=10mm, *Ls*=6.8mm, *L1+Ls*=21.4mm, *L+Ls*=33.8mm, *pxp=pxm*=10.4mm, *pym*=16.8mm, *pyp*=43.2mm).

Figure 2c and Figure 2d show comparison return loss bandwidth and the directive gain between ULPIL (*pxp=pxm*=15mm, *pym*=10mm, *pyp*=50mm), ULPIF (*Ls*=6.8mm, *pxp=pxm*=15mm, *pym*=16.8mm, *pyp*=43.2mm) with different *h* at 2.45 GHz and Base Fed IF antenna (*h*=10mm, *Ls*=6.8mm, *L1+Ls*=21.4mm, *L+Ls*=33.8mm, *pxp=pxm*=10.4mm, *pym*=16.8mm, *pyp*=43.2mm). The antenna bandwidth increases linearly, by increase the antenna height.

Figure 3 shows the directive gain of ULPIF antenna (*h*=10mm, *pxp=pxm*=15mm, *pym*=16.8mm, *pyp*=43.2mm) by investigate on length of short stub *Ls*.

Figure 4a shows the photograph of fabricated ULPIF antenna. Figure 4b and Figure 4c show the return loss and the input impedance characteristics of the ULPIF antenna, respectively. In the calculation the parameters are *h*=10mm, *Ls*=6.8mm, *L1+Ls*=17.9mm, *L+Ls*=34.6mm, *pxp=pxm*=15mm, *pym*=16.8mm, *pyp*=43.2mm and in the measurement are *h*=10mm, *Ls*=6.6mm, *L1+Ls*=17.1mm, *L+Ls*=34.1mm, *pxp=pxm*=15mm, *pym*=16.8mm,

pyp=43.2mm. The measured results are agree well with the calculated results.

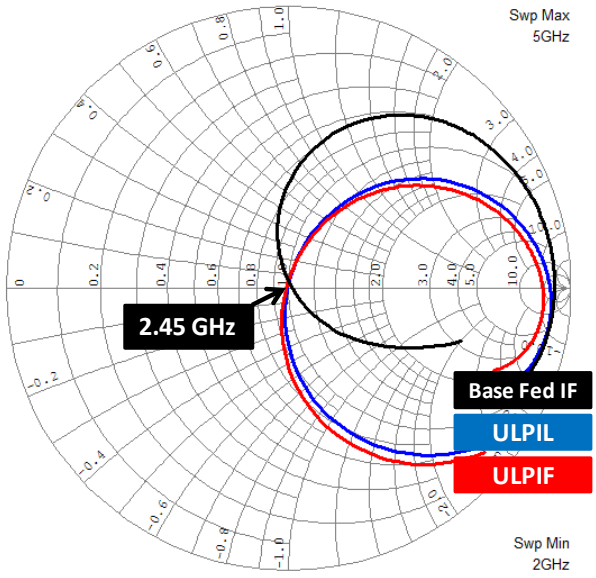

Fig. 2a. Input Impedance characteristic of ULPIL (*h*=10mm, *pxp*=*pxm*=15mm, *pym*=10mm, *pyp*=50mm), ULPIF (*h*=10mm, *Ls*=6.8mm, *pxp*=*pxm*=15mm, *pym*=16.8mm, *pyp*=43.2mm) and Base Fed IF antenna (*h*=10mm, *Ls*=6.8mm, *L1*+*Ls*=21.4mm, *L*+*Ls*=33.8mm, *pxp*=*pxm*=10.4mm, *pym*=16.8mm, *pyp*=43.2mm).

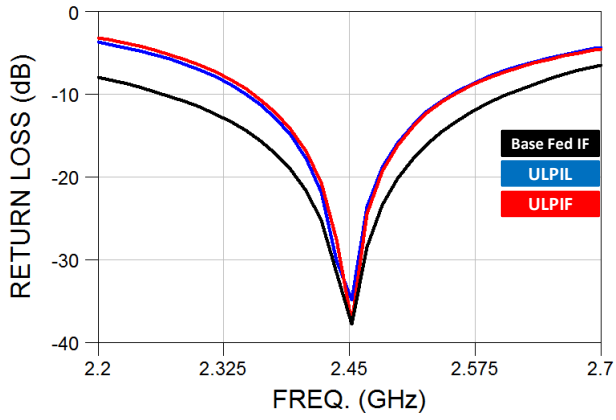

Fig. 2b. Return Loss characteristic of ULPIL (*h*=10mm, *pxp*=*pxm*=15mm, *pym*=10mm, *pyp*=50mm) ULPIF (*h*=10mm, *Ls*=6.8mm, *pxp*=*pxm*=15mm, *pym*=16.8mm, *pyp*=43.2mm) and Base Fed IF antenna (*h*=10mm, *Ls*=6.8mm, *L1*+*Ls*=21.4mm, *L*+*Ls*=33.8mm, *pxp*=*pxm*=10.4mm, *pym*=16.8mm, *pyp*=43.2mm).

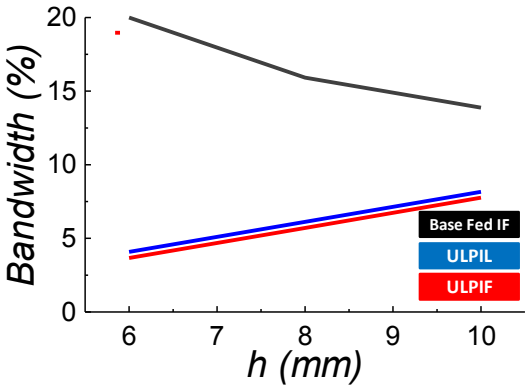

Fig. 2c. Comparison the return loss bandwidth between ULPIL, ULPIF and Base Fed IF antenna with different *h* at 2.45 GHz.

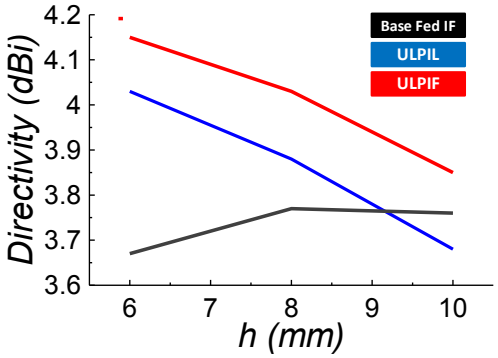

Fig. 2d. Comparison the directive gain between ULPIL, ULPIF and Base Fed IF antenna with different *h* at 2.45 GHz.

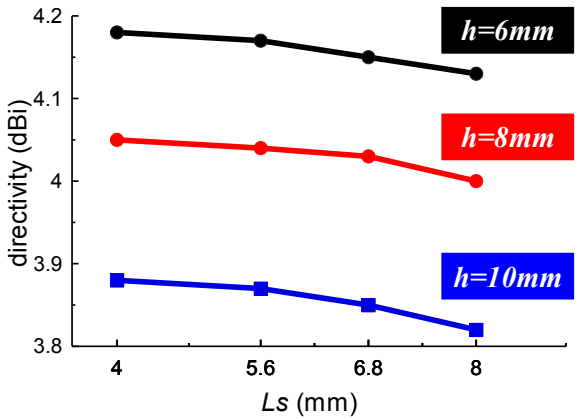

Fig.3. The directive gain of ULPIF at 4.25GHz (*pxp*=*pxm*=15mm, *pym*=16.8mm, *pyp*=43.2mm) with different *Ls*.

IV. Conclusion

The ULPIF antenna on a rectangular conducting plane has been proposed. The return loss and the directive gain of this antenna has been compared with those of the base fed inverted F antenna and the ULPIL antenna. The directive gain of proposed antenna is higher than that of base fed inverted F antenna. When the size of conducting plane is 0.245 λ by 0.49 λ and antenna height is λ/20, the return loss bandwidth less than -10 dB becomes 3.67 % and the directive gain is 4.15 dBi. The measurement results are agree well with the calculation results. This ULPIF antenna may be promising as the base station antenna or mobile terminal antenna of the wireless communication system.

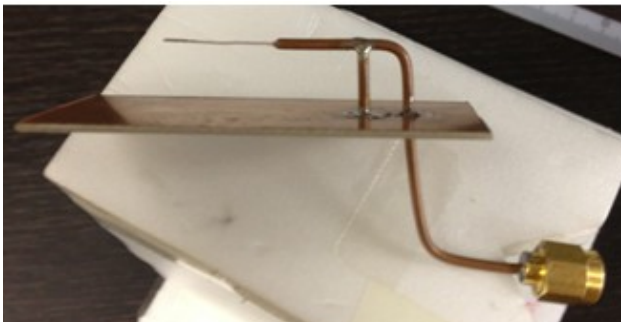

Fig. 4a. The photograph of fabricated ULPIF antenna (*h*=10mm, *Ls*=6.6mm, *L1*+*Ls*=17.1mm, *L*+*Ls*=34.1mm, *pxp*=*pxm*=15mm, *pym*=16.8mm, *pyp*=43.2mm).

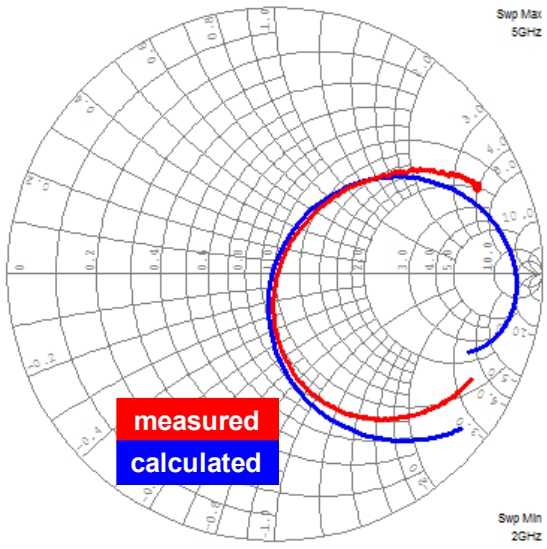

Fig. 4b. Input Impedance characteristic of ULPIF (Calculation; *h*=10mm, *Ls*=6.8mm, *L1*+*Ls*=17.9mm, *L*+*Ls*=34.6mm, *pxp*=*pxm*=15mm, *pym*=16.8mm, *pyp*=43.2mm) and (Measurement; *h*=10mm, *Ls*=6.6mm, *L1*+*Ls*=17.1mm, *L*+*Ls*=34.1mm, *pxp*=*pxm*=15mm, *pym*=16.8mm, *pyp*=43.2mm).

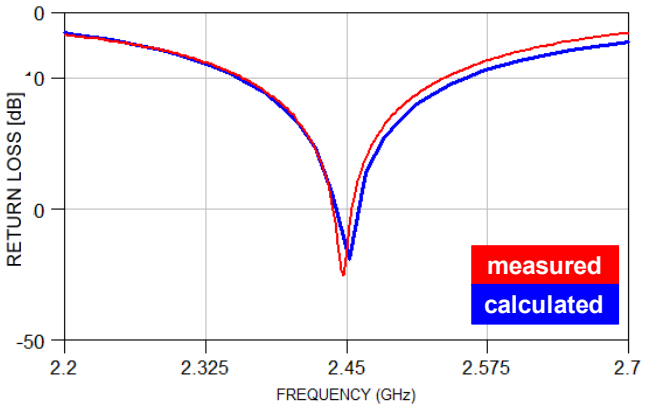

Fig. 4c. Return Loss characteristic of ULPIF (Calculation; *h*=10mm, *Ls*=6.8mm, *L1*+*Ls*=17.9mm, *L*+*Ls*=34.6mm, *pxp*=*pxm*=15mm, *pym*=16.8mm, *pyp*=43.2mm) and (Measurement; *h*=10mm, *Ls*=6.6mm, *L1*+*Ls*=17.1mm, *L*+*Ls*=34.1mm, *pxp*=*pxm*=15mm, *pym*=16.8mm, *pyp*=43.2mm).

Acknowledgment

Erfan Rohadi wants to thank to the General of Higher Education, Ministry Education and Culture of Republic Indonesia for providing the scholarship on the doctoral course program.

References

[1] Douglas B. Miron, *"Small Antenna Design"*, Communication Engineering Series, pp. 2-5, Elsevier Inc. Burlington, USA 2006.

[2] Y. Rahmat-Samii and Z. Li, Handset communication antenna, including human interactions, in *Wireless Network: From Physical Layer to Communication, Computing, Sensing and Control*, G. Franceschetti and S. Stonelli (Eds.), Academic Press, New York, 2006.

[3] Y. X. Guo, M. Y. W Chia, and Z. N. Chia, "Miniature built-in multiband antennas for mobile handset", *IEEE Trans. on Antennas Propagation,* vol. 52, pp 1936-1944. August 2004.

[4] G. Y. Lee and K. L. Wong, " Very low profile bent planar monopole antenna for GSM/ DCS dual-band mobile phone", *Microwave and Optical Technology Letters*, Vol. 34, No. 6 September, 2002.

[5] D. Liu and B. P. Gaucher, The inverted-F antenna height effects on bandwidth, *Proc. IEEE Antenna Propag. Symp.*, Vol. 2A, pp. 367-370, July 2005.

[6] C. Rowell, A brief survey of internal antennas in GSM phones: 1998 to 2004, Proc. *UNSC/URS/National Radio Science Meeting*, July 2005.

[7] K. Fujimoto, A. Henderson, K. Hirasawa and J. R. James, *Small Antennas*, pp.116-151, Research Studies Press, Letchworth, 1987.

[8] T. Yamashita and M. Taguchi, "*Ultra Low Profile Inverted L Antenna on a Finite Conducting Plane"*, Proc. International Sympoisum on Antennas and Propagation, pp.361-364, Oct.2009.

[9] S. Schulteis, C. Waldschmidt, C. Kuhnert and W. Wiesbeck, " *Design of a Capacitively Loaded Inverted F Antenna* ***for.*** *Wireless-LAN Applications*"' Proc. International ITG-Conference on Antennas, Berlin, 178:187-190, Sept.2003.

[10] WIPL-D d.o.o.: http://www.wipl-d.com/

Ultra Low Profile Antenna for 2.45 GHz Wireless Communication

Erfan Rohadi
Graduate School of Engineering, Nagasaki University
1-14 Bunkyo-machi, Nagasaki-shi, 852-8521 JAPAN,
bb52211281@cc-nagasaki-u-ac.jp

Mitsuo TAGUCHI
Graduate School of Engineering, Nagasaki University
1-14 Bunkyo-machi, Nagasaki-shi, 852-8521 JAPAN,
mtaguchi@nagasaki-u.ac.jp

***Abstract*—The ultra low profile, conventional base fed F antenna is analyzed numerically and its characteristics are compared with those of the unbalanced fed, ultra low profile inverted L antenna. The design frequency is 2.45 GHz. When the size of conducting plane is 0.17 λ by 0.49 λ and the antenna height is 0.08 λ, the return loss bandwidth less than -10 dB becomes 15.92 % and the directivity is 3.94 dBi. In the numerical analysis, the electromagnetic simulator "WIPL-D" based on the method of moment is used.**

Keywords: *Ultra low profile antenna, Inverted F antenna, Conventional base fed antenna, WIPL-D*

I. INTRODUCTION

Recent technologies enable wireless communication devices to become physically smaller in size. Antenna size is obviously a major factor that limits miniaturization. In the few years, the designs of low-profile antennas for handheld wireless devices have been developed [1]. The low profile antennas do not extend very far from the surface they are mounted on. On the other hand, the height of previous antennas are λ/10 (λ: wavelength) or more. An example of low profile antennas is a base fed inverted L antenna. The input impedance of base fed inverted L antenna is close to that of the monopole antenna with reactance value due to additional horizontal section parallel to the antenna ground plane. It has a low resistance and high reactance characteristics. The degradation due to impedance mismatch can be recovered by feeding the antenna on the horizontal element.

Since the mismatch loss decreases radiation efficiency, it is desirable to modify the structure of the inverted L antenna to achieve a nearly resistive input impedance that is easily matched to a standard coaxial line. Reducing the antenna height has the disadvantage of reducing the bandwidth, but offers the advantages of smaller size and improved radiation characteristics.

The authors have proposed an ultra low profile, unbalanced fed inverted L antenna located very close on a rectangular conducting plane [2]. We may call this antenna as "ULPIL antenna" for convenience. This antenna consists of a coaxial cable. The inner conductor of the coaxial cable is extended from the end of outer conductor. Therefore, this antenna is excited at the end of outer conductor. The antenna height is around λ/30. This antenna is a horizontally polarized antenna. The length of horizontal element of this antenna is almost λ/4. The input impedance of this antenna is matched to 50 Ω by adjusting the position of feed point. When the size of conducting plane is 0.245 λ by 0.49λ, the return loss bandwidth less than -10 dB becomes 2.45 % and the directivity is 4.24 dBi. In this antenna, the current flows on the conducting plane. Therefore the current on the horizontal element and on the conducting plane contribute to the radiation.

The inverted F antenna and planar inverted F antenna are well known as the other typical low-profile antennas. The inverted F antenna can be configured by bending a quarter wavelength monopole element mounted on a conducting plane into an L shape and by feeding at a point offset from the mounting point [3]. The inverted F antenna possesses good properties as required for wireless local area network application and mobile application at 2.45 GHz and it also provide a fairly return loss bandwidth [4, 5, 6, 7 and 8].

In this paper, the ultra low profile, conventional base fed inverted F antenna (ULPIF antenna) on a rectangular conducting plane is numerically analyzed and its characteristics are compared with the previously proposed ULPIL antenna. The inverted F antenna in Figure 1(b) is identical to a transmission line antenna of length $h + L + Ls$ fed at the tap point (shorted element) Ls. Alternately, the configuration is treated as a small loop inductor, consisting of the feed probe and the inverted-L element behind the feed point, resonated with the capacitance of a horizontal wire above a ground plane. The addition of the element is done to simplify the input impedance settings. The elements may be extruded from the wire form to a planar form to realize an increase in impedance and gain bandwidth. However, a small degradation in gain may be seen [9].

In the numerical analysis, the electromagnetic simulator WIPL-D based on the method of moment is used. The method of moment is effective for analyzing the characteristics of antennas mounted on the portable radio equipment with the dimensions comparable to the wavelength. To improve the characteristics of the ULPIF antenna such as the impedance characteristics, the return loss bandwidth and the electric fields radiation pattern, the length of antenna element, the antenna height, the length of shorting element, and the size conducting plane are optimized [3, 10]. The advantages of the design of the

antenna are the small size, the height less than λ/10 and the low cost material.

II. ANALYTICAL MODEL

Figure 1(a) shows the structure of the unbalanced fed ULPIL antenna located on a rectangular conducting plane, and Figure 1(b) shows the conventional base fed ULPIF antenna. The size of conducting plane is *pxp+pxm* by *pyp+pym*. The coaxial radiator is mounted on the conducting plane. The radius of the outer conductor is 1.095 mm and that of the inner conductor is 0.255 mm. The inner conductor of the coaxial cable is extended from the end of outer conductor, this antenna is excited at the end of outer conductor. The height *h* of antenna is from 5 mm to 12 mm, and the length *Ls* of shorted antenna element is from 3.3 mm to 10mm. The length of horizontal elements *L* and *L1* are optimized. The design frequency is 2.45 GHz. The wavelength λ at 2.45 GHz is 122.45 mm. The size of conducting plane is considered as 20.8 mm by 60 mm. At the design frequency of 2.45 GHz, the size of conducting plane becomes 0.17 λ by 0.49 λ.

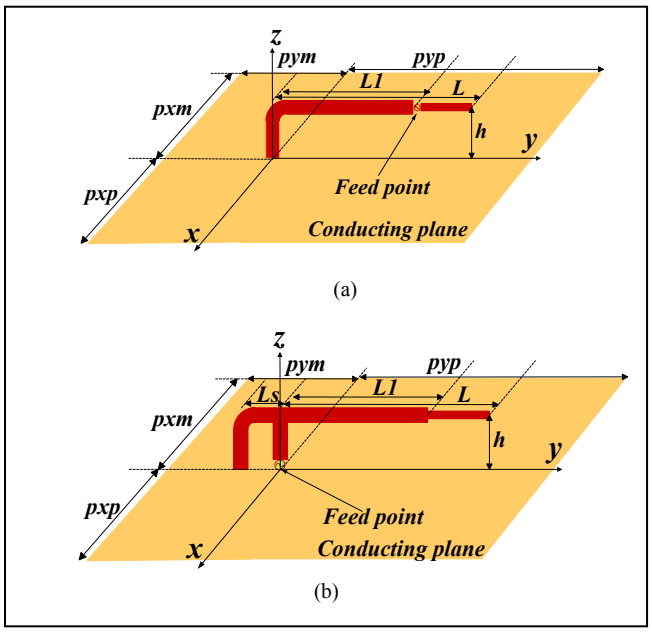

Figure 1. The structure of Unbalanced fed Ultra Low Profile Inverted L Antenna (ULPIL Antenna) and Conventional base fed Ultra Low Profile Inverted F Antenna (ULPIF Antenna) on finite conducting plane.

III. RESULTS AND DISCUSSION

In the ULPIF antenna, the addition of the extra inverted *L* element behind the feed point tunes the input impedance of the antenna. To obtain the impedance of 50 Ω, the length of horizontal elements *L, L1,* and shorted element *Ls* must be adjusted, while considering the current distribution on the conducting plane by adjusting its size. For ULPIF antenna, the impedance is adjusted by also changing the antenna height *h*, otherwise the size of finite conducting plane may be not changed [3].

Figure 2 shows the equivalent circuit of ULPIF antenna. One end of the ULPIF antenna is open and the other end is shorted. Consequently, the current is zero at the open end and it becomes a maximum in the shorted end.

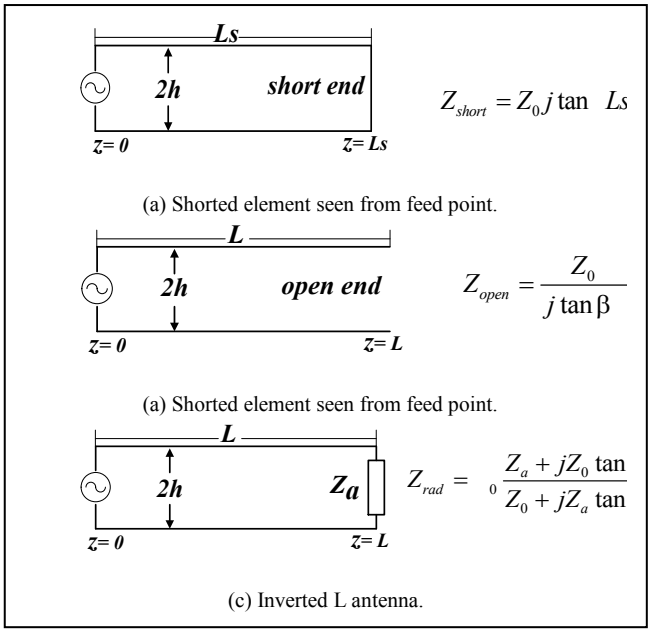

Figure 2. Equivalent circuit of ULPIF antenna.

The current flows on the *z* direction on the short circuit, and then flows in *y* direction at antenna element from the short circuit edge to opposite open circuited edge of antenna element. At the open circuited edge, the displacement current may be on the conducting plane, hence the current flows back to the short-circuited element on the conducting plane [11]. Figure 2(a) shows the equivalent circuit of the shorted element seen from the feed point. Figure 2(b) shows the equivalent circuit of the antenna end seen from the feed point. Figure 2(c) shows the equivalent circuit of the inverted L antenna. This antenna is expressed by the radiation resistance loaded on the transmission line. Since the length *L* of inverted L antenna is almost a quarter wavelengths, the input impedance Z_{open} becomes negligible. Therefore the input impedance of the ULPIF antenna is expressed the parallel connection of Z_{short} and Z_{rad}. Then the input impedance is tuned by adjusting the length *Ls* of shorted element.

A. Impedance and Electric field radiation pattern characteristics

Figure 3 (a) illustrates how the calculated input impedance of an ULPIF antenna changes when the antenna height *h* is altered while the length of shorted antenna element is fixed as *Ls* = 3.3 mm. Figure 3 (b) shows the calculated input impedance of ULPIL antenna with different antenna height *h*.

Figure 3 (c) shows the calculated input impedance of ULPIF antenna with antenna height *h* = 10 mm, length of horizontal antenna elements *L* = 26.6 mm and *L1* = 14 mm, the shorted antenna element *Ls* = 6.8 mm, the size of conducting plane is 20.8 mm by 60 mm and ULPIL antenna with antenna height *h* = 10 mm, length of horizontal antenna elements *L* = 27 mm and *L1* = 10.2 mm, and the size of conducting plane is 30 mm by 60 mm.

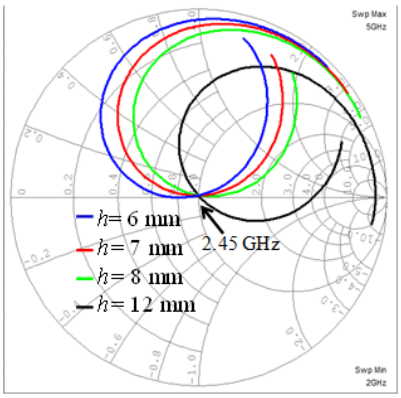

(a) ULPIF antenna (*Ls*=3.3mm)

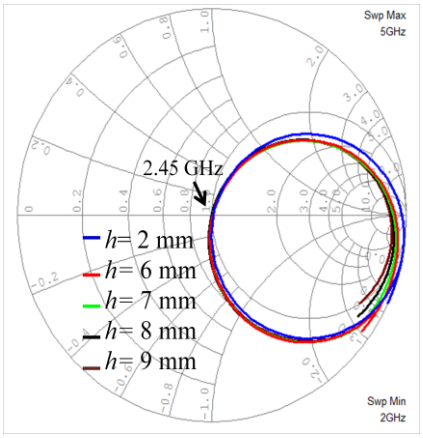

(b) ULPIL antenna

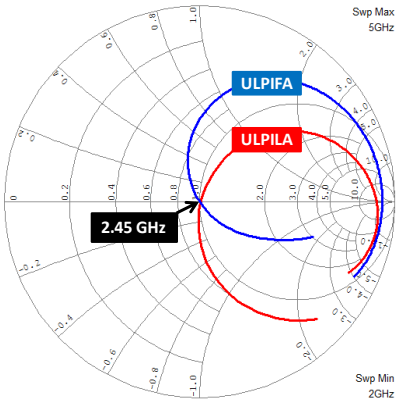

(c) ULPIL antenna and ULPIF antenna with *Ls*=6.8mm

Figure 3. Input impedance characteristics of Unbalanced fed ULPIL antenna and Conventional base fed ULPIF antenna (*Ls*=6.8 mm).

In Figure 3(c), the length of shorted antenna element *Ls* is extended to 6.8 mm for the ease of fabrication.

The energy radiated by the antenna in a particular direction is measured in terms of field strength at a point which is at a particular distance from antenna. The radiation pattern of the antenna is a graph which shows the variation of actual field strength of electromagnetic field at all points which are at equal distance from antenna [12].

Figure 4 (a) shows the computed electric field radiation patterns of ULPIL antenna and Figure 4 (b) shows the computed electric field radiation patterns of the base fed ULPIF antenna. The calculation condition are antenna height h = 10 mm, horizontal antenna elements L = 26.6 mm and $L1$ = 14 mm, shorted element Ls = 6.8 mm, and the size of conducting plane is 20.8 mm by 60 mm and ULPIL antenna with antenna height h = 10 mm, horizontal elements L = 27 mm and $L1$ = 10.2 mm, and the size of conducting plane 30 mm by 60 mm. From these figures it is clear that the antenna will give desired radiation characteristics.

The vertically polarized gain of the ULPIF antenna is maximum in the equatorial plane with a vertical null in the z direction. There is not a null in the y-z plane due to currents on the horizontal antenna elements. The maximum directivities in the z direction are 3.88 dBi for ULPIL antenna and 3.94 dBi for ULPIF antenna. The vertically directed currents on the ULPIF antenna cause a cross polarization component in the x-z plane.

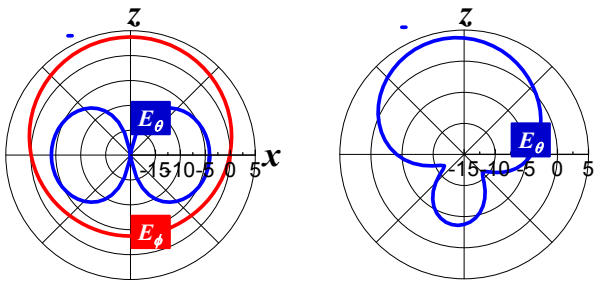

(a) ULPIL antenna

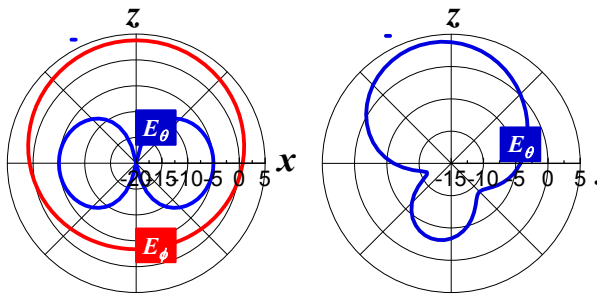

(b) ULPIF antenna (*Ls*=6.8mm)

Figure 4. Electric field radiation patterns of Unbalanced fed ULPIL antenna and Conventional base fed ULPIF antenna (*Ls*=6.8 mm) at 2.45 GHz

B. Returns Loss Bandwidth Characteristics

Table I shows the calculated return loss bandwidth less than -10 dB and the directive gain of ULPIF antenna in the z direction by adjusting the antenna height h and length of shorted antenna element *Ls*. Since the height of ULPIF antenna is reduced, the shorted element becomes narrower.

TABLE I. RETURN LOSS BAND WIDTH AND DIRECTIVE GAIN OF CONVENTIONAL BASE FED ULPIF ANTENNA FOR DIFFERENT *h* and *Ls*.

h [mm]	Ls [mm]	L [mm]	L1 [mm]	Return Loss Bandwidth [%]	Directive gain at 2.45 GHz [dBi]
12	3.30	24.10	15.60	11.84	3.44
	6.00	24.40	16.10	14.29	3.53
	7.00	24.40	16.20	14.69	3.54
	10.00	24.40	16.20	13.88	3.47
11	3.30	24.70	16.00	12.24	3.58
	6.00	25.10	16.30	13.88	3.67
	10.00	25.30	16.40	11.02	3.62
10	3.30	25.10	17.00	11.43	3.69
	6.00	25.60	17.10	11.84	3.78
	10.00	25.90	17.30	5.71	3.74
9	3.30	26.50	13.10	9.80	3.88
	6.00	26.80	13.10	8.57	3.97
	8.00	27.00	13.20	4.49	3.99
	9.00	27.00	13.30	N/A	3.98
8	3.30	27.10	13.30	7.76	3.98
	6.00	27.40	13.40	2.04	4.08
	7.00	27.50	13.50	N/A	4.09
7	3.30	27.80	13.60	5.71	4.08
	4.00	27.80	13.70	4.08	4.12
	5.00	27.90	13.70	N/A	4.16
6	3.30	28.40	14.30	2.45	4.17
	4.00	28.40	14.30	N/A	4.20
5	3.30	29.10	14.80	N/A	4.25

TABLE II. RETURN LOSS BAND WIDTH AND DIRECTIVE GAIN OF UNBALANCED FED ULPIL ANTENNA FOR DIFFERENT *h*.

h [mm]	L [mm]	L1 [mm]	Return Loss Bandwidth			Directive gain at 2.45 GHz [dBi]
			f_low [GHz]	f_high [GHz]	%	
6	29.9	18.3	2.4	2.51	4.490	4.09
7	29.4	16.4	2.38	2.52	5.714	4.00
8	28.3	14.3	2.36	2.56	8.163	3.94
9	27.9	12.3	2.35	2.56	8.571	3.84
10	27.0	10.2	2.34	2.57	9.388	3.88

TABLE III. RETURN LOSS BAND WIDTH AND DIRECTIVE GAIN OF CONVENTIONAL BASE FED ULPIF ANTENNA FOR DIFFERENT *h* (*Ls=6.8mm*).

h [mm]	L [mm]	L1 [mm]	Return Loss Bandwidth			Directive gain at 2.45 GHz [dBi]
			f_low [GHz]	f_high [GHz]	%	
6	28.5	17.0	2.12	2.67	22.45	3.79
7	28.1	16.0	2.19	2.63	17.96	3.83
8	27.6	15.6	2.18	2.64	18.78	3.92
9	27.0	15.2	2.22	2.63	16.74	3.95
10	26.6	14.0	2.24	2.63	15.92	3.94

.

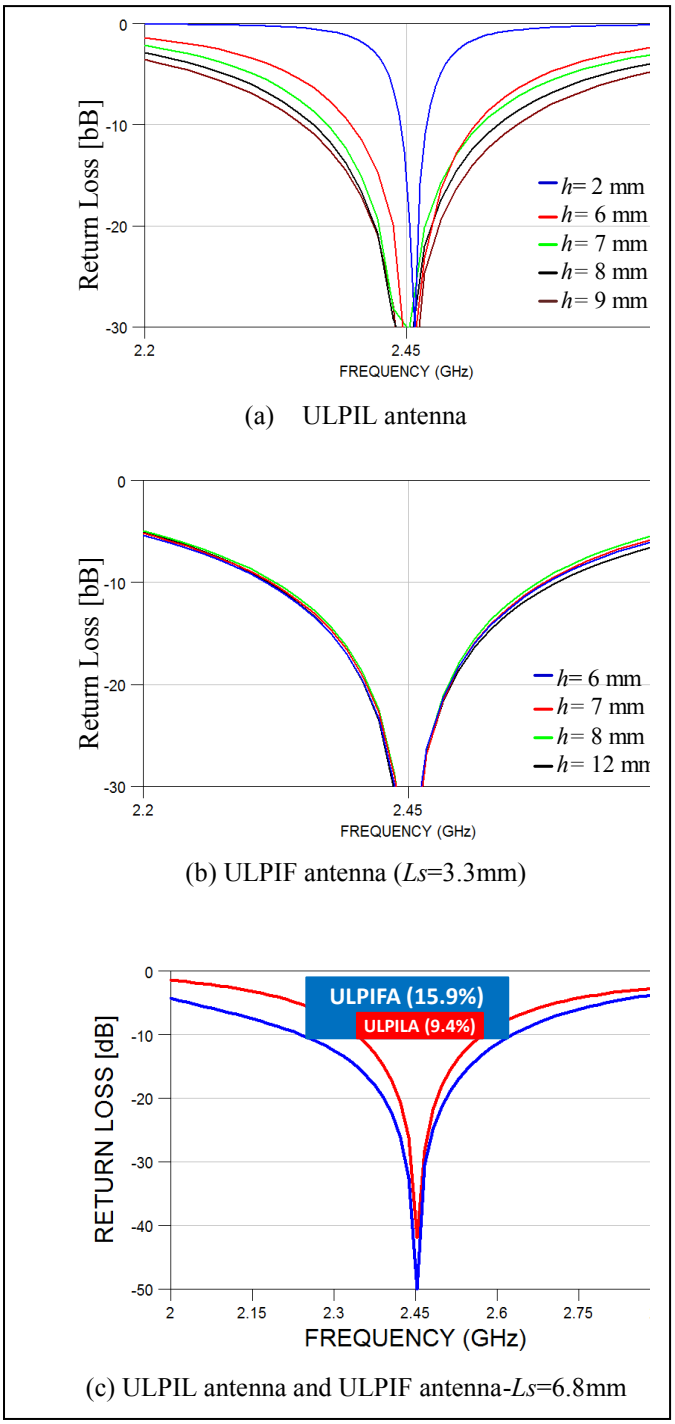

Figure 5. Return Loss Characteristics of Unbalanced fed ULPIL antenna and Conventional base fed ULPIF antenna at 2.45 GHz.

Table II shows the calculated return loss bandwidth of ULPIL antenna and the directive gain in the z direction for different antenna height *h*. The parameters of horizontal antenna element *L* and *L*1 are optimized to match the input impedance to 50 Ω at the frequency of 2.45 GHz.

Table III shows the calculated return loss bandwidth and the directive gain in the z direction of the conventional base fed ULPIF antenna for different antenna height *h*. The shorted

element *Ls* is fixed as 6.8 mm. When the antenna height *h* is 10 mm, the directive gain of ULPIF antenna becomes larger than that of ULPIL antenna. This may be due to that the total length of horizontal element of the ULPIF antenna *L+L1 + Ls* is a little bit longer than that of ULPIL antenna.

Figure 5 (a) shows the calculated return loss characteristics of ULPIL antenna for different antenna height *h*. Figure 5 (b) shows the return loss characteristics of ULPIF antenna. The lengths of shorted element *Ls* and antenna height *h* are adjusted. Figure 5 (c) shows the calculated return loss characteristics of ULPIF antenna with antenna height *h* = 10 mm, horizontal antenna elements *L* = 26.6 mm and *L1* = 14 mm, shorted element *Ls* = 6.8 mm, and the size of conducting plane is 20.8 mm by 60 mm and ULPIL antenna with antenna height *h* = 10 mm, horizontal elements *L* = 27 mm and *L1* = 10.2 mm, and the size of conducting plane 30 mm by 60 mm.

As the antenna height of the ULPIL antenna becomes higher, the upper frequency of the return loss bandwidth less than -10 dB increases and the lower frequency decreases. On the other hand, the return loss characteristics of the ULPIF antenna is almost same for dirrerent antenna height for shorted element *Ls* of 3.3 mm.

The directive gain becomes larger as the antenna height *h* becomes lower when the minimum length of shorted element *Ls* is 3.3 mm while the minimum height *h* of this antenna is 6 mm. On the other hand, its return loss bandwidth becomes narrow.

Figure 6 shows the calculated return loss bandwidth with different antenna height *h* of ULPIF antenna with shorted antenna element *Ls* = 6.8 mm and ULPIL antenna. The ULPIF antenna has smaller mutual coupling between currents on the antenna and on the conducting plane. On the ULPIL antenna, the stronger coupling occurs between the currents on the antenna element on the conducting plane and its bandwidth is narrower than ULPIF antenna.

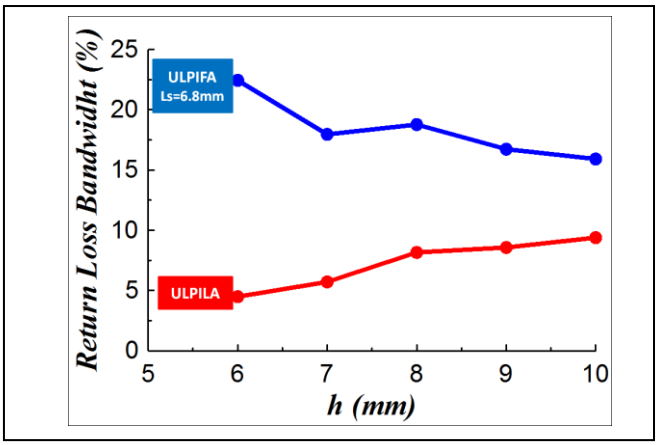

Figure 6. Return Loss Bandwidth of Unbalanced fed ULPIL antenna and Conventional base fed ULPIF antenna (*Ls*=6.8 mm) at 2.45 GHz.

IV. Conclusion

The ultra low profile, base fed inverted F antenna (ULPIF antenna) on a rectangular conducting plane has been analyzed numerically. The calculated return loss and the directive gain of this antenna has been compared with those of the unbalanced fed ULPIL antenna. The directive gain of ULPIF antenna is higher than that of ULPIL antenna. When the size of conducting plane is 0.17 λ by 0.49 λ and antenna height is 0.08 λ, the return loss bandwidth less than -10 dB becomes 15.92 % and the directivity is 3.94 dBi. The antenna height is less than 0.1 λ, this may be promising as the base station antenna or mobile terminal antenna of the wireless communication system. The proposed antenna will be validated through measurement.

Acknowledgment

Mr Erfan Rohadi wants to thank to the General of Higher Education, Ministry of Education of Republic Indonesia for providing the scholarship on the doctoral course program.

References

[1] Douglas B. Miron, *"Small Antenna Design"*, Communication Engineering Series, pp. 2-5, Elsevier Inc. Burlington, USA 2006.

[2] T. Yamashita and M. Taguchi, "Ultra Low Profile Inverted L Antenna on a Finite Conducting Plane", Proceedings of the 2009 International Symposium on Antennas and Propagation, pp.361-364, Oct. 2009.

[3] K. Fujimoto, A. Henderson, K. Hirasawa and J. R. James, *Small Antennas*, pp.116-151, 160-161, Research Studies Press, Letchworth, 1987.

[4] Y. Rahmat-Samii and Z. Li, Handset communication antenna, including human interactions, in *Wireless Network: From Physical Layer to Communication, Computing, Sensing and Control*, G. Franceschetti and S. Stonelli (Eds.), Academic Press, New York, 2006.

[5] Y. X. Guo, M. Y. W Chia, and Z. N. Chia, "Miniature built-in multiband antennas for mobile handset", *IEEE Trans. on Antennas Propagation,* vol. 52, pp 1936-1944. August 2004.

[6] G. Y. Lee and K. L. Wong, " Very low profile bent planar monopole antenna for GSM/ DCS dual-band mobile phone", *Microwave and Optical Technology Letters*, Vol. 34, No. 6 September, 2002.

[7] D. Liu and B. P. Gaucher, The inverted-F antenna height effects on bandwidth, *Proc. IEEE Antenna Propag. Symp.*, Vol. 2A, pp. 367-370, July 2005.

[8] C. Rowell, A brief survey of internal antennas in GSM phones: 1998 to 2004, Proc. *UNSC/URS/National Radio Science Meeting*, July 2005.

[9] T. Taga, Analysis of planar inverted-F antennas and antenna design for portable radio equipment, in *Analysis, Design, and Meauserement of Small and Low-Profile Antenna*, K. Hirasawa and M. Haneishi (Eds.), Arctech House, Norwood, MA, 1992.

[10] WIPL-D d.o.o.: http://www.wipl-d.com/, WIPL-D Pro v7.0, 2008.

[11] Kazuhiro Hirasawa, Misao Haneishi: *Analysis, Design, and Measurement of Small and Low-Profile Antennas,* pp. 165-169, Artech house, Inc. 1992.

[12] Constantine A Balanis., "*Antenna Theory Analysis and Design*." 3rd ed., pp. 873, 1021-1023, Hoboken, NJ, John Willey & Sons. Inc., 2005.